Addis Ababa University

Addis Ababa Institute of Technology

School of Graduate Studies

Simulation of Runoff under the past impacts of land use land cover and future climate change

(Case Study of Anger sub basin)

A thesis Submitted to the School of Graduate Studies in Partial fulfillment of the Requirements for the Degree of Master of Science in Civil Engineering (Major Hydraulic Engineering)

By:

Getachew Rabo

ID GRS /1281/08

Advisor:

Dr. Eng Dereje Hailu

Addis Ababa University Ethiopia

October, 2018

Addis Ababa Institute of Technology

School of Civil and Environmental Engineering

Simulation of Runoff under the past impact of land use land cover and future climate change

(Case study of Anger Sub Basin)

Submitted in partial fulfillment for the degree of Masters of Science in Civil Engineering

(Major in Hydraulic Engineering)

By:

Getachew Rabo

Approval by Board of Examiners

Name	Signature	Date
……..	……	…….
Chairman (department of graduate committee)		
……..	……	…….....
Advisor		
……..	……..	……...
Internal Examiner		
……..	……	…….....
External Examiner		

Acknowledgement

My deep gratitude spirits to my advisor Dr. Eng Dereje Hailu of Addis Ababa University for his encouragement, advice, support and, his valuable guidance throughout the course of this study and, all his contribution through materials support and also his trust and confidence makes me to work on my interest topic.

I would like to acknowledge the Ministry of Water, Irrigation and Electricity (MOWIE) particularly hydrology, GIS department and Library and the Ethiopia Meteorological Service Agency for providing me the relevant data and information required free of payment.

My deepest thank is to my beloved parents. Their absolute love, motivation and always encouraging me, support me, and give me strength to go through my study. A special group of friends also supported me through their friendship and professional help; among them I would like to mention: Jemal Ibrahim, Hailu Kebede, Shimelis Tesfaye and Robera Girma, Who stands with me through contribution his appreciable ideas.

Above all, sincere thanks go to the Almighty God for making this thesis success. This day what God have done for me is really beyond what I can imagine and I have dreamt. Indeed, thanks for everything you have been doing for me.

Abstract

Water resources are substantially affected by LULC and climate change. It was crucial to assess the impact of past LULC and future climate change on water resource. However, conflicting results on the effect of the LULC and climate change on runoff volume have been reported for Anger sub-basin which is located in East Wollega Zone of Oromia National Regional State (ONRS) of Ethiopia. ArcGIS was used to process preliminary data, extracting, layer stake, mosaic satellite images, and image classification. In addition to this Soil and Water Assessment Tool (SWAT) was adopted to perform runoff simulation. The good performance of the SWAT model was confirmed, with a Nash-Sutcliffe model efficiency coefficient (Ens) and determination coefficients (R^2) of 0.76 and 0.90 respectively, for monthly runoff during calibration, and 0.63 and 0.84, respectively, during validation.

This study focused on assessing the past LULU and future climate change on runoff volume change. As research finding show that from the year 1986 to 2010, agricultural land increased by 39.3% and built up area increased by 0.5%. And also, shrub-land, forest area, and water body decreased by 32.9%, 6.6%, and 0.3% respectively during the study. The accuracy of LULC classification was achieved by overall accuracy, user's accuracy, producer's accuracy, and kappa coefficient.

Due to population growth, economic development and deforestation both maximum and minimum temperature increased differently during different scenarios. The temperature of this sub-basin increased by 0.52 C^o, 0.68 C^o, 0.40 C^o, 1.74 C^o, and 2.54C^o, 3.04C^o during the 2020s, 2050 and 2080 0respectively. On the other hand, precipitation of sub-basin decreased differently during different scenarios. It decreased by 2.06%, 7.63% and 17.67% during 2020s, 2050s and 2080s respectively.

From this study, it was observed that, due to urbanization, deforestation and agricultural expansion, past LULC change affect runoff volume of the sub-basin differently in different scenarios. The simulated runoff result indicated that runoff volume increased by 12.54Mm^3 and 25.29 Mm^3 between 1986-2000 LULC and 2000-2010 LULC respectively. And also due to future climate change, the runoff volume will decrease from baseline period (1990s) by 16.76Mm^3, 44.96 Mm^3 and 54.29 Mm^3 during the 2020s, 2050s, and 2080s respectively.

Lastly, past LULC change affect water yield volume of the sub-basin differently in different scenarios. The simulated runoff result indicated that water yield volume decreased by 22.16Mm^3 and 20.76Mm^3 between 1986-2000 LULC and 2000-2010LULC respectively. And also due to future climate change the water yield volume will decrease from baseline period (1990s) by 14.50Mm^3, 39.32 Mm^3 and 78.85 Mm^3 during the 2020s, 2050s and 2080s respectively.

KEYWORDS: SWAT, Arc GIS, Anger sub-basin, Land use land cover and climate change

Table of Contents

Acknowledgement ii
Abstract iii
List of figures viii
List of tables x
List of Abbreviations xi
1 INTRODUCTION 1
1.1 Background 1
1.2 Problem of statement 2
1.3 Objectives of the study 3
1.3.1 General objective 3
1.3.2 Specific objectives: 3
1.4 Research Questions 3
1.5 Significance of the Study 3
1.6 Software and Materials used 4
1.7 Organization of the Thesis 4
2 LITERATURE REVIEW 5
2.1 Introduction 5
2.1.1 Land use land cover change 5
2.1.2 Land use land cover changes studies in Ethiopia 6
2.1.3 Land use land cover changes in the study area 8
2.2 Climate change 8
2.2.1 Climate Change in Ethiopia 9
2.2.2 Climate Change in the Study Area 10
2.3 Application of remote sensing on LULCC 10
2.1 Hydrological Models 11
2.1.1 SWAT Model 12
3 MATERIALS AND METHODS 15
3.1 Description of the study area 15
3.1.1 Location 15
3.1.2 Topography 16
3.1.3 Climate 16
3.1.4 Temperature 16

3.1.5 Rainfall 17
3.1.6 Evaporation 18
3.1.7 Land use and land cover 19
3.1.8 Soil type 22
3.1.9 Geology 23
3.1.10 Socio Economic aspect of the sub basin 24
3.1.11 Administrative structure of the sub basin 24
3.2 Hydrological Model Selection Criteria 24
3.2.1 Reasons for selecting SWAT model 24
3.2.2 Description of SWAT Model 25
3.2.3 Surface runoff 27
3.2.4 Potential Evapotranspiration 28
3.2.5 Ground water flow 28
3.2.6 Flow routing phase 29
3.3 Methodology 30
3.3.1 Data acquisitions 31
3.3.2 Image processing 31
3.4 Land use and land cover mapping 33
3.4.1 Land use land cover classes 33
3.4.2 Image classification 33
3.5 Classification Accuracy Assessment 34
3.5.1 Kappa coefficient 34
3.6 Model input data collection 35
3.6.1 Digital Elevation Model 35
3.6.2 Meteorological data 35
3.7 Model input data analysis 37
3.7.1 Filling missing data 37
3.7.2 Areal rainfall determination 38
3.7.3 Homogeneity test 39
3.7.4 Consistency 40
3.8 Inverse Distance methods (IDM) 41
3.9 Bias correction of precipitation 42

3.10 Bias correction of Temperature 42
3.11 Trend Analysis of Metrological data 43
3.11.1 Maximum and minimum temperature analysis 43
3.11.2 Precipitation Analysis 43
3.11.3 Hydrological Data 44
3.11.4 Sub-basin and seasonal rain fall variation profile 45
3.12 Model Setup 46
3.12.1 Watershed Delineation 46
3.12.2 Hydrologic Response Units Analysis 47
3.12.1 *Weather Generator`* 48
3.12.2 Sensitivity analysis 49
3.13 Model Calibration and Validation 49
3.13.1 Model Performance Evaluation 50
4 RESULT AND DISCUSSION 52
4.1 Accuracy Assessment 52
4.2 Land use Land Cover Change Analysis 55
4.3 Baseline Scenario developed for Anger station 58
4.3.1 Minimum temperature 58
4.3.2 Maximum Temperature 59
4.3.3 Precipitation 59
4.4 Sub basin Climate change analysis 60
4.5 Annual average and monthly variability of Precipitation 62
4.6 Annual average and monthly variability of minimum temperature 64
4.7 Annual average and monthly variability of maximum temperature 67
4.8 Dryness indexes (EO/P) Analysis 69
4.9 Stream Flow Modeling 70
4.9.1 Sensitivity Analysis 70
4.9.2 Flow Calibration 71
4.9.3 Uncertainty 72
4.9.4 Model Validation 72
4.10 LULC and climate changes Impact analysis 74
4.10.1 Land use land cover change impact analysis 74

4.10.2 Climate change impact analysis 75
4.10.3 The sub-basin reaches annual surface run off variability 76
5 CONCLUSION AND RECOMMENDATION 78
5.1 CONCLUSION 78
5.2 RECOMMENDATION 79
References 80
Appendix: A 86
Appendix _B value of constant a and b for each station 87
Appdeix_C Trend analysis of Tmax and Tmin for each station 88
Appendix _ F Base line Tmax Scenario developed for all station 93
Appendix G Base line PCP Scenario developed for all station 94
Appendix –H observed stream flow for calibration and validation (1990-2005) 97

List of figures

Figure 3-1: Major river basin in Ethiopia and location map of Anger sub basin 15
Figure 3-2: Maximum Temperature in Anger Sub Basin 16
Figure 3-2: Minimum Temperature in Anger Sub Basin 17
Figure 3-3: Rainfall distribution of Anger Sub Basin 17
Figure 3-4: monthly average rainfall, maximum and minimum Temperature of sub basin 18
Figure 3-5: Potential Evapotranspiration of Anger Sub Basin (Atlas of the Blue Nile Basin) 19
Figure 3-6: Anger Land use Land cover during 1986 (GLCF wave site) 20
Figure 3-7: Anger Land Use Land cover during 2000 (GLCF Wave site) 21
Figure 3-8: Anger Land use Land Cover during 2010 (GLCF Wave site) 21
Figure 3-9: Map of the soil types of Anger Sub Basin (Atlas of the Blue Nile Basin) 23
Figure 3-10: Geology of Anger Sub Basin (Atlas of the Blue Nile Basin) 23
Figure 3-11: Population Density of woredas in Anger Sub Basin (Atlas of the Blue Nile Basin)24
Figure 3-12: Land phase of hydrological cycle 26
Figure 3-13: Work flow of the study 30
Figure: A. 3-14: “False color" composite satellite Image of sub basin during 1986 32
Figure 3-15: Digital Elevation Model of Anger Sub Basin (MOWIE) 35
Figure 3-16: Location of Meteorological stations in around the Anger sub Basin (NMAE) 36
Figure 3-17Thiessen polygon for selected rainfall stations 39
Figure 3-18: Homogeneity test analysis for all Meteorological stations 40
Figure 3-19: Double mass curve of all station 41
Figure3-20: Homogeneity test of flow data 44
Figure 3-21: Comparison of Seasonal Rainfall Variation in the major stations 45
Figure 3-22: Seasonal Rainfall Variations for the Study Area 46
Figure3-23: Sub Basin Map of Anger Sub Basin 46
Figure 4-1 LULC Area in percentage 55
Figure 4-2 LULC Area change in percentage 55
Figure 4-3 LULC classification during 1986 (GLCF wave site) 56
Figure 4-4 LULC classification during 2000 (GLCF wave site) 57
Figure 4-5 LULC classification during 2010(GLCF wave site) 57
Figure 4-6 observed & Downscaled monthly mean Tmin for the baseline 58
Figure 4-7 Variance of Observed & Downscaled Tmin for the Baseline period 58
Figure 4-8 Observed & downscaled monthly mean Tmax for the baseline period 59
Figure 4-9 Variance of Observed & downscaled Tmax for baseline period 59
Figure 4-10 Mean monthly Observed & downscaled precipitation for the baseline period 60
Figure 4-11 Variance of Observed & Downscaled Precipitation for the baseline period 60
Figure 4-12 Change in mean monthly precipitation of sub basin 61
Figure 4-13 change in mean monthly Tmin of sub basin 61
Figure 4-14 Change in mean monthly Tmax of sub basin 61
Figure 4-15 change in mean monthly Pcp at Anger 62

Figure 4-16 change in mean monthly Pcp at G_Ayana 62
Figure 4-17 Change in mean monthly Pcp at Nekemte 63
Figure 4-18 change in mean monthly Pcp at Shanbo 63
Figure 4-19 change in mean monthly Pcp at Alibo 64
Figure 4-20 change in mean monthly Tmin at Anger 64
Figure 4-21 change in mean monthly Tmin at G_Ayana 65
Figure 4-22 change in monthly Tmin at Nekemte 65
Figure 4-23 change in mean monthly Tmin at Shanbo 66
Figure 4-24 change in mean monthly Tmin at Alibo 66
Figure 4-25 change in mean monthly Tmax at Anger 67
Figure 4-26 change in mean monthly Tmax at G_Ayana 67
Figure 4-27change in mean monthly at Nekemte 68
Figure 4-28change in mean monthly Tmax at Shanbo 68
Figure 4-29change in mean monthly Tmax at Alibo 69
Figure 4-30 sub basin variability of dryness index 69
Figure 4-31monthly variability of dryness index 70
Figure 4-32: calibration of stream flow from (1990-1999). 71
Figure 4-33: validation of stream flow from (2000-2005) 72
Figure 4-34 Fitted line between observed and simulated stream flow for calibration. 74
Figure 4-35: Fitted Line Between observed and simulated stream flow for validation 74
Figure 4-36 seasonal surface runoff change due to LULC change 75
Figure 4-37seasonal water Yld change due to LULC change 75
Figure 4-38seasonal surface runoff change due to climate change 76
Figure 4-39 seasonal water Yld change due to climate change 76
Figure 4-40: different reaches of Anger sub basin 77

List of tables

Table 2-1: Description of three selected semi-distributed hydrological models 12
Table 3-1: Land use land cover of Anger sub basin 19
Table 3-2: LULC classification of Anger sub basin during 1986..... 20
Table 3-3: LULC classification of Anger sub basin during 2000..... 21
Table 3-4: LULC classification of Anger sub basin during 2010..... 22
Table 3-5: Soil types of Anger sub basin with their symbols and areal coverage 22
Table 3-6: The acquisition dates, sensor, path row, resolution and producers of the image 31
Table 3-7 Kappa statics ranges 34
Table 3-8: Location of meteorological stations in and around the Anger sub basin (NMAE)..... 36
Table 3-9: Areal rainfall interpolated using Thiessen polygon method for sub basin..... 39
Table 3-10: Mean Monthly Rainfall of all stations in (mm)..... 45
Table 3-11: Slope class of Anger sub basin and Area coverage in percent..... 47
Table 4-1 confusion matrix for the classification of 1986..... 53
Table 4-2 confusion matrix for the classification of 2000..... 54
Table 4-3 confusion matrix for classification of 2010..... 54
Table 4-4 LULC Area change in percentage 55
Table 4-5 LULC Area during 1986 56
Table 4-6 LULC Area during 2000 56
Table 4-7 LULC Area during 2010 57
Table 4-8: Sensitive parameters and their rank with t-stat and p-value for stream flow...... 70
Table 4-10: Average monthly stream flow for calibration and validation. 73

List of Abbreviations

CC: - climate change

DEM:-digital elevation model

ETM+:-Enhanced Thematic Mapper Plus

ENS:-Nash-Suttclife model efficiency coefficient

ETO:-Calculator

FAO:-Food and Agricultural origination of united state

GIS: -Geographical Information System

GWQ:-Ground Water Flow

GLCF:-Global land cover facility

HEC-HMS: -Hydraulic Engineering Centre-Hydrologic Modeling System

HBV: -HydrologisikaBayraansVattenbalans-avediling

HRU:-hydrological response units

IGBP-IHDP:-international Geosphere-Biosphere Program and The International Human Dimension Program

IPCC: -Intergovernmental Panel on climate change

LULCC: - land use land cover change

MWIE: - Ministry of Water, Irrigation and Electricity

NMAE: - national metrological agency of Ethiopia

NRCS:-Natural resources conservation service

ONRS:-Oromia National Regional State

PET:-Potential Evapotranspiration

R^2:-determination coefficients

RS:-Remote sensing

SWAT:-Soil and Water Assessment Tool

SCS:-soil conservation service

SCE-UA:-Shuffled Complex Evolution Algorithm

S1_S7:- Scenario one to Scenario seven

TM: - thematic mapper

USDA-ARS: -United States Department of Agriculture-Agricultural Research Service

USGS:-United States Geological Survey

WGS:-World Geodetic System

WXGEN: - weather generator

1 INTRODUCTION

1.1 Background

Water resources are currently under severe pressure because of impacts of climate change and human activities, which include land-use change, increasing population growth, and economic development (IPCC, 2013). Assessing water resources becomes a complex task that must consider many aspects, of which climate and land-use change and variability are identified as key factors (Elfert. S., and Bormann.H., 2010).Whereas land-use change can cause changes in components in a basin, such as evapotranspiration, surface runoff and groundwater. Thus, separating the effects of climate and land-use changes on runoff is important to produce accurate predictions of runoff simulation and to provide useful information to land-use planning and water resources management (Pechlivanidis I.G., 2011).

Distributed hydro logical models, which use input parameters directly representing land surface characteristics, have been applied to assess the impact of LULC(land use/Land cover) and climate changes on runoff in water resource management areas (Yang, 2008). The effects of LULC and climate changes on runoff are considerably more sensitive, and the drying climate will make the degraded environment and serious water crises even worse (Leng, 2016).In addition, regional impacts of climate and land-use changes on runoff vary from place to place and need to be investigated on a local scale (Wang, 2014).

Some researchers said that climate change had stronger impacts than land-use change on runoff simulation. And others, concluded that land-use change was the main driving factors for the decrease or increase in runoff simulation. In Abby basin, most studies have focused on the impact of climate changes on runoff simulation without considering land-use change as well as Others have only addressed the changes in runoff simulation with impact of land-use and land-cover change. Furthermore, no studies considering both land-use land-cover and climate change have been performed in the Abby basin, therefore this research focus on runoff simulation under the impacts of climate and land use/cover change in Anger sub basin.

Hence, Anger basin runoff simulation under impacts of climate and land use/cover change was particularly important in improving water management efficiency and benefiting various water use needs such as irrigation and small scale hydro power on Anger sub basin and also it might be used for recreation, and environmental protection. Besides the mentioned purposes highly it will be

used for better management and planning of reservoirs. The overall objective of this study is to model runoff volume change of Anger sub-basin under past impact of LULC and future climate change using the SWAT model. The specific objectives are:- (1) to assess the past LULC and future climate change of the sub basin. (2) To calibrate and validate SWAT model for stream flow of study area. (3) To quantify impacts of past LULC and future climate change on runoff volume of sub basin through scenario simulation.

This study provides important information that decision-makers will need in order to assist with water resources management in the Anger sub basin under changing environmental conditions.

1.2 Problem of statement

Water resource play a crucial role in the economic development of the developing countries with water stressed water resource like Ethiopia. The region's explosive population growth and resulting new demands on limited water resources require efficient management of existing water resources and building new facilities to meet the challenge. In water resources management system, it is well known that to combat water shortage issues, maximizing water management efficiency based on runoff simulation was crucial. Runoff simulation is vital importance to flood mitigation and water resources management and planning. While short-term simulation such as hourly or daily simulation is crucial for flood warning and defense, long-term simulation based on monthly, seasonal or annual time scales is very useful in reservoir operations and irrigation management decisions such as scheduling releases, allocating water to downstream users, drought mitigation and managing river treaties or implementing compact compliance.

In Abbay basin, most studies have been focused on the impact of climate change on runoff simulation without considering LULC change and also other researchers only addressed impact LULC change on runoff simulation. Furthermore, no studies considering both land-use/cover and climate change have been performed in the Abbay basin, therefore this research focused on runoff simulation under the impacts of past land use/cover and future climate change in Anger sub basin. Hence, the sub basin runoff simulation under impacts of land use/cover and climate change were particularly important in improving water management efficiency and benefit various water uses such as irrigation and small scale hydro power on the sub basin and also it might be used for recreation, and environmental protection.

Besides the mentioned purposes highly it will be used for better management of sub basin and planning of reservoirs under changed environmental conditions.

1.3 Objectives of the study

1.3.1 General objective

- The objective of this research is to model runoff volume change of Anger sub-basin under the past impact of LULC and future climate change using the SWAT model.

1.3.2 Specific objectives:

- To assess the past LULC and future climate change of the sub-basin.
- To calibrate and validate SWAT model for stream flow of the study area.
- To quantify the impact of past LULC and future climate change on runoff volume change of the sub-basin through scenario simulation.

1.4 Research Questions

To address the above objectives, the following research questions were designed.

- What the trends of past LULC and future climate change of the sub basin looks like?
- How well can the SWAT model simulate stream flow in the sub basin?
- How the effect of the past LULC and future climate change does affect run-off of the sub basin?

1.5 Significance of the Study

The past LULC and future climate change have a significant impact on natural resources, socioeconomic and environmental system. However, to assess the effect of past LULC and future climate change on runoff simulation, it is important to have an understanding of the past LULC and future climate change patterns and the hydrological processes of the sub basin. Understanding the types and impacts of past LULC and future climate change is an essential indicator for resource base analysis and development of effective and appropriate response strategies for sustainable management of natural resources in the country in general and at the study area in particular. Moreover, the study presents a method to quantify past LULC and future climate change and their impact on the hydrological regime. This has been achieved through a method that combines the

hydrological model (SWAT) to simulate the hydrological processes, ArcGIS and remote sensing techniques to analyze the land use and land cover change.

1.6 Software and Materials used

To meet the objectives of this study, various software and materials were used. Among them:-

- ArcGIS was used to process preliminary data, extract, composite (layer stake), mosaic satellite image and image classification.
- SWAT model embedded in ArcGIS was used to simulate runoff of the sub basin.
- XLSTAT was used to analysis hydro meteorological data
- Rainbow was used to test stream flow homogeneity
- Swatdatabse was used to prepare the SWAT input table and weather generator
- Excel was used to analysis SWAT output

1.7 Organization of the Thesis

For simplification purpose, this research paper is organized into five chapter: Under chapter one:- an introduction, statement of the problem, the objective of the study, the research question and the significance of the study were well presented. Under chapter two:- review of related literature, the definition and concepts of LULC and climate change, LULC and climate change in Ethiopia, the application of remote sensing on LULC change, an introduction to the SWAT model, and application of the SWAT model in Ethiopia were presented. Under chapter three:- description of the study area, image processing and classification, Hydrological model selection criteria, Collection of input data and data analysis, model setup, model performance evaluation were well presented.

Under chapter four:- result and discussion, including LULC changes analysis, LULC maps, accuracy assessment, and LULC change statistics and runoff modeling include sensitivity analysis, calibration, and validation of the model and lastly evaluation of runoff due to LULC and climate change.

Finally; under chapter five: - conclusions and recommendations of the study were presented.

2 LITERATURE REVIEW

2.1 Introduction

In this literature review part, important points like definition and theory of LULC and climate change, empirical review of LULC and climate change in Ethiopian context, use of remote sensing on LULC changes, the overview of hydrological models and, the SWAT model in Ethiopia. Mostly, the assessments concentrated on the review of related literature by evaluating the scientific works which associated with the subject of this study.

2.1.1 Land use land cover change

The international Geosphere-Biosphere Program and The International Human Dimension Program (IGBP-IHDP, 1999), land cover states to the physical and biological cover over the surface of earth, including distribution of vegetation, water, bare soil and artificial structures. Land use states to the planned use or management of the land cover type by human beings such as agriculture, forestry and building construction. Land use land cover change (LUCC) is generally grouped in to two broad categories (Meyer and Truner, 1994): alteration and variation. Alteration states to a change from one cover or category to another (e.g. from forest to grassland). Variation, on the other hand, characterize a change within one land use or land cover category (e.g. from rain fed cultivated area to irrigated cultivated area) due to changes in its physical or purposeful qualities. These changes in land use land covers systems have vital environmental consequences through their impacts on soil and water, biodiversity, and microclimate (Lambin, 2003).

Land cover changes have been influenced by both the increase and decrease of a given population (Lambin, 2003). In most developing countries like Ethiopia population growth has been a leading cause of land use land cover change than other forces (Sage, 1994). These is an important statistical relationship between population growth and land cover alteration in most of African, Asian, and Latin American countries (Meyer and Turner, 1994). Due to the increase demands of food production, agricultural lands are increasing at the expenditure of natural vegetation and grassland (Lambin, 2003).Land use and land cover features have numerous influences with hydrological cycle. The land use and land cover type can disturb both the infiltration and runoff amount by the following the falling of precipitation (Houghton, (1995). Both surface runoff and ground water flow are meaningfully pretentious by types of land cover (Abebe, 2005).

Surface runoff and ground water flow are the two constituents of stream flow. Surface runoff is typically subsidized directly from precipitation, whereas ground water flow is subsidized from infiltrated water. However, the source of stream flow is typically from surface runoff during the rainy months the stream flows from the ground water. Rise of crop lands and reduction of forest, results rise of stream flow because of the crop soil moisture demand. Crops need less soil moisture than forest; therefore, the rainfall fulfills the storage of soil moisture in agricultural lands more rapidly than in forests there by generating more runoff when the area under agricultural land is widespread. Hence, this indicates rise in stream flow. In addition, deforestation also has its own impact on hydrological processes, leading to declines in rainfall, and more rapid runoff after precipitation (Legesse, 2003). Therefore, such changes of land use land cover may have impacts on stream flow during wet and dry months, and on the component of stream flow (surface runoff and ground water flow) and assessing such impacts is the core of this study.

Generally, knowing of impacts of land use and land cover change on the natural resources like water resources depends on understanding of the past land use practices, current land use land cover patterns, and projection of future land use land cover, as affected by population size and distribution, economic development, technology, and other factors. The land use and land cover change assessment is an important step in planning sustainable land management that can help to minimize agro-biodiversity losses and land degradation, especially in developing countries like Ethiopia (Hadgu, 2008).

2.1.2 Land use land cover changes studies in Ethiopia

In Ethiopia, the land used to grow crops, trees, animals for food, as building sites for houses and roads, or for recreational purposes. Most of the land in the country is being used by smallholders who farm for subsistence. With the rapid population growth and in the absence of agricultural intensification, smallholders require more land to grow crops and earn a living; it results in deforestation and land use conversions from other types of land use cover to cropland. The researches that have been conducted in different parts of Ethiopia have shown that there were considerable land use land cover changes in the country. Most of these studies indicate that croplands have expanded at the expanse of natural vegetation including forests and scrublands; for example Minichil, (2016); Haile (2011): Gashaw (2017): Sileshi (2016) and Getahun (2015) in Blue Nile basin of Ethiopia.

In their study, they reported the decline of natural forests and grazing lands due to conversions to cultivated lands. In Didessa basin much of the original forest have already been converted to agricultural lands. These changes would aggravate serious problems related to water scarcity in dry periods and hill slope erosion during wet periods (Minichil.J, 2016). The changes of land use land cover from (1986–2001) in Upper Gilgel Abbay catchment, Blue Nile basin –Ethiopia shows an increase in agricultural land by 67.34% while it decreased in forest area by 50.9%. The expansion of agricultural land from (1986–2001) is larger than in the previous time (Haile TA, 2011). And also, the changes of Land Use/Cover in Gumara Watershed, Upper Blue Nile Basin, Ethiopia shows the expansion of cultivated land by 98.7% and built-up area and the withdrawing of forest area, shrub land and grassland by 75.19% were further continued in 2030 and 2045 (Gashaw G. and Mamaru A, 2015). Lastly, the change of Land-Use from 2009 to 2025 in the Upper Blue Nile Basin shows the agricultural land will continue to expand from 69.5% in 2009 to 77.5% in 2025 in the catchment albeit at a declining rate when compared with the period from 1986 to 2009 (Seleshi G. Yalew & A., 2016). The changes of Land Use-Cover from 1986 to 2003 in Melka Kuntrie Sub basin, Upper Awash River Basin-Ethiopia shows an expansion of cultivated land by 63% and reduction in forest, grass, or shrub land by 44% in sub basin. Land use in 2003, which was mostly converted to agriculture land from forest, grass, or shrub land than land use during 1986 (Getahun YS, 2015).

The changes of land use land cover that occurred from 1971/71 to 2000 in Yerer Mountain and its surrounding results an expansion of cultivated land by 25% in 1971/72 to 56.4% in 2000. The increase in cultivated land in three decades was 125%, which was mainly at the expense of the grasslands. At the same time, grasslands decreased from 65.35% in 1971/72 to 32.7% in 2000. (Gebrehiwet, 2004). Hadgu (2008) identified that decrease of natural vegetation and expansion of agricultural land over the period of 41 years in Tigray, northern part of Ethiopia. He concluded that population pressure was an important deriver for expansion and intensification of agricultural land in recent periods. Garedew, (2010) in the semiarid areas of the central Rift valley of Ethiopia, during the period of 1973-2000 cropland coverage has increased and woodland cover lost. Similarly, Feoli, et al, (2002) reported the expansion of evergreen vegetation with increase of population. According to many literatures, population growth has a paramount impact on the environment. For instance, population pressure has been found to have negative effect on Riverine tree in Chemoga watershed (Bewket W. a., 2005), and natural forest cover in Dembecha Woreda

north-western Ethiopia (Zeleke, 2001). And also, Pender et al, (2001) exhibited that the population growth has significant effect on land degradation, poverty and food insecurity in the northern Ethiopia highlands. However, most of the empirical evidences indicated that land use land cover changes and socioeconomic dynamics have a strong relationship (i.e. as population increases the need for cultivated land, grazing land, fuel wood; settlement area also increases to meet the growing demand for food and energy, and livestock population). Thus, population pressure, lack of awareness and weak of management are considered as the major causes for the deforestation and degradation of natural resources in Ethiopia.

2.1.3 Land use land cover changes in the study area

Anger was one of the main tributaries of the Didessa basin which is the sub-basin of the Blue Nile basin. Most of the studies related to the Blue Nile basin focused on the northern part. But, Anger sub-basin is the southern part of the basin which is the less studied area. The research conducted on southern part mainly focused on Didessa basin and took Anger sub-basin as a similar area. The study carried out by Minichil.J, (2016) shows much of the original forest in the Dedissa basin has already been converted to agricultural lands due to population growth and economic development. These changes would aggravate already serious problems related to water scarcity in dry periods and hill-slope erosion during wet periods in the sub-basin.

2.2 Climate change

Climate is the average weather or the regular variations in weather in a region over a period of years. It defines typical weather conditions for a given area based on long-term averages, usually decades or longer. For example, it could show up a change in climate normal (expected average values for temperature and precipitation) (IPCC, 2007).Climate change states to a change of climate that is recognized directly or indirectly to human activity that changes the composition of the global atmosphere and that is in addition to natural climate variability observed over comparable time periods, whether due to natural variability or as a result of human activity (IPCC, 2007). Climate change is facing the entire world nowadays. It is now widely received that climate change is by now happening and further change is unavoidable; the global average combined land and ocean surface temperature data calculated shows a warming of 0.85oc over the period 1880 to 2012 (IPCC, 2014). This is more strongly after 1970; many studies discovery specifies that most of the increase in average global surface temperature over the last 50 years is attributable by human

activities (Endalkachew, G., 2012). It was estimated that, change and sea level is expected to rise at rate of about 1.7 mm/yr. as the ocean expands as heat is gradually diffused downwards in the ocean (Endalkachew, G., 2012). The IPCC also notes that observations over the past century shows, changes were occurring in the amount, intensity, frequency and types of precipitation globally (IPCC, 2007).

The IPCC was established in 1988 by the World Meteorological Organization and the United Nations Environment Program, and its role is to "assess on a comprehensive, objective, open and transparent basis the scientific, technical and socio-economic information relevant to understanding the scientific basis of risk of human-induced climate change, its potential impacts and options for adaptation and mitigation". Among the different assessment that were carried out by the IPCC, the most recent which published in 2007, states the projected global surface warming lies within the range 0.6 to 4.0oc, whereas the projected see level rise lies within the range 18 to 59 cm at the end of next century (IPCC, 2007). The major effect of climate change is increasing temperatures which will in turn increase Evapotranspiration and thus crop water demand (FAO and MoWIE , 2013).

2.2.1 Climate Change in Ethiopia

For the past four decades, the average annual temperature in Ethiopia has been increasing by 0.37oC every ten years, which is slightly lower than the average global temperature rising (Emerta, A., 2013). According to Emerta, the greater part of the temperature rise was observed during the second half of the 1990's and temperature rise is more pronounced in the dry and hot spots of the country, which are located in the northern, northeastern, and eastern parts of the country. The lowland areas are the most affected, as these areas are largely dry and exposed to flooding during extreme precipitation in the highlands.

Future temperature projections of the IPCC mid-range scenario show that the mean annual temperature will increase in the range of 0.9 to 1.1ºC by 2030, in the range of 1.7 to 2.1ºC by 2050, and in the range of 2.7 to 3.4ºC by 2080 in Ethiopia compared to the 1961 to 1990 (Emerta, A., 2013). However the country has both dry and wet periods over the past four decades, precipitation has a general decreasing trend since the 1990s (Abayneh, A., 2011). The decrease in precipitation has multiple effects on water availability for irrigation and other farming uses, especially in the north, northeastern, and eastern lowlands of the country. The average change in rainfall is projected to be in the range of 1.4 to 4.5 percent, 3.1 to 8.4 percent, and 5.1 to 13.8 percent over 20, 30, and

50 years, respectively, compared to the 1961 to 1990 usual. According to Abayneh, the overall trend in the entire country is more or less constant. Related with rainfall and temperature change and variability, there was a recurrent draught and flood events in the country. There was also observation of water level rise and dry up of lakes in some parts of the country depending on the general trend of the temperature and rainfall pattern of the regions.

2.2.2 Climate Change in the Study Area

Some studies conducted in Abbay and Awash basins show that these basins are climate sensitive. The catchments under consideration are found in the Anger sub basin; therefore climate change should be considered to evaluate the present and future condition of the runoff of this sub basin.

2.3 Application of remote sensing on LULCC

Remote sensing (RS) is defined as the science of obtaining information about an object, area, phenomenon through the analysis of data acquiring by a device that is not in contact with the object, area, or phenomenon under investigation (Bawahidi, 2005). It provides a large amount of data about the earth surface for detailed analysis and change detection with the help of sensors. Most of data inputs to the hydrological (SWAT) model is directly or indirectly extracted from remotely sensed data. Some of the important data used in hydrological modeling that are obtained from remote sensing include digital elevation model (DEM), land cover maps. Some of the application of remote sensing technology in mapping and studying of the land use and land cover changes are; map and classify the land use and land cover, assess the spatial arrangement of land use and land cover, allow analysis of time-series images used to analyze landscape history, report and analyze result of inventories including inputs to Geographical Information System (GIS), provide a basis for model building.

Land use and land cover is changing rapidly in most parts of world. In this situation, accurate, meaningful and availability of data is highly essential for planning and decision making. Remote sensing is particularly attractive for the land cover data among the different sources. Stefanov et al (2001) reported that in 1970's satellite remote sensing techniques have started to be used as a modern tool to detect and monitor land cover change at various scales with useful results. William et al (1991) showed that the information of land use and land cover change which is extracted from remotely sensed data is vital for updating land cover maps and the management of natural resources and monitoring phenomena on the surface. The importance of land cover mapping is to show the land cover changes in the watershed area and to divide the land use and land cover in

different classes of land use and land cover. For this purpose, remotely sensed imagery play a great role to obtaining information on both temporal trends and spatial distribution for projecting land cover changes but also to support changes impact assessment (Atasoy, 2006). To monitor the rapid changes of land cover, to classify the types of land cover, and to obtain timely land cover information, multi temporal remotely sensed images are considered effective data sources.

2.1 Hydrological Models

Hydrological models are mathematical descriptions of components of hydrological cycle. They have been developed for many different reasons and therefore have many different forms. However, hydrological models are in general designed to meet one of the two primary objectives. The one objective of the watershed hydrologic modeling is to get a better understanding of the hydrologic processes in watershed and of how changes in the watershed may these phenomena. The other objective is for studying potential impacts of changes in land use and land cover or climate. On the basis of process description, the hydrological models can be classified in to three main categories (Cunderlik J. , 2003).

- **Lumped models.** Parameters of lumped hydrologic models do not vary spatially within the basin and thus, basin response is evaluated only at outlet, without explicitly accounting for response of individual sub-basins. The parameters often do not represent physical features of hydrologic processes and usually involve certain degree of empiricism. These models are not usually applicable to event-scale processes. If the interest is primarily in the discharge prediction only, then these models can provide just as good simulations as complex physical based models.
- **Distributed models.** Parameters of distributed models are fully allowed to vary in space at the resolution usually chosen by the user. Distributed modeling approach attempts to incorporate data concerning the spatial distribution of parameter variations together with computational algorithms to evaluate the influence of this distribution on simulated precipitation-runoff behavior. Distributed models generally require large amount of (often unavailable) data. However, the governing physical processes are modeled in detail, and if properly applied, they can provide the highest degree of accuracy.
- **Semi-distributed models.** Parameters of semi-distributed (simplified distributed) models are partially allowed to vary in space by dividing the basin in to a number of a smaller sub-basins. The main advantage of these models is that their structure is more physically - based than the

structure of lumped models, and they are less demanding on input data than fully distributed models. SWAT (Arnold J. G., 1993), HEC-HMS (U. S. ACE, 2001), HBV (Bergström, 1995), are considered as semi-distributed models.

Hydrologic models can be further divided in to event-driven models, continuous processes models, or models capable of simulating both short-term and continuous events. Event –driven models are designed to simulate individual precipitation-runoff events. Their emphasis is placed on infiltration and surface runoff. Typically, event models have no provision for moisture recovery between storm events and, therefore, are not suited for the simulation of dry –weather flows. On the other hand, continuous –process models simulate instead a longer period, predicting watershed response both during and between precipitation events. They are suited for simulation of daily, monthly or seasonal stream flow, usually for long-term runoff volume forecasting and for estimating of water yield (Cunderlik J. , 2003).

Generally for this study, semi-distributed models are selected because of their structure is more physically- based than the structure of lumped, and they are less demanding on input data than fully distributed models.

Therefore, three selected semi-distributed models were reviewed (table: 2.1).

Description	SWAT	HEC-HMS	HBV
Model type	Semi-distributed physically-based long-term	Semi-distributed physically-based	Semi-distributed conceptual model
Model objective	Predict the impact of land management practices on water and sediment	Simulate the rainfall runoff process of watershed	Simulate rainfall runoff process and floods
Temporal scale	Day+	Day-	Day-
Spatial scale	Medium+	Flexible	Flexible
Process modeled	Continuous	Continuous and event	Continuous and event
Cost	Public domain	Public domain	Public domain

Table 2-1: Description of three selected semi-distributed hydrological models

2.1.1 SWAT Model

2.1.1.1 Introduction to SWAT Model

The SWAT (Soil and Water Assessment Tool) watershed model is one of the most recent models developed at the USDA-ARS (Arnold J. G., 1998) during the early 1970's. SWAT model is semi-

distributed physical-based simulation model and can predict the impacts of land use change and management practices on hydrological regimes in watersheds with varying soils, land use and management conditions over the long periods and primarily as a strategic planning tool (Neitsch, 2005).The interface of SWAT model is compatible with Arc GIS that can integrate numerous available geospatial data to accurately represent the characteristics of watershed. In SWAT model, the impacts of spatial heterogeneity in topography, land use, soil and other watershed characteristics on hydrology are described in subdivisions. There are two scale levels of subdivision ; the first is that the watershed is divided into a number of sub- watersheds based upon drainage areas of the attributes, and the other one is that each sub-watershed is further divided in to a number of hydrological response units (HRUs) based on land use and land cover, soil and slope characteristics. The SWAT model simulates eight major components: hydrology, weather, sedimentation, soil temperature, crop growth, nutrients, pesticides, and agricultural management (Neitsch, 2005). Major hydrologic processes that can be simulated by the model include Evapotranspiration, surface runoff, infiltration, percolation, shallow aquifer and deep aquifer flow, and channel routing (Arnold J. G., 1998). Stream flow is determined by its components (surface runoff and ground water flow from shallow aquifer).

2.1.1.2 SWAT Model Application in Ethiopia

The SWAT model application was calibrated and validated in some parts of Ethiopia, frequently in Blue Nile Basin. Through modeling of Didessa Watershed (in Abbay basin) (Minichil.J, 2016) indicated that stream flow and sediment yield simulated with SWAT were reasonable accurate. The same study conducted on similar long term data can be generated from ungauged watershed using the SWAT model and modeling of Lake Tana basin with SWAT also showed that the SWAT model was successfully calibrated and validated (Setegn S. S., 2008). This study reported that the model can produce reliable estimates of stream flow and sediment yield from complex watersheds. Gessese (2008) used the SWAT model performed to predict the Lagedadi Reservoir Sedimentation. According to this study, the SWAT model performed well in predicting sediment yield to Legedadi reservoir. The study further put that the model proved to be useful in capturing the process of stream flow and sediment transport of watersheds of the Lagedadi reservoir. In addition to the above, the SWAT model was tested for prediction of sediment yield in Anjeni gauged watershed by (Setegn S. S., 2008). The study found that the observed values showed a good agreement at Nash-Sutcliff efficiency (ENS) of 80%. In light of this, the study suggested that the

SWAT model can be used for further analysis of different management scenarios that could help different stakeholders to plan and implement appropriate soil and water conservation strategies. The SWAT model showed a good match between measured and simulated flow and sediment yield in Gumara watershed both in calibration and validation periods (Asres and Awulachew, 2010). (Tekle, 2010) Through modeling of Bilate watershed also indicated that SWAT Model was able to simulate stream flow at reasonable accuracy. The literature reviewed and presented above showed that SWAT is capable of simulating hydrological and soil erosion process with reasonable accuracy and can be applied to large and complex watershed.

3 MATERIALS AND METHODS

3.1 Description of the study area

3.1.1 Location

Anger sub-basin is the largest tributary of Didessa basin, Ethiopia. This sub-basin is located in East Wollega Zone of Oromia National Regional State (ONRS) of Ethiopia. The sub-basin area comprises of 15 woredas, namely:- Wayu Tika, Bila Seyo, Sibu Sire, Guto Gida, Sasiga, Gudaya Bila, Bilo Jegonfoy, Abe Dongoro, Horo, Gida Kiremu, Yaso, Limu, Haro, Jarti Jadeja, and Amuru. In terms of geographic coordinate system, the watershed lies between 10.95^{o} and 11.80^{o} North latitudes and 36.70^{o} and 37.40^{o} East longitudes. It originates from the Northwestern side of the watershed and flows into the Northeast direction and forms part of the Didessa basin as shown in (Figure 3-1) below. The total area is estimated to be 7,980 km^2 and accessed by the main asphaltic road from Addis Ababa to Nekemte and gravel roads to Gida Ayana cross the sub-basin. The sub-basin is also accessed by other gravel roads which connect Bure, Gida Ayana, and Nekemte Town.

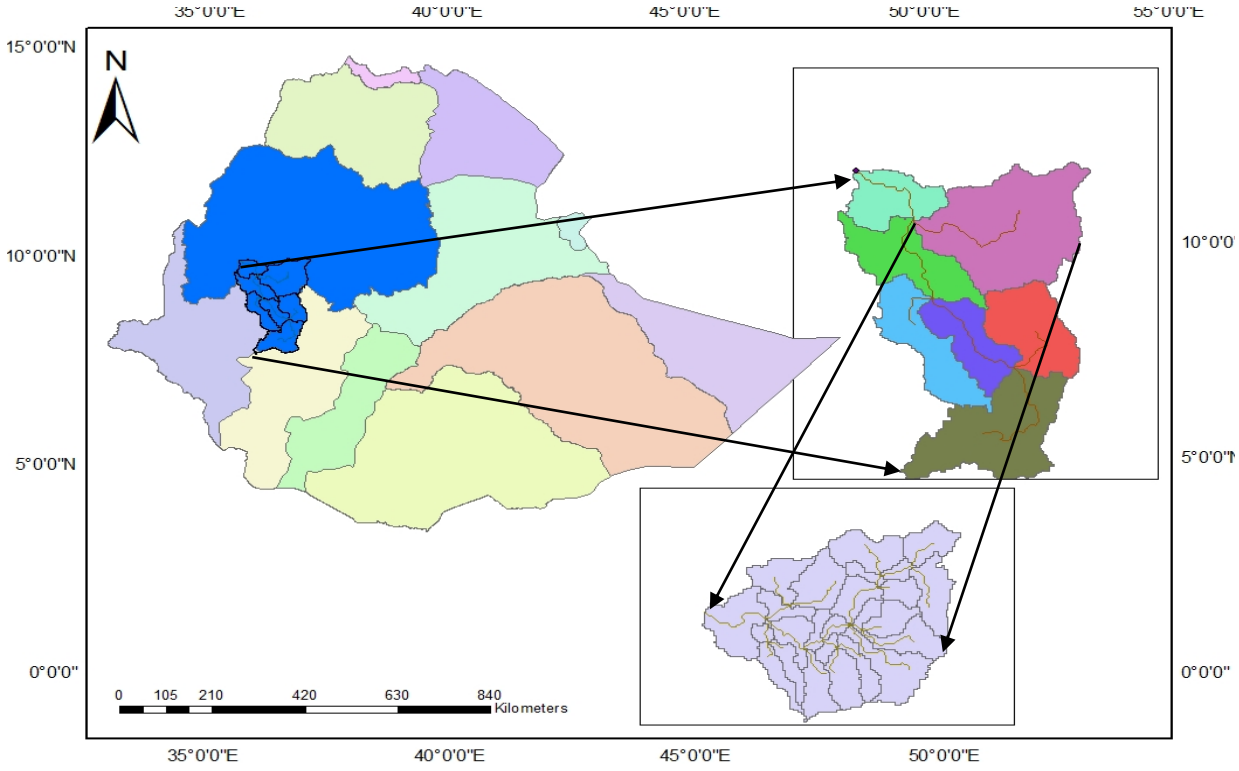

Figure 3-1: Major river basin in Ethiopia and location map of Anger sub basin

3.1.2 Topography

Anger sub basin has an area of 7,980 km^2. The altitude in the sub basin ranges approximately between 868 masl and 3144 masl. The highlands of the sub basin are higher in altitude, greater than 1800 masl up to 3144 masl. The lowlands have lower altitude less than 1200 masl in the western lowlands of the sub basin.

3.1.3 Climate

The climate of Ethiopia can be classified in different ways including the Traditional koppen's, Throthwaite's, Rainfall regimes and also Agro –climatic zone classification systems. The most common used classification system, are traditional and agro-ecological zones (NMSA , 2001). The traditional classification system, this mainly relies on altitude and temperature; accordingly there are five climatic zones namely: -

- Wurch (cold climate at more than 3000 Mts. altitude)
- Dega (temperature like climate - high lands with 2500-3000Mts. altitude)
- WoinaDega (warm at 1500-2500 Mts. Altitude)
- Kola (hot and arid type, less than 1500m in altitude) and
- Berha (hot and hyper-arid type) climate.

The sub basin is characterized by tepid to cool and sub humid mid high lands, and hot to warm sub humid lowlands and the lowlands in the eastern parts of the watershed being hot to warm moist lowlands (Aster D. Y. and Seleshi B. A., 2009).

3.1.4 Temperature

The annual maximum and minimum temperature in the sub basin varies between 22^0C – 30^0C and 11^0C - 15^0C respectively. Temperature is higher in the western lowlands at Anger metrological gauging station with a maximum of 29.33^0C and minimum at Alibo metrological gauging station of 11.34^0C.

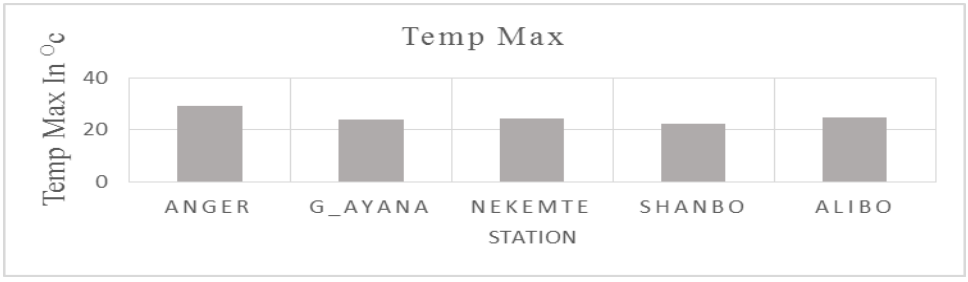

Figure 3-2: Maximum Temperature in Anger Sub Basin

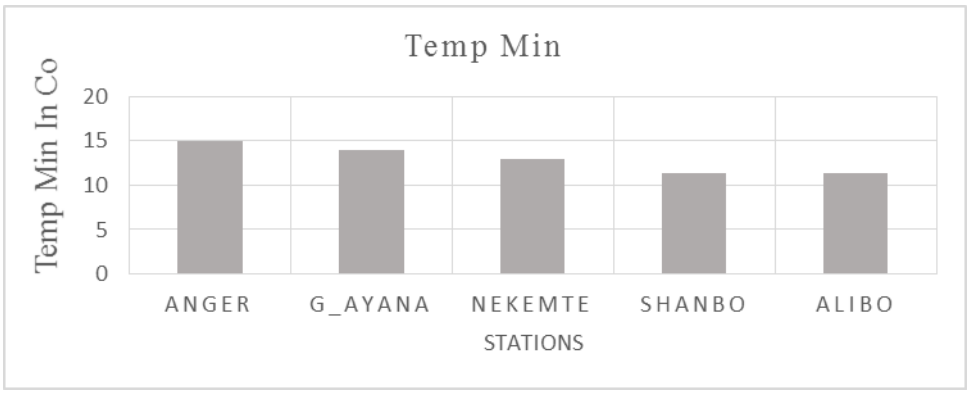

Figure 3-3: Minimum Temperature in Anger Sub Basin

3.1.5 Rainfall

The sub basin has an annual rainfall ranging approximately between 1230 mm and 2000 mm. Lower annual rainfall less than 1600 mm in the major sub basin and higher rain fall greater than 1600 mm in same high lands of sub basin.

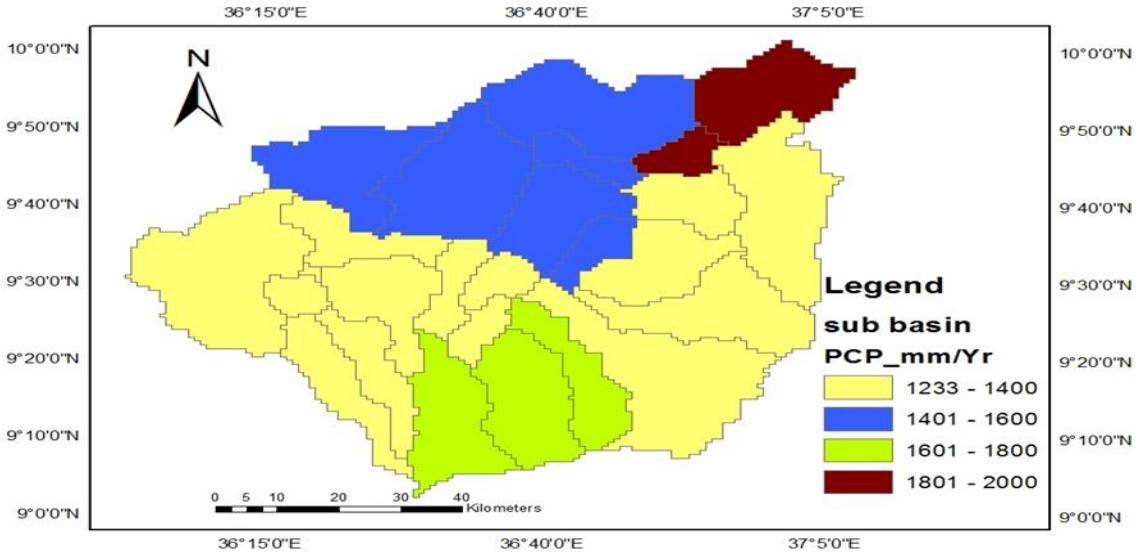

Figure 3-4: Rainfall distribution of Anger Sub Basin

The mean annual rainfall of sub basin ranging from 1817mm at Alibo meteorological gauging station and 1320 mm at Anger gauging stations.so the highest rainfall distribution occurs in the high lands of the sub basin and low distribution around the low lands of the sub basin.

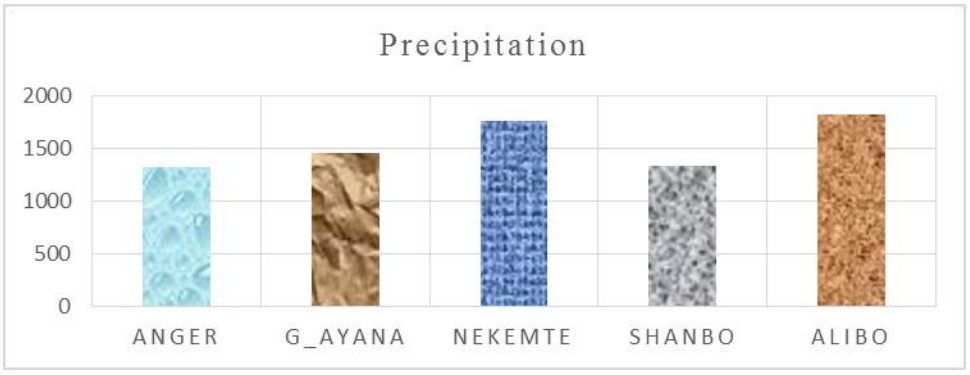

The monthly average rainfall, Max temperature and Min temperature distribution of sub basin were presented for same selected meteorological station on Figure *3-5* below. And for other attached on Appendix A

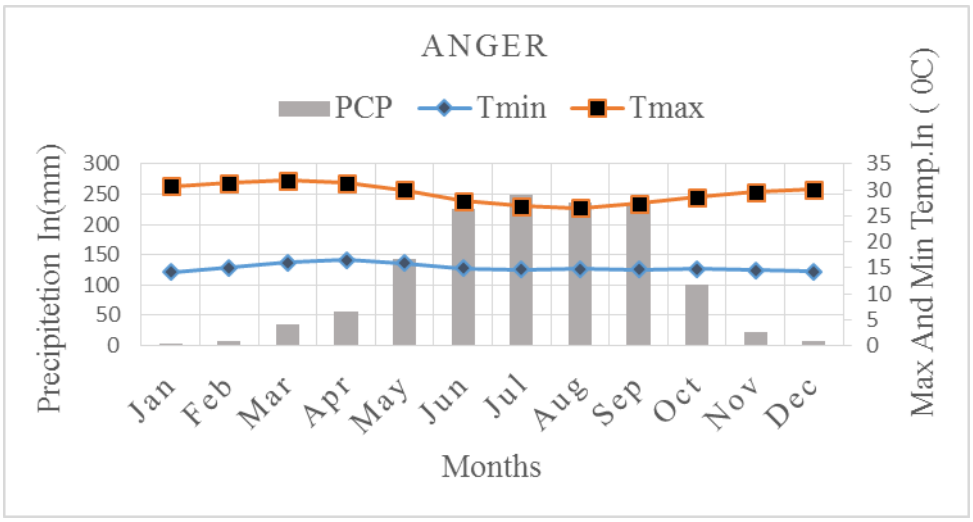

Figure 3-5: monthly average rainfall, maximum and minimum Temperature of sub basin

3.1.6 Evaporation

Potential Evapotranspiration (PET) in the sub basin is generally between 1360 mm and 1925 mm per year. PET is higher greater than 1800 mm/yr., in the lowlands where high temperature is observed. The highlands of the basin show lower PET, less than 1600 mm/yr. (Aster D. Y. and Seleshi B. A., 2009)

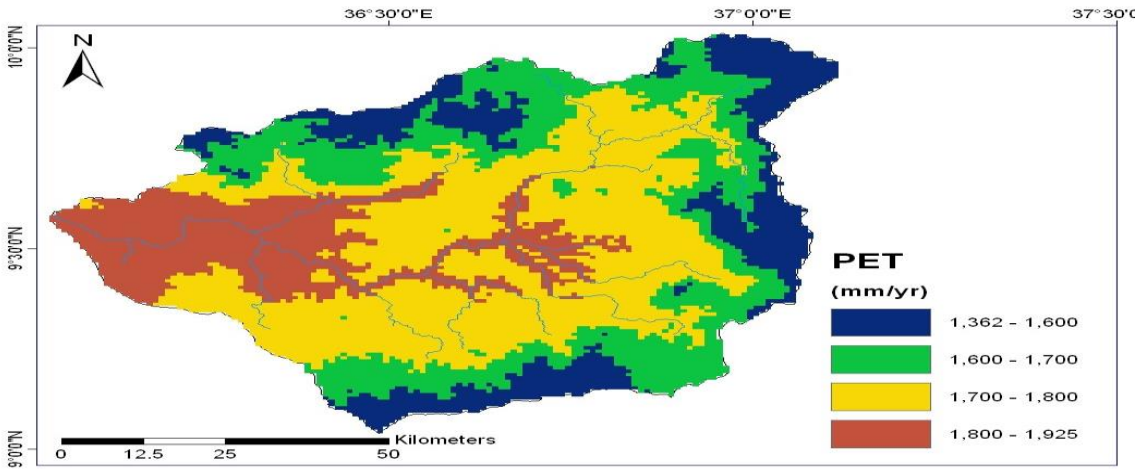

Figure 3-6: Potential Evapotranspiration of Anger Sub Basin (Atlas of the Blue Nile Basin)

3.1.7 Land use and land cover

Land use is a highly influencing factor of hydrological properties of watershed. It is one of the main input data of the SWAT model to describe the hydrological response units (HRUs) of the watersheds. The SWAT model has predefined four letter codes for each land use category (table: 3-1). These codes were used to link or associate the land use map of the study area to SWAT land use databases. Hence, while preparing the lookup-table, the land use types were made compatible with the input needs of the model. The land covers of the sub basin are dominated by cultivated land and forest. Shrub Land was also used in the sub basin, with urban area and water or marsh land is the parts of sub basin.

Land use/ Land cover	Land use according to SWAT database	SWAT code
Cultivated land	Agricultural land close to grown	AGRC
Forest land	Forest mixed	FRST
Shrub and grass land	Forest deciduous	FRSD
Urban and built up area	Residential-Low Density	URLD
Water and marshy land	Water	WATR

Table 3-1: Land use land cover of Anger sub basin

In the sub basin the area covered by different land use land cover in percent during 1986 were 43.2% Agricultural land, 10.3% forest land, 45.8 %s shrub and grass land, 0.4% Built Up area and 0.4%water body. And also, during 2000 were 50.9% Agricultural land, 7.2 % forest land, 41 %shrub and grass land, 0.6 % Built Up area and 0.2%water Body. Lastly, during 2010 were 82.5% Agricultural land, 3.6% forest land, 12.9%shrub and grass land, 0.8% Built Up area and 0.1% water body. So Agricultural land, shrub land and forest were dominate the sub basin during the study period and Built Up area and water body was also the parts of the watershed. For detail information presented tables and figures below.

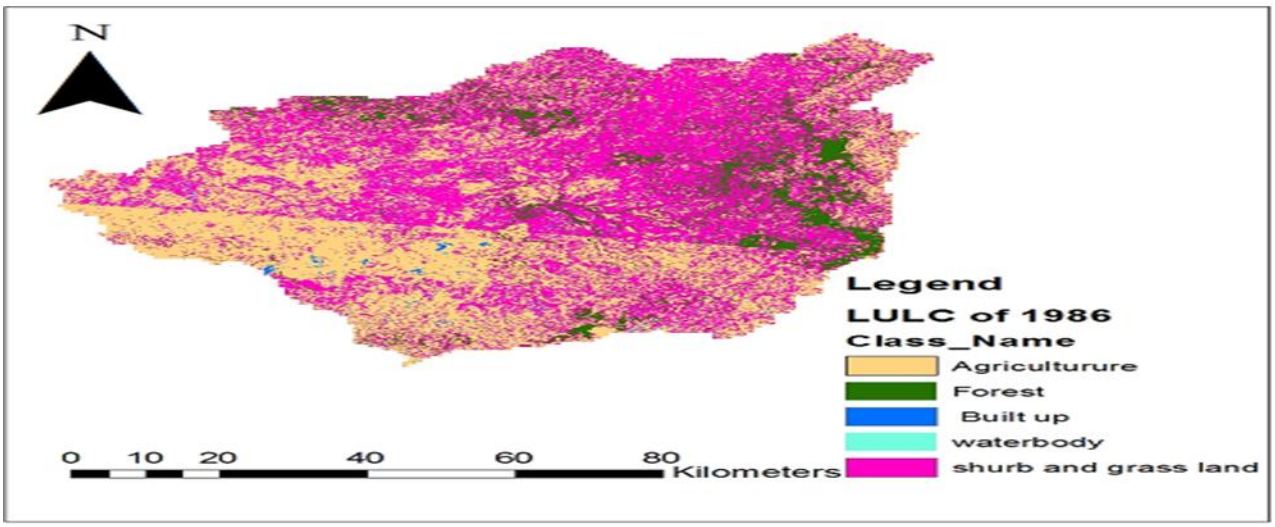

Figure 3-7: Anger Land use Land cover during 1986 (GLCF wave site)

Land use / Land cover type	Land use according to SWAT database	SWAT code	Area	
			Km^2	%
Agricultural land	Agricultural land close to grown	AGRC	3450	43.2
Shrub and Grass land	Forest deciduous	FRSD	819	45.8
Forest	Forest mixed	FRST	3661	10.3
Built Up	Residential-Low Density	URLD	28	0.4
Water body	Water	WATR	31	0.4

Table 3-2: LULC classification of Anger sub basin during 1986

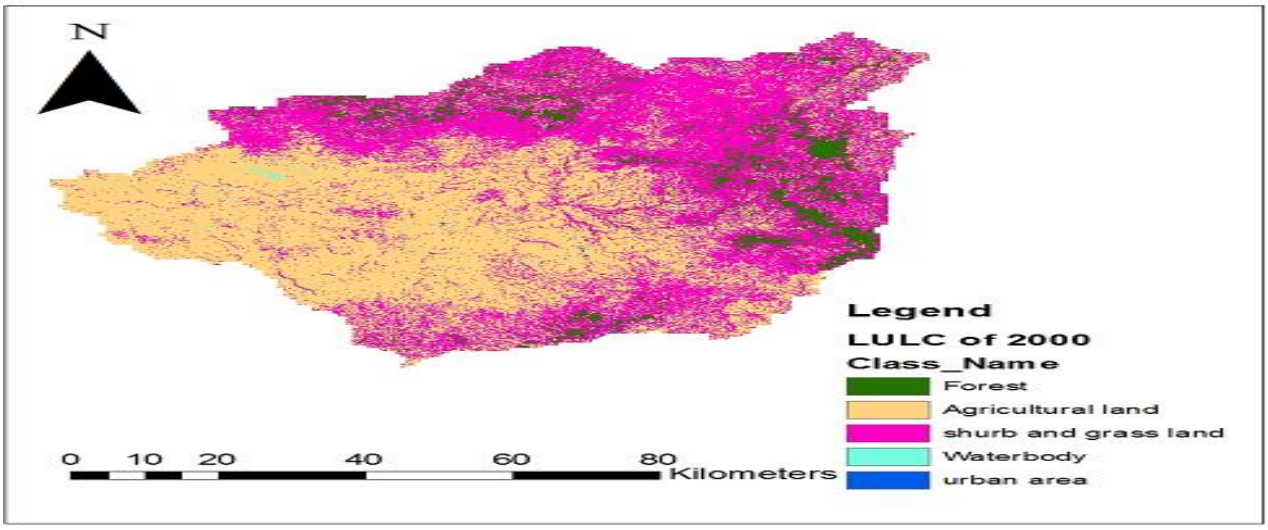

Figure 3-8: Anger Land Use Land cover during 2000 (GLCF Wave site)

Land use / Land cover type	Land use according to SWAT database	SWAT code	Area	
			Km^2	%
Agricultural land	Agricultural land close to grown	AGRC	4067	50.9
Shrub and Grass land	Forest deciduous	FRSD	3278	41.0
Forest	Forest mixed	FRST	579	7.2
Built Up	Residential-Low Density	URLD	44	0.6
Water body	Water	WATR	19	0.2

Table 3-3: LULC classification of Anger sub basin during 2000

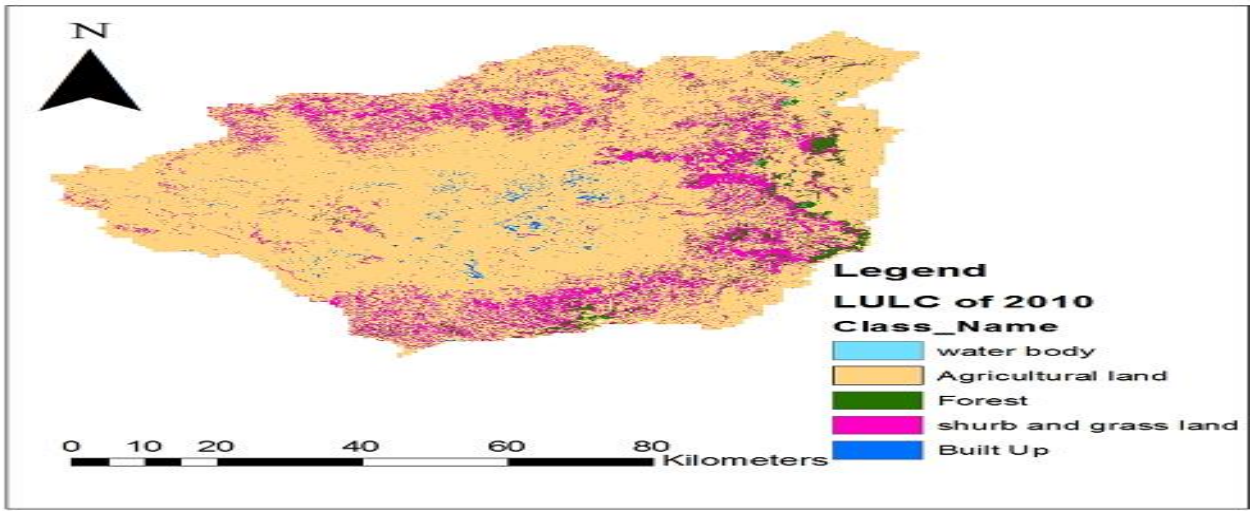

Figure 3-9: Anger Land use Land Cover during 2010 (GLCF Wave site)

Land use / Land cover type	Land use according to SWAT database	SWAT code	Area	
			Km^2	%
Agricultural land	Agricultural land close to grown	AGRC	6590	82.5
Shrub and Grass land	Forest deciduous	FRSD	1031	12.9
Forest	Forest mixed	FRST	290	3.6
Built Up	Residential-Low Density	URLD	66	0.8
Water body	Water	WATR	9	0.1

Table 3-4: LULC classification of Anger sub basin during 2010

3.1.8 Soil type

According to FAO/UNESCO-ISRIC classification, nine major soil groups were identified in the Anger sub basin presented in Figure 3-10. SAWT model requires soil chemical and physical properties such as soil texture, available water content, hydraulic conductivity, bulk density and organic carbon content for different layers of each soil type. These data were obtained from Minister of Water irrigation and Energy (MOWIE).To integrate the soil map with SWAT model, a user soil database which contains textural and chemical properties of soil was prepared for each soil layers and added to the SWAT user soil databases using the data management add tool in ArcGIS. The symbol and areal coverage of the soil type are presented in (Table.3-5). The sub basin were dominated by HaplicAlisols, HaplicAcirisols, RahodicNitisols and DystricLeptosols. And also HaplicNitisols, EutricVertisols and EutricRegosols were the soils of sub basin.

Soil type	Symbol	Area	
		Ha	%
HaplicAlisols	ALh	314102.5970	39.36
HaplicAcirisols	ACh	211205.4140	26.47
RahodicNitisols	NTr	122534.0501	15.35
DystricLeptosols	LPd	100628.0340	12.61
HaplicNitisols	NTh	28451.6384	3.57
EutricLeptosols	LPe	18415.0175	2.31
EutricVertisols	VRe	2618.2489	0.33
EutricRegosols	RGe	87.2750	0.01

Table 3-5: Soil types of Anger sub basin with their symbols and areal coverage

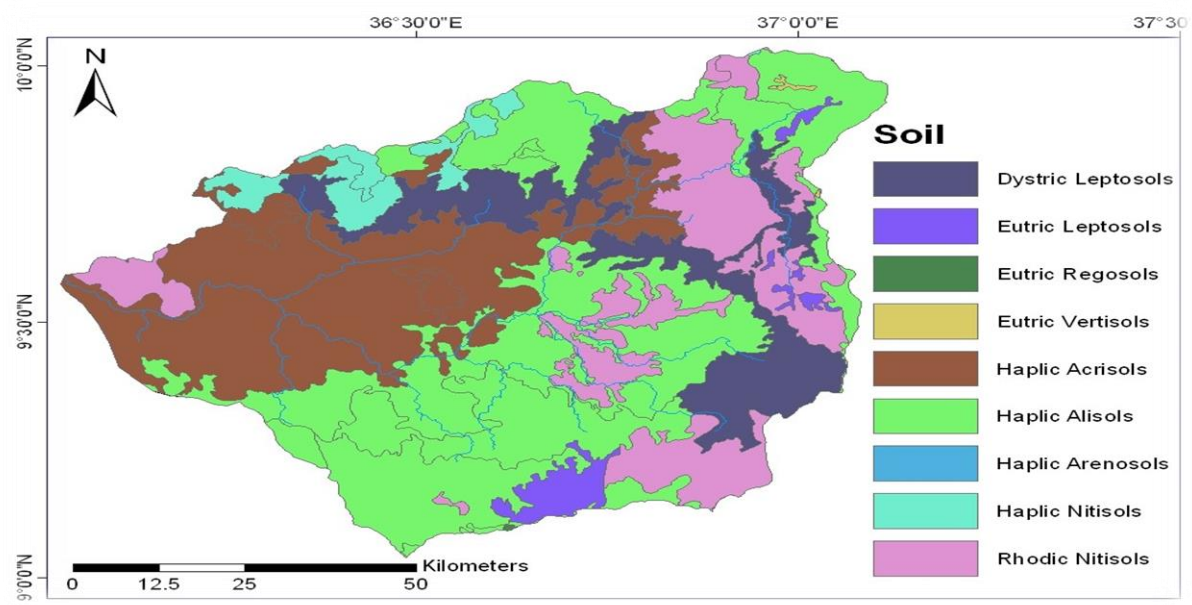

Figure 3-10: Map of the soil types of Anger Sub Basin (Atlas of the Blue Nile Basin)

3.1.9 Geology

The regional geology of the Anger sub basin is mainly dominated by undifferentiated lower complex, Wollega basalts and Adigrat sandstone. And also granite and classic's deposits were the parts of the sub basin. (Aster D. Y. and Seleshi B. A., 2009).

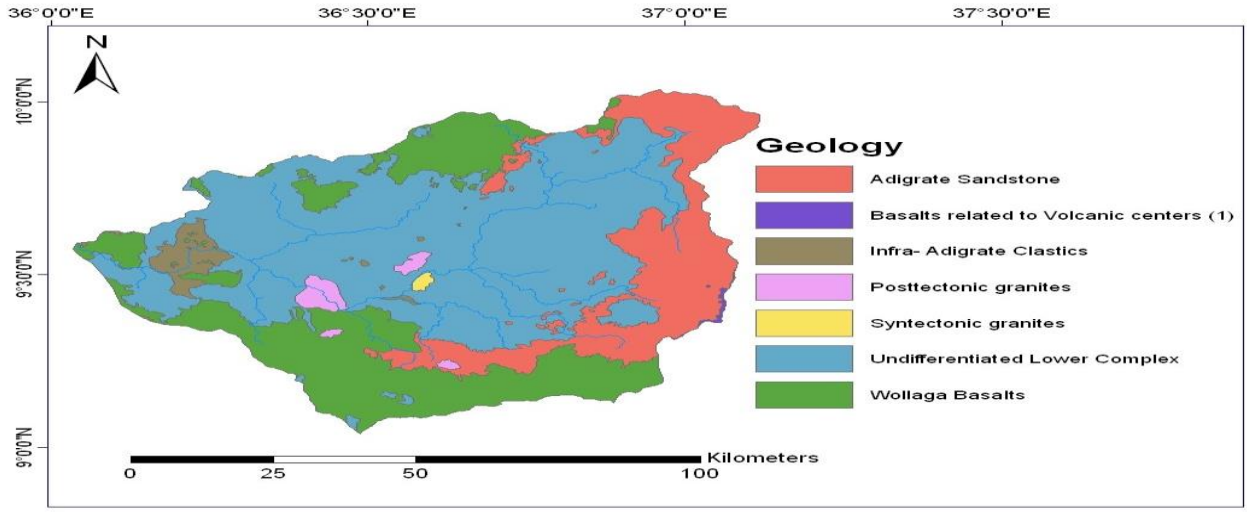

Figure 3-11: Geology of Anger Sub Basin (Atlas of the Blue Nile Basin)

3.1.10 Socio Economic aspect of the sub basin

3.1.11 Administrative structure of the sub basin

Anger sub basin covers 15 woredas; Wayu Tika, Bila Seyo, Sibu Sire, Guto Gida, Sasiga, Gudaya Bila, Bilo Jegonfoy, Abe Dongoro, Horo, Gida Kiremu, Yaso, Limu, Haro, Jarti Jardega, and Amuru. The total population of the woredas is 1,375,209 people (Aster D. Y. and Seleshi B. A., 2009)

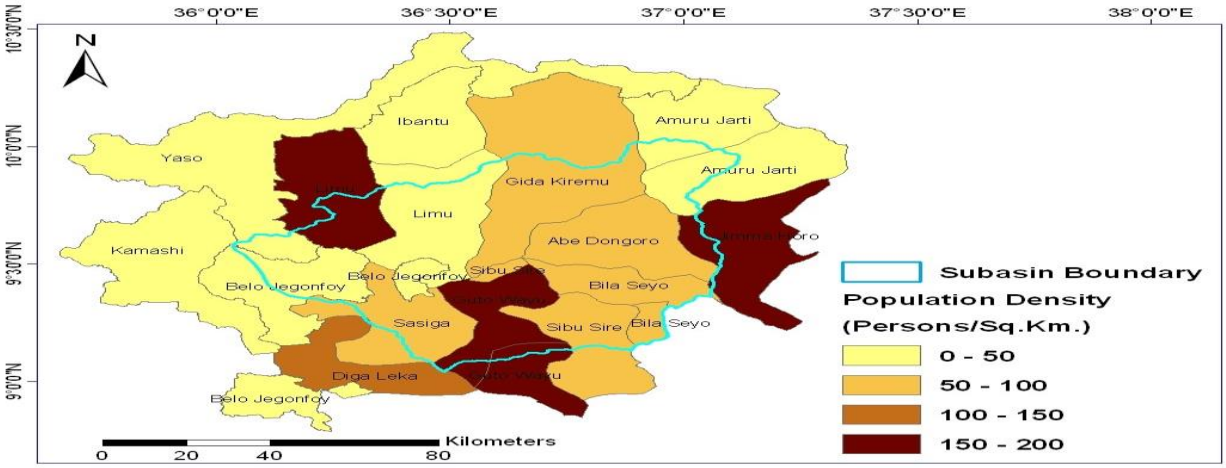

Figure 3-12: Population Density of woredas in Anger Sub Basin (Atlas of the Blue Nile Basin)

3.2 Hydrological Model Selection Criteria

There are various criteria which can be used for choosing the right hydrological model for specific problem. These criteria are always project dependent, every project has its own specific requirements and needs. Further, some criteria are user dependent (and therefore subjective). Among the various project–dependent selection criteria there are four common, fundamental that must be always answered (Cunderlik J. , 2003).

3.2.1 Reasons for selecting SWAT model

The reasons, for selecting SWAT model for this study are:-

- The model was applied for land use and land cover and climate change impact assessment in different parts of the world.
- To model and simulate the major hydrological process in the watersheds
- It is less demanding on input data, and
- It is readily and freely available.

A major limitation to large area hydrological modeling of SWAT is the spatial detail required to correctly simulate environmental processes. For example, it is difficult to capture the spatial variability associated with precipitation with in watershed. Another limitation is data files can be difficult to manipulate and can contain several missing records. The model simulations can only be as accurate as the input data. The third limitation is that, the SWAT model does not simulate detailed event-based flood and sediment routing.

3.2.2 Description of SWAT Model

Soil and water assessment tool (SWAT) was applied in the Anger sub basin to assess the impact of land use/land cover and climate change on hydrological components. The standard used to select this method is based on benefits it provides to meet the objectives of study area. The SWAT model is embodied in Arc GIS that can integrate various readily available geospatial data to accurately represent the characteristics of watershed. The SWAT watershed model is one of the most recent models developed by the USDA-ARS to predict the impacts of land management practices on water, sediment and agricultural chemicals yields in watersheds with varying soils, land use and management practices over long periods of time (Neitsch S, 2005).The model is a physical based, semi- distributed, continuous time, and operating on daily time step (Neitsch S, 2005).

As a physical model, SWAT uses hydrological response unit (HRU) to describe spatial heterogeneity in terms of land use, soil types and slope with in watershed. In order to simulate hydrological processes in watershed, SWAT divides the watershed in to sub watersheds based upon drainage areas of the tributaries. The sub watersheds are further divided in to smaller spatial modeling unit known as HRUs, depending on land use land cover, soil and slope characteristics.

One of the main advantages of SWAT is that it can be used to model watershed with less monitoring data. For simulation, SWAT needs digital elevation model; land use and land cover map, soil data and climate data of the study area. These data are used as input for the analysis of hydrological simulation of surface runoff and groundwater recharge. SWAT splits hydrological simulations of a watershed in two major phases: the land phases and routing phases. The land phases of the hydrological cycle control the amount of water, sediment, nutrient, and pesticide loadings to the main channel in each sub basin. While the routing phases considers the movement of water, sediment and agricultural chemicals through the channel network to the watershed outlet (Ma X, 2009).The land phases of hydrological cycle is modeled in SWAT based on water balance equation (Neitsch S, 2005).

$$SWt = SWo + \sum_{i=1}^{t}(Rday - Qsurf - Ea - Wseep - Qgw) \_\_\_\_\_ (3.1)$$

Where:-

- **SWt** is the final soil water content (mm)
- SWo is the initial water content (mm)
- **t** is time in (days)
- **Rday** is the amount of precipitation on day i(mm)
- **Qsurf** is the amount of surface runoff on day i(mm)
- **Ea** is the amount of Evapotranspiration on day i(mm)
- **Wseep** is amount of water entering the vadose zone from the day i(mm),and
- **Qgw** is the amount of return flow on day i(mm)

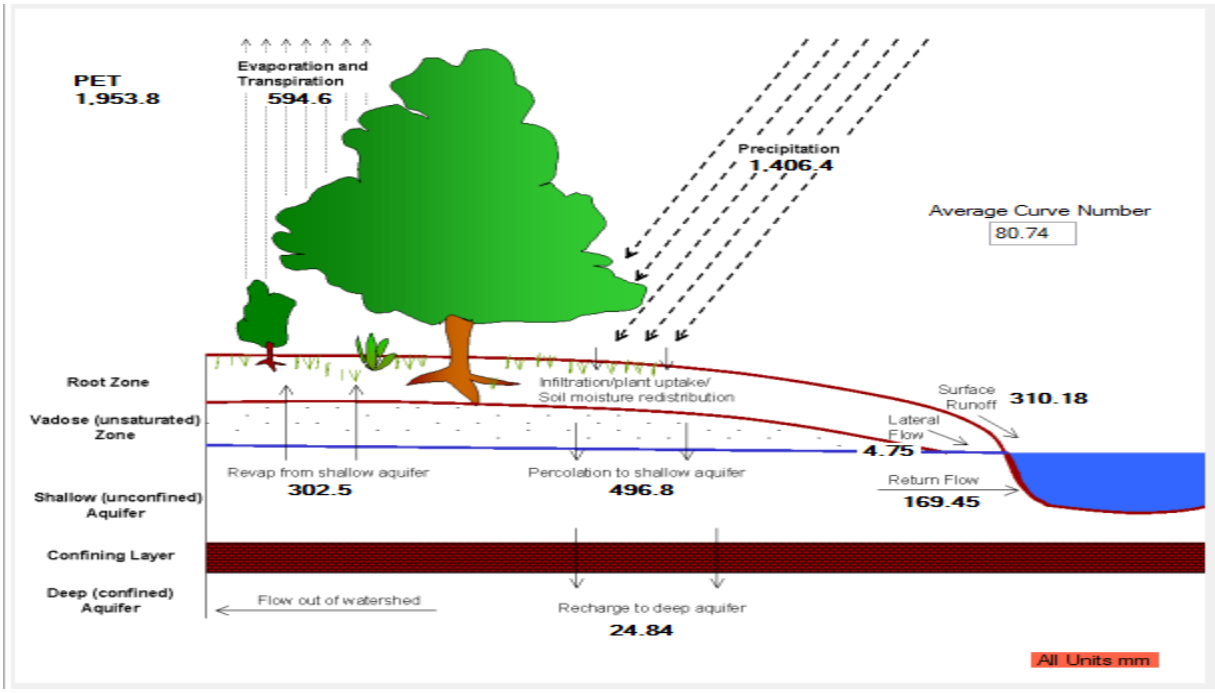

Figure 3-13: Land phase of hydrological cycle

The model has eight major components: hydrology, weather, sedimentation, soil temperature, crop growth, nutrients, pesticides, and agricultural management (Neitsch S, 2005). However, brief description of some of the SWAT computation procedures which are considered in this study are presented under the following subsections. For complete model description, one may refer to SWAT theoretical documentation (Neitsch S, 2005).

3.2.3 Surface runoff

Surface runoff refers to the portion of rainwater that is not lost to interception, infiltration and Evapotranspiration (Solomon, H. , 2005). Surface runoff occurs whenever the rate of precipitation exceeds the rate of infiltration. SWAT offers two methods to estimating the surface runoff: the soil conservation service (SCS) curve number method (USDA - SCS, 1972) or the Green and Ampt infiltration method (Green. W.H. and Ampt G.A., 1911).The Green and Ampt method needs sub-daily time step rainfall which made it difficult to be used for this study due to unavailability of sub-daily time step rainfall data. Therefore, the SCS curve number method was adopted for this study.

The general equation for the SCS curve number method is expressed equation (3.2).

$$Qsurf = \frac{(Rday - Ia)^2}{(Rday - Ia + S)} \quad (3.2)$$

Where:-

- **Qsurf** is the accumulated runoff or rainfall excess (mm),
- **Rday** is the rainfall depth for the day (mm water),
- **Ia** is initial abstraction which includes surface storage, interception and infiltration prior to runoff (mm water),
- **S** is retention parameter (mm water).

The retention parameter varies spatially due to changes with land surface features such land use, slope and management practices. This parameter can also be affected temporal due to change in soil water content. It is mathematically expressed as:-

$$S = 25.4 * \left(\frac{1000}{CN} - 10\right) \quad (3.3)$$

Where, CN is the curve number for the day its value is the function of land use soil permeability and soil hydrologic group.

The initial abstraction, Ia, is commonly approximated as 0.2S and equation (3.3) becomes

$$Qsurf = \frac{(Rday - 0.2S)^2}{(Rday + 0.8S)} \quad (3.4)$$

For the definition of hydrological groups, the model uses the U.S.Natural resources conservation service (NRCS) classification. The classification defines a hydrological model group as a group of soils having similar runoff potential under similar storm and land cover conditions. Thus, soils are

classified in to four hydrological groups (A,B,C, and D) based on infiltration which represent high, moderate, slow, and very slow infiltration rates, respectively.

3.2.4 Potential Evapotranspiration

Potential Evapotranspiration is a collective term that includes evaporation from the plant (transpiration) and evaporation from the water bodies and soil. Evaporation is the primary mechanism by which water is removed from sub basin. An accurate estimation of Evapotranspiration is critical in the assessment of water resources and the impacts land use and climate change on these resources. There are many methods that are developed to estimate potential Evapotranspiration (PET) SWAT provided three options for PET calculation: Penman-Monteith (Monteith, 1965), Priestley-Taylor (Priestley, 1972), and Hargreaves (Hargreaves et al, 1985), methods. The methods have varies data needs of climate variables. Penman- Monteith method requires solar radiation, air temperature and relative humidity and wind speed; Priestley – Taylor method requires solar radiation, air temperature and relative humidity; whereas Hargreaves method requires air temperature only. For this study, the Penman –Monteith method was selected as the method is widely used and all climatic variable required by the model are available for the four stations in and around the study sub basin.

3.2.5 Ground water flow

To simulate the ground water, SWAT partitions groundwater in to two aquifer systems: a shallow, unconfined aquifer which contributes return flow to stream within the watershed and deep, confined aquifer which contributes return flow to streams outside the watershed (Arnold J. G., 1993). In SWAT the water balance for a shallow aquifer is calculated with equation (3.5).

$$\boldsymbol{aq\ shi = aq\ shi - 1 + W\ rchrg - Q\ gw - W\ revap - Wdeep - Wpump, sh} \quad (\mathbf{3.5})$$

Where:-

- **aqshi** is the amount of water stored in the shallow aquifer on a day I (mm),
- **Aqsh i-1** is the amount of water stored in the shallow aquifer on day i-1(mm),
- **W rchrg** is the amount of recharge entering the aquifer on day I (mm),
- **Qgw** is the ground water flow, or base flow, or return flow, in to the main channel on day I (mm)
- **Wrevap** is amount of water moving in to soil zone in response to water deficiencies on day I (mm),

- **W deep** is the amount of water percolating from the shallow aquifer in to the deep aquifer on day I (mm), and
- **Wpumpsh** is the amount of water removed from the shallow aquifer by pumping on day I (mm).

3.2.6 Flow routing phase

The second component of simulation of the hydrology of watershed is the routing phase of hydrological cycle. It consists of movement of water, sediment and other constituents (E.g. nutrients, pesticides) in the stream network. Two options are available to route the flow in the channel network: the available storage and Muskingum methods.

The available storage method uses a simple continuity equation in routing the storage volume, whereas the Muskingum routing method models the storage volume in channel length as combination of wedge and prism storages. In the later method, when a flood wave advances in to reach segment, inflow exceeds outflow and wedge storage is produced. As a flood wave recedes or retreat, outflow exceeds inflow in the reach segment and negative wedge is produced. In addition to the wedge storage, the reach segment contains a prism of storage formed by a volume of constant cross-section along the reach length. The available storage method was used for this study. The method was developed by (Williams, 1969). The equation of the available storage routing is given by:

$$\Delta Vstored = Vin - Vout \quad (3.6)$$

Where:-

- **ΔVstored** is a change in volume of storage during the time step (m^3 water)
- **Vin** is the volume of inflow during the time step (m^3 water), and
- **Vout** is the volume of outflow during the time step (m^3 water)

3.3 *Methodology*

The following framework illustrates the general workflow of the study

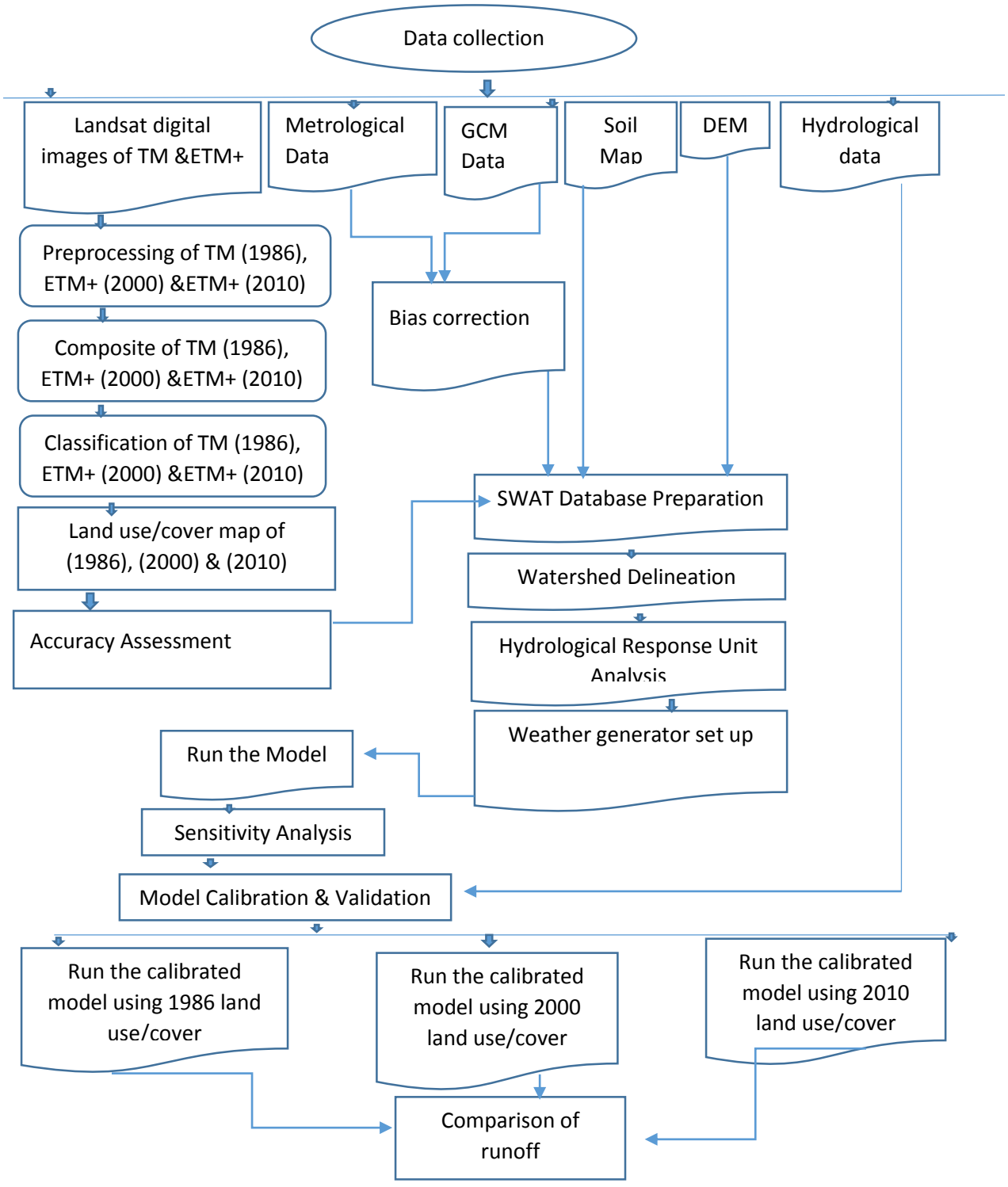

Figure 3-14: Work flow of the study

3.3.1 Data acquisitions

For this study , various data are required that includes topographic data (DEM), land use and land cover data, soil data, daily data of climatic variables (daily data of precipitation, maximum and minimum temperature , relative humidity , wind speed and solar radiation).The land use land cover were obtained from satellite GLCF website. Soil, DEM and hydrological data were collected from the MOWIE. The climatic data were obtained from the national metrological agency of Ethiopia (NMAE).The GCM data of Abbay basin (daily data of precipitation, maximum and minimum temperature, relative humidity, wind speed and solar radiation) were obtained from international water management institutions (IWMI).

3.3.2 Image processing

This study was done using Land sat imageries from (GLCF Wave site) of six bands to identify change in land use land cover distribution in the Anger sub basin over 25 year period from 1986-2010. Land sat TM, ETM+ and ETM+ was selected for the period of 1986, 2000 and 2010 respectively. To avoid a seasonal variation in vegetation pattern and distribution throughout a year, the selection of dates of the acquired data were made as much as possible in the same annual season of acquired years. This images used in this study area were orthorectified to the Universal Transverse Mercator projection using datum WGS (World Geodetic System) 84 zone 37N. In order to view and discriminate the surface features clearly, all the input satellite images were composed using the RGB color composition Figure: A. 3-15. The images provide complete coverage of Anger sub basin. The image data files were downloaded in zipped files from the Global land cover facility (GLCF) website and extracted to Tiff format files. The acquisition dates, sensor, path row, resolution and the producers of satellite images used in this study are summarized in the (table 3:6) below.

Path/row	Acquisition month, date and year	Sensor	Resolution (m)	Producer
170/053&054	Jan 01,1986	TM	30	GLCF
170/053&054	Feb 02,2000	ETM+	30	GLCF
170/053&054	Jan 01 2010	ETM+	30	GLCF

Table 3-6: The acquisition dates, sensor, path row, resolution and producers of the image

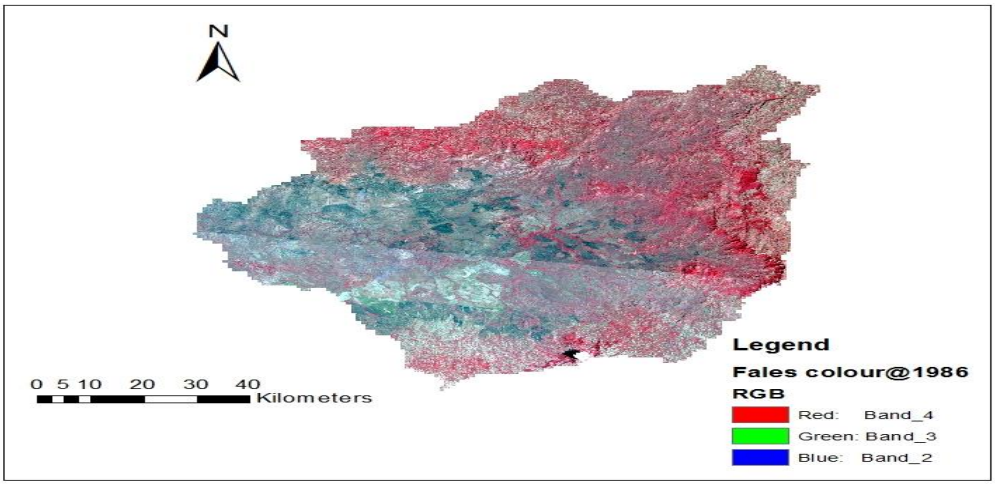

Figure: A. 3-15: "False color" composite satellite Image of sub basin during 1986

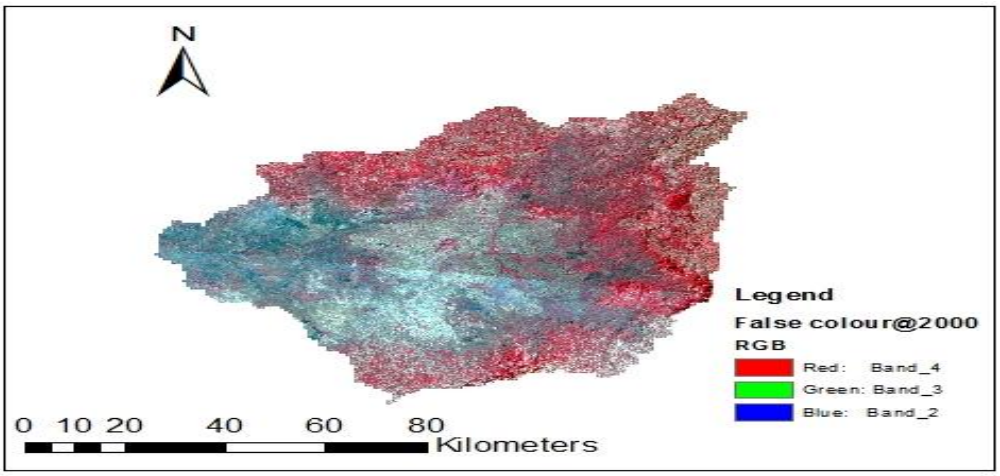

Figure:B During 2000 (GLCF Wave site)

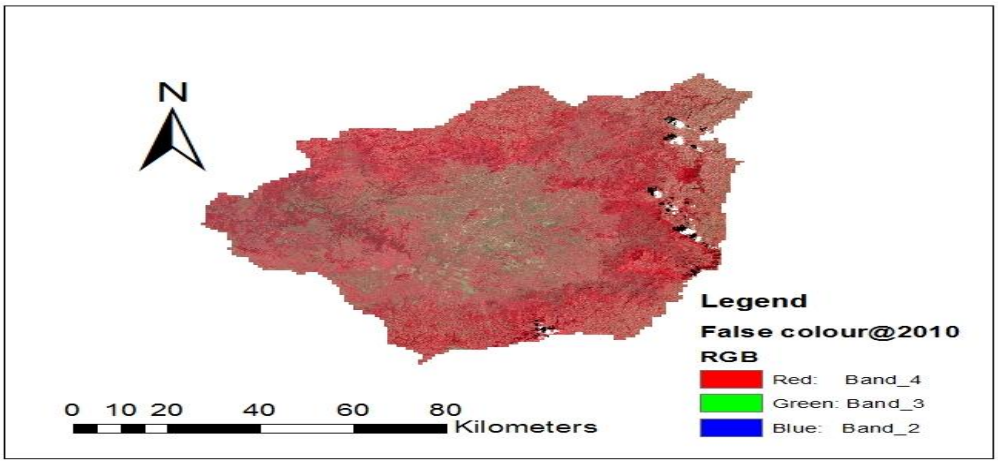

Figure: C. During 2010(GLCF wave site)

3.4 Land use and land cover mapping

3.4.1 Land use land cover classes

The land use and land cover change studies usually need the development and the definition of homogeneous land use and land cover units before the analysis is started. These have to be differentiated using the available data source such as remote sensing, any other relevant information and the previous local knowledge. Hence, based on the priori knowledge of the study area and additional information from previous research in the study area five different types of land use and land cover have been identified for the Didessa sub basin (Minichil.J, 2016).The descriptions of these land use and land covers are given as follows.

- **Cultivated land**: - areas, used for crop cultivation, both annuals and perennials, and the scattered rural settlement that are closely associated with the cultivated fields. Due to the difficulty encountered to identifying the dispersed rural settlements this kind of land cover was combined with the cultivated land during classification.
- **Forest land**: - land covered with dense trees which includes ever green forest land, mixed forest and plantation forests.
- **Shrub and grass land**: - areas covered with shrubs, bushes, small trees, grass and little wood mixed with same grass.
- **Water and marshy land: -** areas which are water logged and swampy throughout the year, the river and its main tributaries.
- **Urban land**: - area covers with building rural residential houses infrastructures roads.

3.4.2 Image classification

Image classification is the process of assigning of pixels of continuous raster image to the predefined land cover classes. It is always a difficult and time consuming task. Different issues to keep in mind to avoid overlapping features and finish with effective classification Leis parallel with the ground truth. The result of the classification is mostly affected by various factors such as classification methods, algorithms, collecting of training sites etc. In remote sensing there are various image classification methods there appropriateness depends on the purpose of land cover maps produced for and the analyst's knowledge of the algorithms is using. However, in most cases the researchers categorized them in to three major categories: supervised, unsupervised and hybrid. For this study, the supervised classification type was applied. It is the most common type of

classification technique in which all pixels with similar spectral value are automatically categorized in to land cover classes or themes. Supervised classification which relies on the prior knowledge of pattern recognition of study area was used. It requires the manual identification of point of interest areas as reference or ground truth within the images, to determine the spectral signature of identified features. For this study the land cover map was produced based on the pixel based supervised classification thought the step such as: first, selecting of the training sites which are typically representative for the land cover classes. The training sites were collected based on the analyst's personal experience and knowledge of the physiographical knowledge of the area. In addition, image enhancement and composition were applied for better discriminating the land cover classes. Using these approaches same training sites were collected as from each image (1986, 2000 and 2010). Second, perform the classification using the Maximum Likelihood classifier.

3.5 Classification Accuracy Assessment

One of the most important final step at classification process is accuracy assessment. The aim of accuracy assessment is to quantitatively assess how effectively the pixels were sampled into the correct land cover classes. Moreover the key emphasis for accuracy assessment pixel selection was on areas that could be clearly identified on both Landsat high resolution image, Google earth and Google Map. So 130, 131 and 141 points (locations) were selected in the classified image of 1986, 2000 and 2010 respectively. The Accuracy Assessment Cell Array Reference column was filled according to the best guess of each reference point.

3.5.1 Kappa coefficient

Kappa analysis is a discrete multivariate technique used in accuracy assessments. According to (Landis, 1977) the acceptable ranges of kappa coefficient is presented below.

1	<0.00	Poor
2	0.00 - 0.20	Slight
3	0.21 - 0.40	Fair
4	0.41 - 0.60	Moderate
5	0.61 - 0.80	Substantial
6	0.81 - 1.00	Almost perfect

Table 3-7 Kappa statics ranges

The Kappa statistic is computed as;

$$K = \frac{\sum_{i=1}^{r} xii - \sum_{i=1}^{r} (xi + Xx + 1}{N^2 - \sum_{i=1}^{r} (xiiXx + 1} \quad \text{(3.7)}$$

Where: - r is number of rows and columns in error matrix,

N is total number of observations (pixels),

Xii is observation in row i and column i,

Xi+ is marginal total of row i, and

X+i is marginal total of column i,

3.6 Model input data collection

SWAT is highly data intensive model that requires specific information about the watershed such as topography, land use and land cover, soil properties, weather data, and other land management practices. These data were collected from different sources and database. The data are analyzed as presented in the next sub-sections.

3.6.1 Digital Elevation Model

Digital Elevation Model (DEM) data is required to calculate the flow accumulation, stream networks, and watershed delineation using SWAT watershed delineator tools. A 30m by 30m resolution ASTER Global Digital Elevation Model was obtained from the (MOWIE).

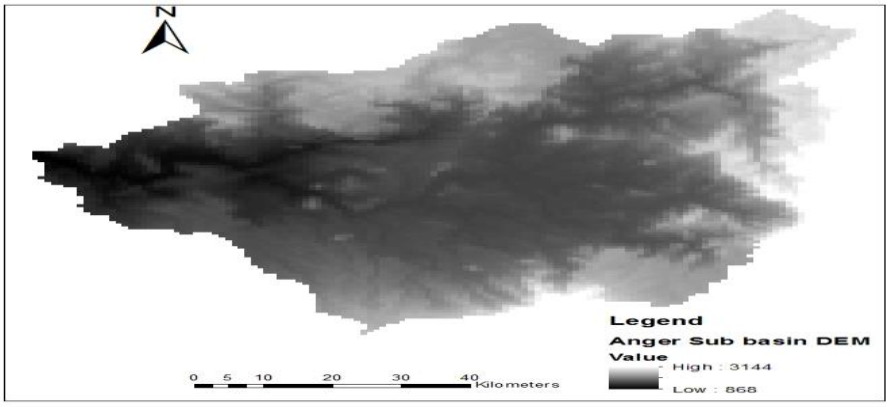

Figure 3-16: Digital Elevation Model of Anger Sub Basin (MOWIE)

3.6.2 Meteorological data

Weather data are among the main demanding input data for the SWAT simulation. The weather input data required for SWAT simulation includes daily data of precipitation, maximum and minimum temperature, relative humidity, wind speed and solar radiation. These were obtained from the Ethiopian National Metrological Agency. The weather data used were represented from five stations in and around the watershed. Such as, G_Ayana, Nekemte, Shambu, Anger and Alibo stations as shown in Figure 3-17. The first three stations are the first classes that have records on

all climatic variables, whereas the last two is the third class station (table: 3-7). The climatic data used for this study covers 30 years from 1986-2015.Based on the class of the stations, the number of weather variables collected varies from station to station that are grouped in to two. The first group contains only rainfall Max and Min temperature data. The second group contains variables like maximum and minimum temperature, humidity, sunshine hours, and wind speed in addition to rainfall. However, missing values were identified in some of the climatic variables. These values were assigned with no data code (-99) which when filled by weather generator embodied in SWAT model from monthly weather generator parameters values. The monthly generator parameters values were estimated from the three weather stations (G_Ayana, Nekemte and Shambu).Finally, the weather data were prepared in Txt format with lookup tables as required by the model.

No	Station name	Latitude (deg)	Longitude (deg)	Rain fall	Max temp	Min temp	Relative humidity	Sun shine hr	Wind speed
1	G_ Ayana	9.87	36.62	✓	✓	✓	✓	✓	✓
2	Nekemte	9.08	36.46	✓	✓	✓	✓	✓	✓
3	Shambu	9.57	37.12	✓	✓		✓	✓	✓
4	Anger	9.26	36.33	✓	✓	✓	X	X	X
5	Alibo	9.89	37.01	✓	✓	✓	X	X	X

Table 3-8: Location of meteorological stations in and around the Anger sub basin (NMAE)

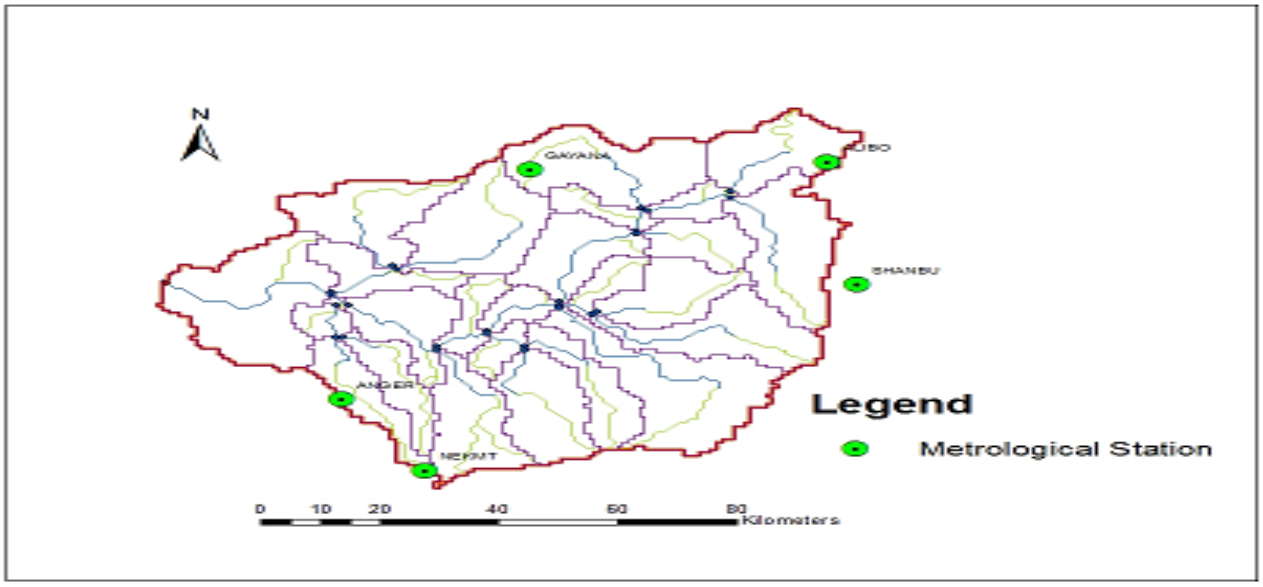

Figure 3-17: Location of Meteorological stations in around the Anger sub Basin (NMAE)

3.7 Model input data analysis

3.7.1 Filling missing data

Missed measured precipitation data may face to many problems in hydrologic analysis and design. Because of the cost associated with data collection and some natural and man-made conditions sometimes make it very difficult to have complete records of data at every stations clearly. Conditions above mentioned sometimes prevent to obtain quantitative and qualitative data of the study area. For gauges that require periodic observation, the failure or absence of the observer to make the necessary visit to the gauge, destruction of recording gauges, and instrument failure because of mechanical or electrical malfunctioning can result in missing data. Any such causes of instrument failure reduce the length and information content of the precipitation record. Hence, there are different methods for filling the missing data from those methods station average and normal ratio method were used for the rainfall in this study area (Richards, 1998).

$$\%difference = \left(\frac{NX - Ni}{NX}\right) * 100 \quad (3.8)$$

NX-Ni must be positive. If Ni>NX the numerator will become Ni-Nx. Then, the b mean of the nearby stations' differences is determined.

$$Px = \frac{1}{n} * \left(\left(\frac{Nx}{N1}\right) * P1 + \left(\frac{Nx}{N2}\right) * P2 + \cdots + \left(\frac{Nx}{Nn}\right) * Pn\right) \quad (3.9)$$

Where Px is the missing data at station x, Nx is the missing data stations normal annual rainfall, Ni is normal annual rainfall at station i. and n is number of nearby gauges. The station-average method for estimating missing data uses n gages from a region to estimate the missing point rainfall, Px, at another gage:

$$Px = \frac{1}{n}\sum_{i=1}^{n} Pi \quad (3.10)$$

In which Pi is the rainfall at gage I (Equation 3.9) is accurate when the total annual rainfall at any of the n regional gages when the mean of percent difference is less than 10%. This method gives equal weight to the rainfall at each of the regional gages. The value 1/n is the weight given to the rainfall at each gage used to estimate the missing rainfall. Most of the rainfall recorded from the stations has missing data ranging about 10%. Therefore before using the data to runoff modeling

it was first essential to apply a gap filling techniques. The other station which has greater than 10% is filling by weather generator.

3.7.2 Areal rainfall determination

In a given drainage basin rain gauge stations are evenly distributed into sub-basin. The rain of one station in a basin may be different from that of the second station in the same catchment. From this idea the average precipitation value on the entire basin is worked out, so as to get average rain catchments to have the limits of the catchment carefully defined. Therefore, rainfall over an area of interest has to be estimated from these point measurements. There are usually three ways of determining the areal precipitation over a catchment from rain gauge measurement. These methods are the Arithmetic means, the Thiessen polygon and the Isohyetal method. However, the Thiessen polygon was used for this study for its sound theoretical basis and availability of computational tools. But the method is dependent on a good network of representative rain gauges and does not allow the hydrologist to consider factors, such as topography (Daniel, 2008).

To determine the mean areal rainfall, the rainfall amount of each station was multiplied by the area of its polygon and the sum of these products was divided by the total area of the catchment.

If P1, P2, P3……Pn are the rainfall magnitudes recorded by the gauging stations 1, 2…….n, respectively and if the areas of Thiessen Polygon A1, A2, and A3……An, then the average rainfall over the catchment is given by:

$$Pavg = \frac{P1 * A1 + P2 * A2 + P3 * A3 ..... Pn * An}{A} \text{ . ---------- 3.11}$$

Where: - Pavg = areal precipitation over the sub-basin (mm); P1, 2…n = precipitation depth in each station (mm);

A1, 2 …n = area of each polygon (km2);

A = total watershed area of sub-basin (km2)

According to Areal rainfall determination in a given drainage basin rain gauge stations are evenly distributed into sub-basin. The rain of one station in a basin may be different from that of the second station in the same catchment. From this idea the average precipitation value on the entire basin is worked out, so as to get average rain catchments to have the limits of the catchment carefully defined. Therefore, rainfall over an area of interest has to be estimated from these point measurements.

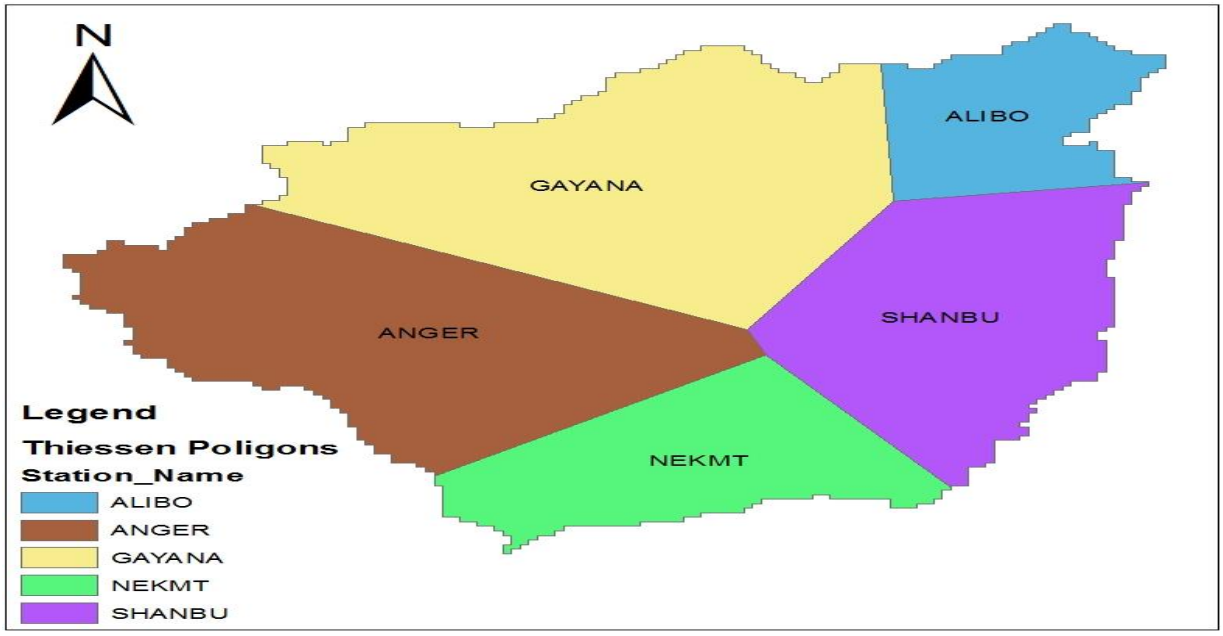

Figure 3-18Thiessen polygon for selected rainfall stations

S/N	Station	Area in (KM^2)	Area ratio	Annual rainfall in (mm)	weighted rainfall in (mm)
1	Alibo	547.8	0.07	1846.621	129.89
2	Nekemte	1116.2	0.14	1797.95	257.68
3	Shambu	1599.8	0.21	1356.85	278.72
4	Anger	2163.96	0.28	1345.83	373.94
5	G_Ayana	2360.4	0.30	1485.51	450.22
	total	7788.16	1.00	1488.74	292.62

Table 3-9: Areal rainfall interpolated using Thiessen polygon method for sub basin

3.7.3 Homogeneity test

Homogeneity analysis was used to separate a change in the statistical properties of the time series data. The causes can be either natural or man-made. These include alterations to land use and relocation of the observation gauging station. Therefore in order to select the representative meteorological station for the analysis of areal rainfall estimation, checking homogeneity of group

stations is essential, the homogeneity of the selected gauging stations daily rainfall records were carried out by non-dimensional equation: (Tadesse T., 2016)

$$Pi = \frac{\overline{Pi}}{\overline{P}} \quad \text{.....3.12}$$

Where: -

- Pi = Non dimensional Value of precipitation for the month i
- $\overline{Pi}$ = Over years averaged monthly precipitation for the station i
- $\overline{P}$ = Over year's average yearly precipitation of the station

According to Homogeneity test analysis**,** the selected stations were plotted for comparison with each other; for illustration Figure 3-19 below show the result of homogeneity analysis result. Same-mode and pattern of the stations are observed and hence group stations selected are homogenous since all the value of Pi are less than 0.3.

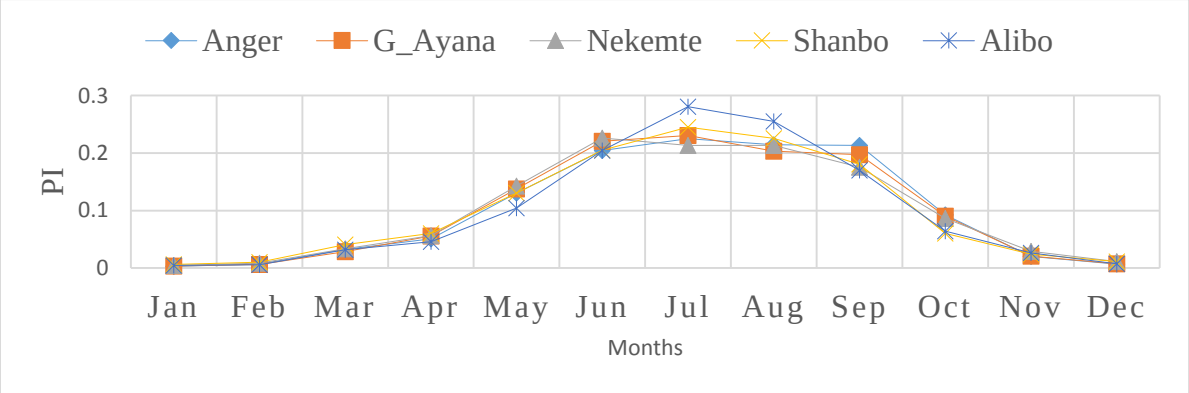

Figure 3-19: Homogeneity test analysis for all Meteorological stations

3.7.4 Consistency

Double mass curve (DMC) was used to check the consistency of rainfall for adjustment of inconsistent data. This technique is based on the principle that when each record data comes from the same parent sample, they are consistent. A group of four base stations in the neighborhood of the station was selected. A consistent record is one where the characteristics of the record have not changed with time. A double-mass curve is graph of the cumulative catch of rain gage of interest versus the cumulative catch of one or more gage in the region that has been subjected to similar hydro metrological occurrence and is known to be consistent. If a rainfall record is consistent estimator of the hydro meteorological occurrences over the period of record, the double-mass curve will have a constant slope. A change in the slope of the double mass curves would suggest

that an external factor has caused changes in character of the measured values. If a change in slope is evident, then either the record needs to be adjusted with the early or the later period of record adjusted (H.Hardision, 1960).

$$\frac{Pa}{Pd} = \frac{\frac{y}{x}}{\frac{yd}{xD}} = \frac{Slope\ of\ original\ line}{Slope\ of\ deviated\ line} = corection\ factor \_\_\_\_\_ (3.13)$$

In which pa=adjusted amount Pd=deviated amount for the concurrent period for which pa is desired.

According to the double mass curves analysis, all the stations in and around Anger sub basin were consistent. For illustration the double mass curves for some stations are presented below.

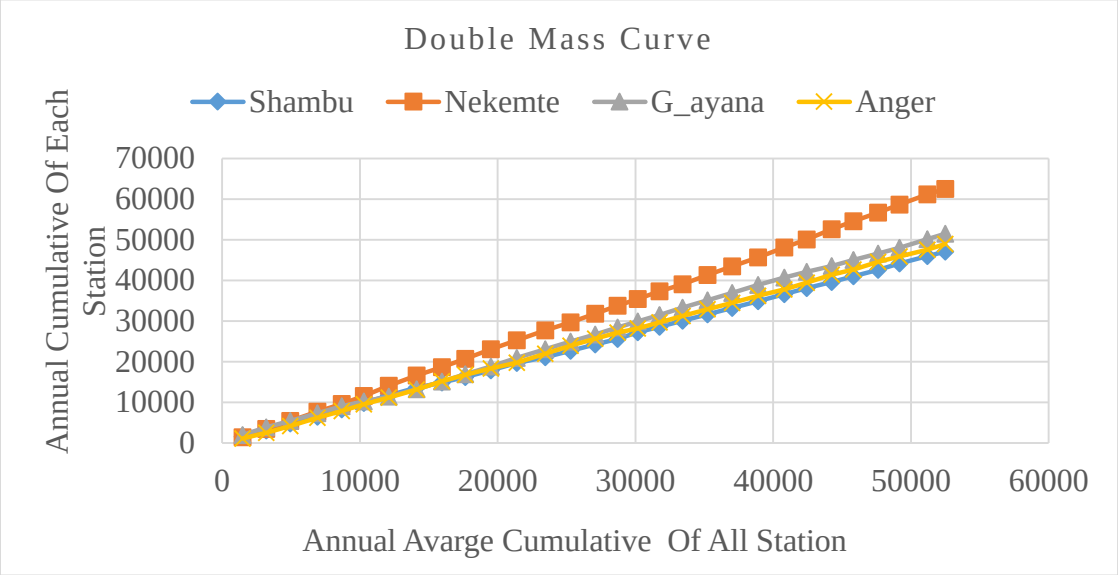

Figure 3-20: Double mass curve of all station

3.8 Inverse Distance methods (IDM)

To covert different GCM grid point to observed metrological station by using Inverse distance methods (IDM) by using the flowing equation.

$$ZP = \frac{\sum_{i=1}^{n} \frac{Zi}{di^{p}}}{\sum_{i=1}^{n} \frac{1}{di}} \_\_\_\_\_ 3.14$$

Where ZP=value of predicted point

Zi=value of I measured point

Di = distance of I measured to the predicted point

P = power function (normal p=2)

n = number of measured point be used.

3.9 Bias correction of precipitation

Because the bias in precipitation and temperature was found to vary spatially, bias corrections were carried out for each of the five stations individually (Leander, 2007)**.** Reference used a power transformation, which corrects the CV (Coefficient of Variation) as well as the mean. In this nonlinear correction each daily precipitation amount *P* is transformed to a corrected $P*$ using:

$$P *= a * P\hat{}b \quad (3.15)$$

The effect of sampling variability is reduced by determine the parameters *a* and *b* for every months period of the year (Leander, 2007). The determination of the *b* parameter is done iteratively. It was determined such that the CV of the corrected daily precipitation matches the CV of the observed daily precipitation. Then the parameter *a is* determined such that the mean of the transformed daily values corresponds with the observed mean. The resulting parameter *a* depends on *b*. The parameter *b* depends only on the CV and is independent of the value of parameter *a*.

The values of constant a and b of Anger station was attached in table below. For other station attached in Appendix-B

months	Jan	Feb	Mar	Apr	May	Jun	Jul	Aug	Sep	Oct	Nov	Dec
a	0.40	0.50	2.68	0.83	0.97	1.30	1.75	1.50	2.17	1.25	1.56	0.37
b	0.51	0.97	0.56	0.98	0.92	0.82	0.71	0.75	0.67	0.84	0.66	0.64

3.10 Bias correction of Temperature

For correcting the daily temperature a different technique is used. The correction of temperature only involves shifting and scaling to adjust the mean and variance (Leander, 2007). For each Station, the corrected daily temperature *T** was obtained as:

$$T *= To + \frac{\sigma(To)}{\sigma(Tm)} * (Tu - To) + (To - Tm) \quad (3.16)$$

Where: - *T u* is the uncorrected daily temperature,

To is the observed daily average temperature and

Tm is the corresponding basin average temperature.

In this equation an over bar denotes the average over the considered period and σ the standard deviation. This method was not appropriate for precipitation because it might cause negative values

3.11 Trend Analysis of Metrological data

3.11.1 Maximum and minimum temperature analysis

Both projected and bias corrected Anger sub basin annual maximum and minimum Temperature shown that an increasing trend over the entire period from 1986-2100 which was presented in figure below. For individual station was attached in Appendix-C.

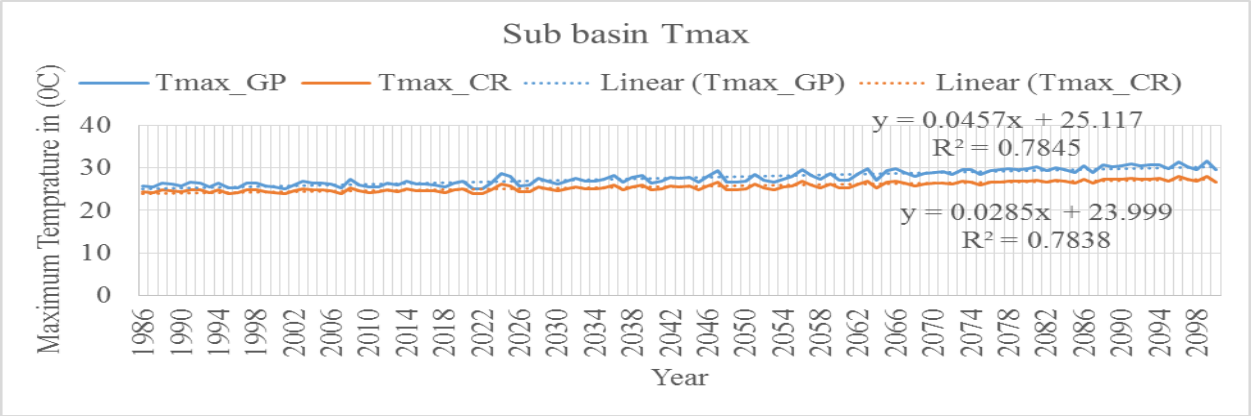

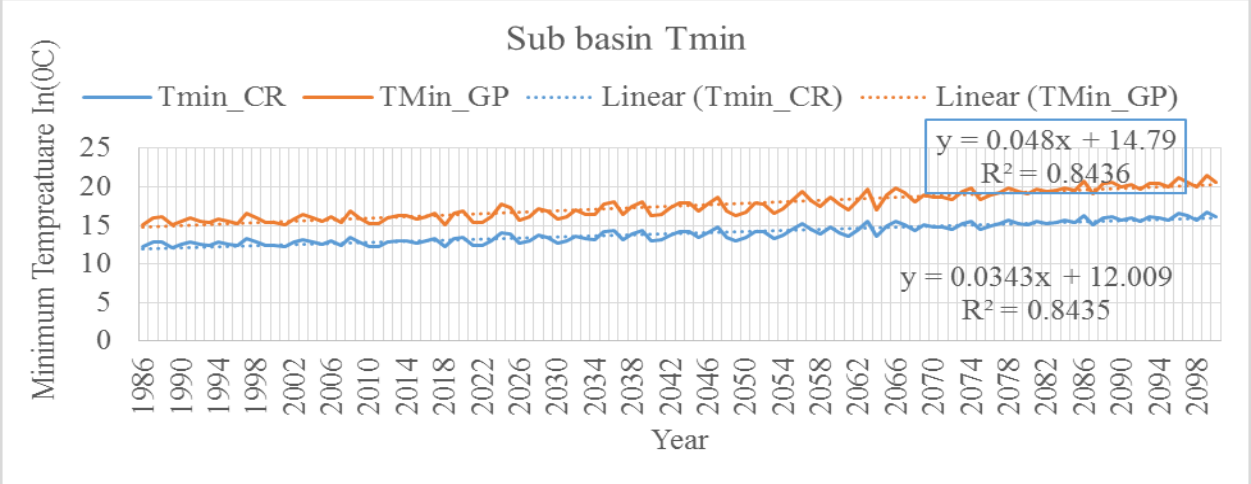

3.11.2 Precipitation Analysis

Both projected and bias corrected Anger sub basin annual precipitation shown that a decreasing trend over the entire period from 1986-2100 which was presented in figure below. For individual station was attached in Appendix-D.

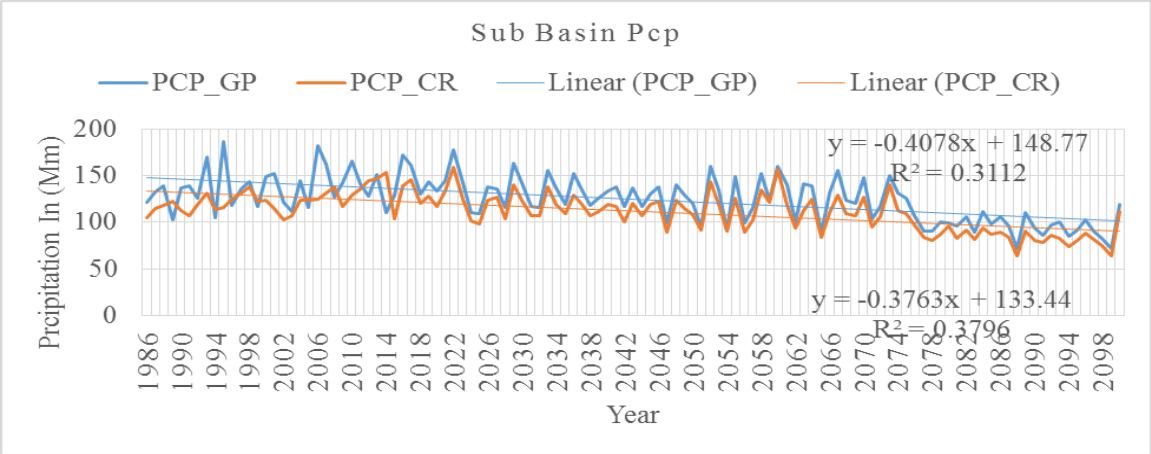

3.11.3 Hydrological Data

Flow data was required for performing sensitivity analysis, calibration and validation of the model from 1990 to 2005 for the period of 16 years. The flow data was also collected from Ministry of Water, Irrigation and Energy of Ethiopia (MOWIE). The flow data was at Great Anger gauging station were collected and arranged as per the requirement of SWAT model. The homogeneity of rainfall and flow data were also checked using RAINBOW (a software package for hydro meteorological frequency analysis and testing the homogeneity of historical data sets). RAINBOW offers a test of homogeneity which is based on the cumulative deviations from the mean. By evaluating the maximum and the range of the cumulative deviations from the mean, the homogeneity of the data of a time series was tested. According to the RAINBOW analysis, the stream flow gauging stations at Great Anger was homogeneous. The detail is illustrated in the Figure3-21 below.

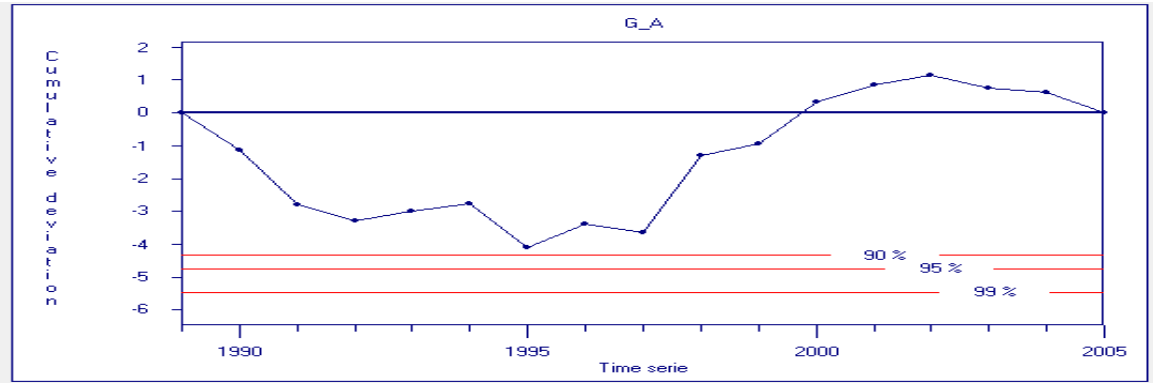

Figure3-21: Homogeneity test of flow data

3.11.4 Sub-basin and seasonal rain fall variation profile

Mean monthly rainfall profile of the entire period from (1986-2015) illustrates local seasonal rainfall variation as well as spatial differences within the basin. Relevant Statistics of the selected key stations base series rainfall values within this region are given in table 3-9. The corresponding profiles are graphically illustrated in Figure 3-22 and Figure 3-23. The monthly profile indicates the occurrence and relative strength of the dry, wet and intermediate season of monthly rainfall in the different location of the catchments area. The rainfall patterns of the study area reflect the Mono-Modal regime.

Stations	Jan	Feb	Mar	Apr	May	Jun	Jul	Aug	Sep	Oct	Nov	Dec	Annual
Anger	3.3	7.3	35.8	55.6	143.6	224.8	247.9	236.3	234.6	101.6	22.3	7.3	1320.4
G_Ayana	3.8	7.7	34.4	67.7	166.9	267.9	279.9	246.9	239.4	109.5	24.8	8.7	1457.6
Nekemte	6.7	12.2	49.5	82.5	209.4	332.7	313.3	313.5	258.3	127.0	42.4	16.6	1764.2
Shambu	6.9	11.2	45.3	66.9	144.6	227.5	271.9	250.4	200.3	67.0	26.6	12.3	1330.9
Alibo	6.8	8.5	48.1	69.1	158.2	309.7	425.3	386.2	257.6	97.2	39.9	10.7	1817.4

Table 3-10: Mean Monthly Rainfall of all stations in (mm)

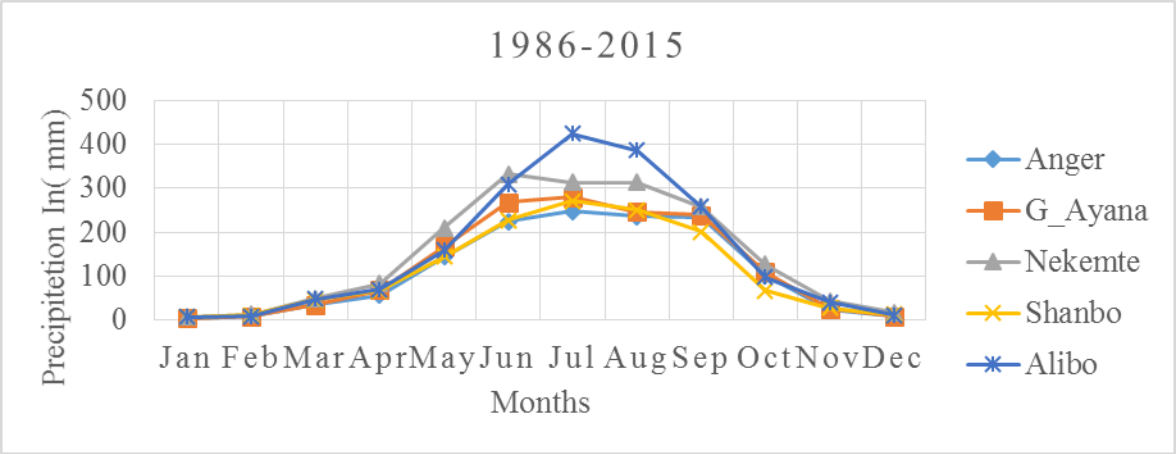

Figure 3-22: Comparison of Seasonal Rainfall Variation in the major stations

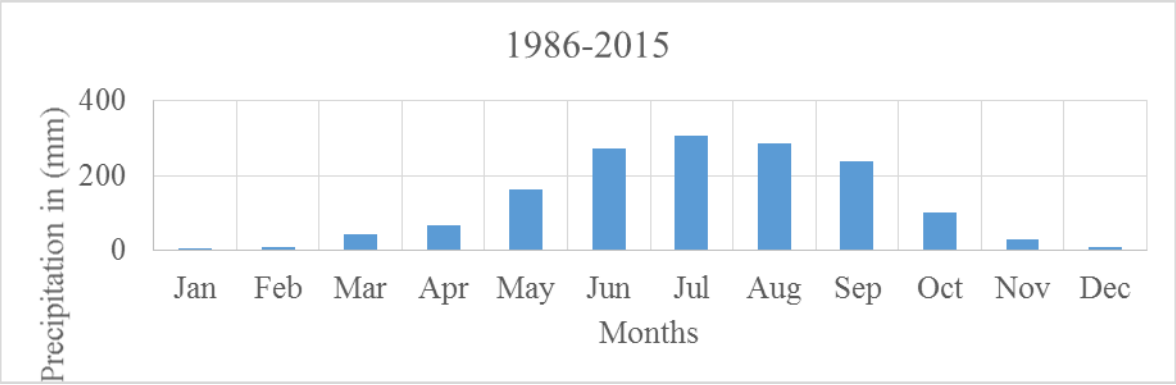

Figure 3-23: Seasonal Rainfall Variations for the Study Area

3.12 Model Setup

3.12.1 Watershed Delineation

The watershed and sub watershed delineation was performed using 30m DEM resolution data using Arc SWAT model watershed delineation function. First, the SWAT project set was created. The watershed delineation processes consists of five major steps, DEM setup, stream definition, outlet and inlet definition, watershed outlet selection definition and calculation of sub basin parameters. Once, the DEM setup was completed and the location of outlet was specified on the DEM, the model automatically calculates the flow direction and flow accumulation. Subsequently, stream networks, sub watersheds and topographic parameters were calculated using the respective tools. The stream definition and the size of sub basins were carefully determined by selecting threshold area or minimum drainage area required to form the origin of streams. Using threshold value suggested by the Arc SWAT interface (8526.27ha), the Anger sub basin was delineated in to 26 sub basins having an estimated total area of 7980.4km2 Figure3-24.

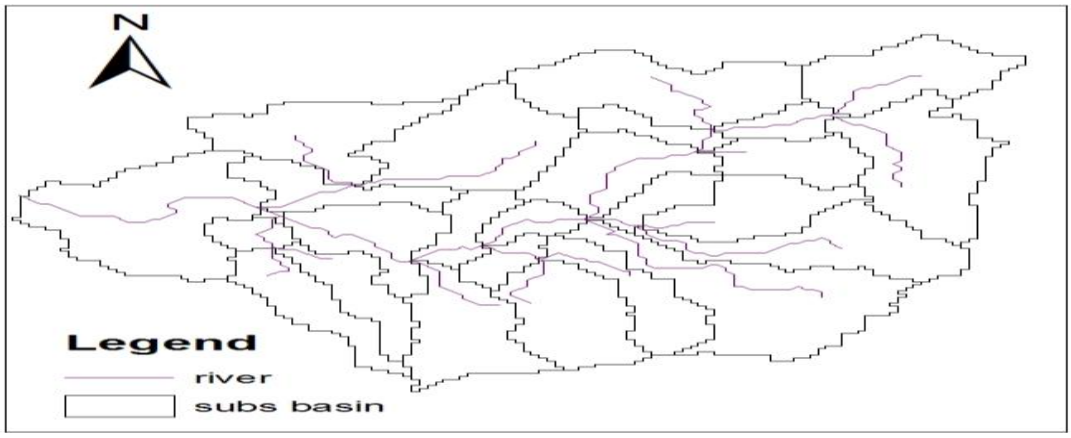

Figure3-24: Sub Basin Map of Anger Sub Basin

During the watershed delineation process, the topographic parameters (elevation, slope) of the watershed and its sub watershed were also generated from the DEM data. Accordingly the elevation of the watershed ranges from 868 to 3144 above mean sea level the height elevation is at the Jarete Jiridiga Mountain and the lowest at the watershed outlet, Balo Jegofay. Slope classification was carried out based on height range of DEM used during watershed delineation. The slope values of the watershed were reclassified in percent. It reclassified into five class.

Classes	Slope range (%)	Area	
		ha	%
Class 1	0-4	410017.7830	51.38
Class 2	4-8	213736.3879	26.78
Class 3	8-15	131174.2716	16.44
Class 4	15-25	39011.9091	4.89
Class 5	> 25	4101.9233	0.51

Table 3-11: Slope class of Anger sub basin and Area coverage in percent

3.12.2 Hydrologic Response Units Analysis

The sub watershed were divided into HRUs by assigning the threshold values of land use and land cover, soil and slope percentage. In general the threshold level used to eliminate minor land use and land covers in sub basin, minor soil within land use and land cover area and minor slope classes within a soil on specific land use and land cover area. Following minor elimination, the area of remaining land use and land covers, soils and slope cases are reapportioned so that 100% of their respective area modeled by SWAT. Land use, soil and slope characterization for Sub basin was performed using commands from HRU analysis menu on the Arc SWAT Toolbar. These tools allowed loading land use and soil maps which are in raster formats in to the current project, evaluates slope characteristics and determining the land use/soil/slope class combinations in the delineation sub basin. In the model, there are two options in defining HRU distribution: assign a single HRU to each sub basin or assign multiple HRUs to each sub basin based on a certain threshold values. The SWAT user's manual suggests that a 20% land use threshold, 10% soil threshold and 20% slope threshold are adequate for most modeling application.

Therefore, for this study, HRU definition with multiple options that accounts for 10% land use, 20% soil and 10% slope threshold combination was used. These threshold values indicate that land

uses which form at least 10% of the sub basin area and soils which form at least 20% of the area within each of the selected land uses will be considered in HRU. Hence, the sub basin was divided in to 203 HRUs, each has a unique land use and soil combinations. The number of the HRUs varies with in the sub watersheds.

3.12.1 *Weather Generator`*

In developing countries, there is a lack of full and realistic long period of climatic data. Therefore, the weather generator solves this problem by generating data from the observed one (Danuso, 2002). The Model requires the daily values of all climatic variables from measured data or generated from values using monthly average data over a number of years. This study used measured data for all climatic variables. However, the weather data obtained for the stations in and around Sub basin had missed records in some of the variables. Therefore, this missed values were filled with the weather generator utility in the Arc SWAT model from the values of weather generator parameters. Weather data of three stations (G_ Ayana, Nekemte and Shambu) with continues records were used as input to determine the values of weather generator parameters. Hence, for weather generator data definition, the weather generators data file wgnstations.txt was selected first. Subsequently, rain fall data, temperature data, relative humidity data, solar radiation data and wind speed data were selected and added to model.

The SWAT Model contain weather generator model called WXGEN (Shapley and Williams, 1990). It is used in SWAT model to generate climatic data or to fill missing data using monthly statistics which is calculated from existing daily data. From the values of weather generator parameters, the weather generator first separately generates precipitation for the day. Maximum temperature, minimum temperature, solar radiation and relative humidity are then generated. Lastly, the wind speed is generated independently. To generate the data, SWAT Weather Database is designed to be a friendly tool to store and process daily weather data to be used with SWAT projects. It is capable of: Storing relevant daily weather information; easily creating .txt files to be used as input information during an Arc SWAT project setup; efficiently calculating the WGEN statistics of several weather stations in one-step run (Essenfelder, A. H., 2016). As for any SWAT project, missing values must be entered as -99.0. Such values will not be used during the calculation of the WGEN statistics. They will, however, be written to the Arc SWAT input .txt files. (Essenfelder, A. H., 2016)

3.12.2 Sensitivity analysis

Calibration is necessary to optimize the values of the model parameters which help to reduce the uncertainty in model outputs. However, such type of model with a multiple parameters, the difficult task is to determine which parameters are to be calibrated. In this case, sensitivity analysis is important to identify and rank parameters that have significant impact on the specific model output interest (Van Griensven, 2006). Therefore, for this study, sensitivity analysis was done prior to the calibration process in order to identify important parameters for model calibration.

The average monthly stream flow data of ten year from 1990-1999 of the sub basin gauging station were used to compute the sensitivity of stream flow parameters. In sensitivity process, by entering the Arc SWAT interface SWAT-CUP sensitivity analysis window, first the SWAT simulation was specified for performing the sensitivity analysis and the location of the sub basin where observed data was compared against simulated output. Then, selected parameters were entered for sensitivity analysis with the default lower and upper parameter bounds. Hence, 26 flow parameters were included for the analysis with default values as recommended by (Van Griensven, 2006). And rank of sensitivity was based on the value of t-sat and p-values.

3.13 Model Calibration and Validation

Following the sensitivity analysis result, model calibration was done to obtain optimum values for sensitive parameters. SWAT provides three options for calibration: manual calibration, auto-calibration and combination of these two methods. For this study, first manual calibration was done to fine tone some of the parameters and some model parameters were adjusted by manual calibration. Then, auto calibration by SWAT-CUP was done on monthly time steps using the average measured stream flow data of the sub basin covering from 1990-1999.There were different calibration procedure methods Generalized Likelihood Uncertainty Estimation (GLUE), Parameter Solution (ParaSol), Sequential Uncertainty Fitting (SUFI2) and Markov chain Monte Carlo (MCMC). For this study, the Sequential Uncertainty Fitting (SUFI2) option was selected. This method was chosen for its applicability to both simple and complex hydrological models. In this procedure, by entering the Arc SWAT interface SWAT_CUP Auto-calibration window, first the SWAT simulation was specified for performing the auto-calibration and the location of the sub basin where observed data could be compared against simulated output. Then, the desired parameters for optimization, observed data file, and methods of calibration were selected.

Hence, seven flow parameters were considered in the calibration process. After the auto calibration runs completed, the model was run using the best parameter output values and the simulations were compared with observed stream flow data using Nash and Sutcliffe coefficient of efficiency (ENS) and coefficient of determination (R^2).Validation was also done to compare the model outputs with an independent data set without making further adjustment of the parameter values. Model validation is comparison of model outputs with an independent data set without making further adjustment which may adjust during calibration process. The measured data of average monthly stream flow data of six years from 2000-2005 were used for the model validation process. In this process, the two model performance values were also checked here to make sure that the simulated values are still within the accurate limits.

3.13.1 Model Performance Evaluation

Model evaluation is an essential measure to verify the robustness of the model. In this study, two model evaluation methods were used, which were Nash-Sutcliffe efficiency (NSE) and coefficient of determination (R^2)

$$ENS = 1 - \frac{\sum((Qi - Pi)^2}{\sum(Qi - Qavr)^2} \quad (3.17)$$

Where:-

- Qi- measured value
- Pi- simulated value and
- Qav- average observed value
- Pav- average simulated value

The determination coefficient (R^2) describes the proportion the variance in measured data by the model. It is the magnitude linear relationship between the observed and the simulated values. R^2 ranges from 0(which indicates the model is poor) to 1 (which indicates the model is good), with higher values indicating less error variance, and typical values greater than 0.6 are considered acceptable (Santhi. C., 2001).

The R^2 is calculated using the following equation:

$$R^2 = \frac{\sum[Qi - Qavr][Pi - Pavr]}{\sqrt{\sum[(Qi - Qavr)]2}\sqrt{\sum[(Pi - Pavr)]2}} \quad (3.18)$$

Where:-

- Qi- measured value
- Pi- simulated value and
- Qavr - average observed value
- Pavr - average simulated value

4 RESULT AND DISCUSSION

4.1 Accuracy Assessment

The accuracy assessment is used to determine the precision of the classified image. It was performed using confusion matrix. Using the original mosaic image and the Google Earth Image as a reference, randomly selected points were compared with the corresponding classification. So 130, 131 and 141 points were selected for the validation of 1986, 2000 and 2010 images respectively. Table 4-2, 4-3 and 4-4 show a confusion matrix for the three Landsat images.

- Overall accuracy

The overall accuracy gives the overall results of the confusion matrix. It is calculated by dividing the total number of correct pixels (diagonals) by the total number of pixels in the confusion matrix. The results show that the overall accuracy for the maps of 1986, 2000 and 2010 were 88%, 87% and 92% respectively. According to (Anderson *et al*, 1976), the minimum accuracy value for reliable land cover classification is 85 %. The other authors (eg. Bedru, 2006), describes that the expected accuracy is determined by the users themselves depending on the type of application the map product will be used later. Accuracy levels are accepted by users may not acceptable by other users for certain task (Bedru, 2006). Therefore, based on table 4-2, 4-3 and 4-4 the classification carried out in this study produces an overall accuracy that fulfils the minimum accuracy level defined by Anderson for those land cover maps of Anger watershed.

- Kappa coefficient

The kappa coefficient gives the agreement between classified image and reference or ground truth. A Kappa coefficient equal to 1 means perfect agreement where as a value close to zero means that the agreement is no better than would be expected by chance. The results indicated that the Kappa coefficient for the maps of 1986, 2000 and 2010 were 81%, 79.5% and 83.2% respectively for each year. Therefore, based on table 4-2, 4-3 and 4-4 the classification carried out in this study produces a kappa coefficient with substantial agreement for the year 1986 and almost prefect agreement for year 2000 and 2010.

- Producer's Accuracy

The producer's accuracy tells us how well a certain area can be classified. It is obtained by dividing the number of correctly classified pixels in the category by the total number of pixels of the category in the reference data. The producer's accuracy is also known as an Omission Error, which

is the probability of a reference pixels being classified correctly. It gives only the proportion of correctly classified pixels. The overall result of the producer's accuracy ranges from 58% to 100%. The lowest values were misclassified due to similar spectral value of different land cover classes. For instance, Water body with forest, Agricultural land with forest cover, Agricultural land during dry season with Built up area (which is classified as Built up area), etc. somehow affects the level of classification.

- User's Accuracy

It is the ratio between the total number of pixels correctly belonging to a class (diagonal elements) and the total number of pixels assigned to the same class by the classification procedure (row total). This quantity describes the probability that a pixel of the classified image truly corresponds to the class to which it has been assigned. In this study, the user's accuracy ranges from 78% to 100%. The lowest value "Forest" were, to some extent, misclassified because of the similarity spectral properties of Forest and Water Body.

Table 4-1 confusion matrix for the classification of 1986

		Ground truth Data						
		AGL	FL	BU	WB	SL	Grand Total	User's Accuracy
Classification Data	AGL	48	1			2	51	94%
	FL	1	10			1	12	83%
	BU	1		4			5	80%
	WB	1			5		6	83%
	SL	7	2			47	56	84%
Grand Total		58	13	4	5	50	130	
Producer's Accuracy		83%	77%	100%	100%	94%		Overall Accuracy=88%

Kappa coefficient=81%

Note: AGL=Agricultural land; WB=Water Body; FL=Forest land, SL=Shrub land; BU= Built Up.

Table 4-2 confusion matrix for the classification of 2000

		Ground truth Data						
		FL	AGL	SL	WB	BU	Grand Total	User's Accuracy
Classification Data	FL	8	1				9	89%
	AGL	3	54	5			62	87%
	SL	2	4	43		1	50	86%
	WB			1	4		5	80%
	BU					5	5	100%
Grand Total		13	59	49	4	6	131	
Producer's Accuracy		62%	92%	88%	100%	83%		Overall Accuracy=87%

Kappa coefficient=79.5%

Note: AGL=Agricultural land; WB=Water Body; FL=Forest land, SL=Shrub land; BU= Built Up.

Table 4-3 confusion matrix for classification of 2010

		Ground truth Data						
		WB	AGL	FL	SL	BU	Grand Total	User's Accuracy
Classification Data	WB	4					4	100%
	AGL		97	3	1	1	101	96%
	FL	1	1	7			9	78%
	SL		1	3	18		22	82%
	BU		1			4	5	80%
Grand Total		5	100	12	19	5	141	
Producer's Accuracy		80%	97%	58%	95%	80%		Overall Accuracy=92%

Kappa coefficient=83.2%

Note: AGL=Agricultural land; WB=Water Body; FL=Forest land, SL=Shrub land; BU= Built Up.

4.2 Land use Land Cover Change Analysis

The three-land use /cover maps of 1986, 2000 and 2010 generated from the land sat TM and ETM+ imaginary classification (Figure 4-7,4-8 and 4-9 respective years). It is easily shown that there is an increase of Agricultural land and built up area, and decrease of forested areas, shrub and grassland and water bodies over 25 years. In general, during 25-year period the Agricultural land increases at about 39.3% whereas the Shrub and grass land decreased by 32.9% and also forested area decreased by 6.6%. For the individual class area and change statistics for the three periods are summarized as follows in Figure 4-1: bellow.

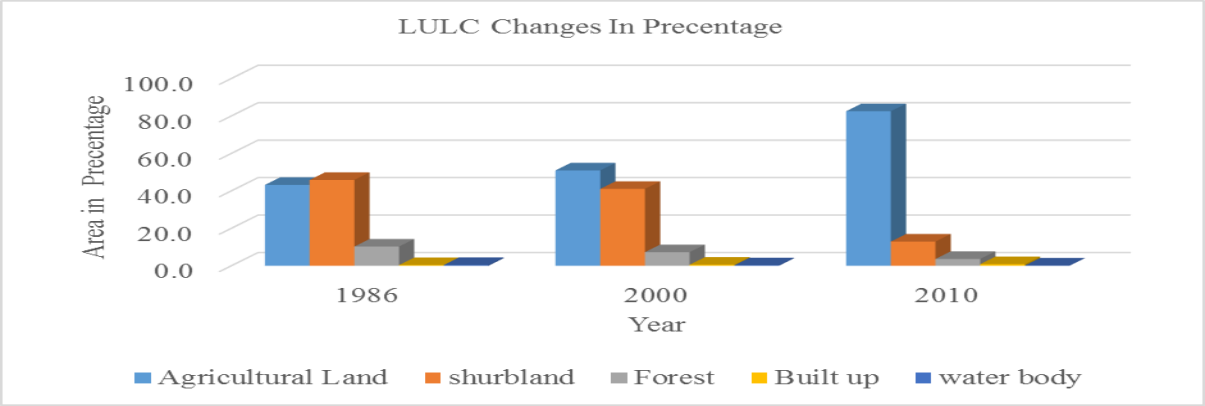

Figure 4-1 LULC Area in percentage

LULC Type	LULC Area Change in %		
	2000-1986	2010-2000	2010-1986
Agricultural Land	7.7	31.6	39.3
shrub land	-4.8	-28.1	-32.9
Forest	-3.0	-3.6	-6.6
Built up	0.2	0.3	0.5
water body	-0.2	-0.1	-0.3

Table 4-4 LULC Area change in percentage

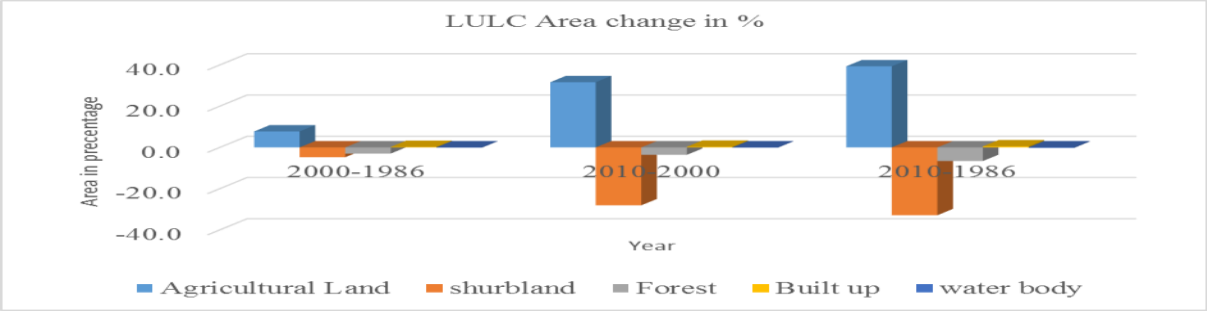

Figure 4-2 LULC Area change in percentage

In the sub basin the area covered by different land use land cover in percent During 1986 were 43.2% Agricultural land, 10.3% forest land, 45.8 %s shrub and grass land, 0.4% Built Up area and 0.4%water body. And also, during 2000 were 50.9% Agricultural land, 7.2 % forest land, 41 %shrub and grass land, 0.6 % Built Up area and 0.2%water Body. Lastly, during 2010 were 82.5% Agricultural land, 3.6% forest land, 12.9%shrub and grass land, 0.8% Built Up area and 0.1% water body. So Agricultural land, shrub land and forest were dominate the sub basin during the study period and Built Up area and water body was also the parts of the watershed. For detail information presented tables and figures below.

Land use / Land cover type	Land use according to SWAT database	SWAT code	Area	
			Km^2	%
Agricultural land	Agricultural land close to grown	AGRC	3450	43.2
Shrub and Grass land	Forest deciduous	FRSD	819	45.8
Forest	Forest mixed	FRST	3661	10.3
Built Up	Residential-Low Density	URLD	28	0.4
Water body	Water	WATR	31	0.4

Table 4-5 LULC Area during 1986

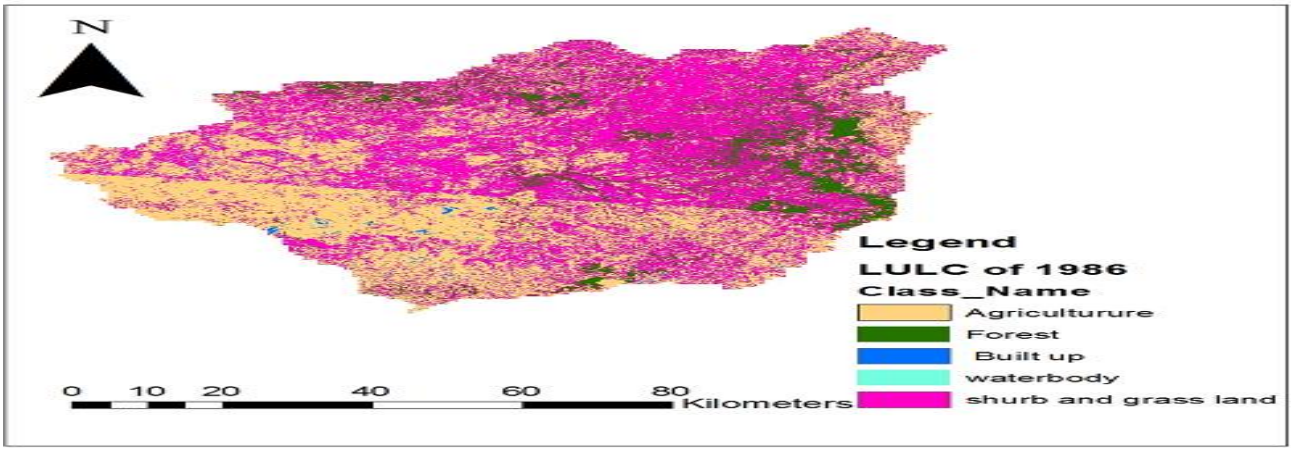

Figure 4-3 LULC classification during 1986 (GLCF wave site)

Land use / Land cover type	Land use according to SWAT database	SWAT code	Area	
			Km^2	%
Agricultural land	Agricultural land close to grown	AGRC	4067	50.9
Shrub and Grass land	Forest deciduous	FRSD	3278	41.0
Forest	Forest mixed	FRST	579	7.2
Built Up	Residential-Low Density	URLD	44	0.6
Water body	Water	WATR	19	0.2

Table 4-6 LULC Area during 2000

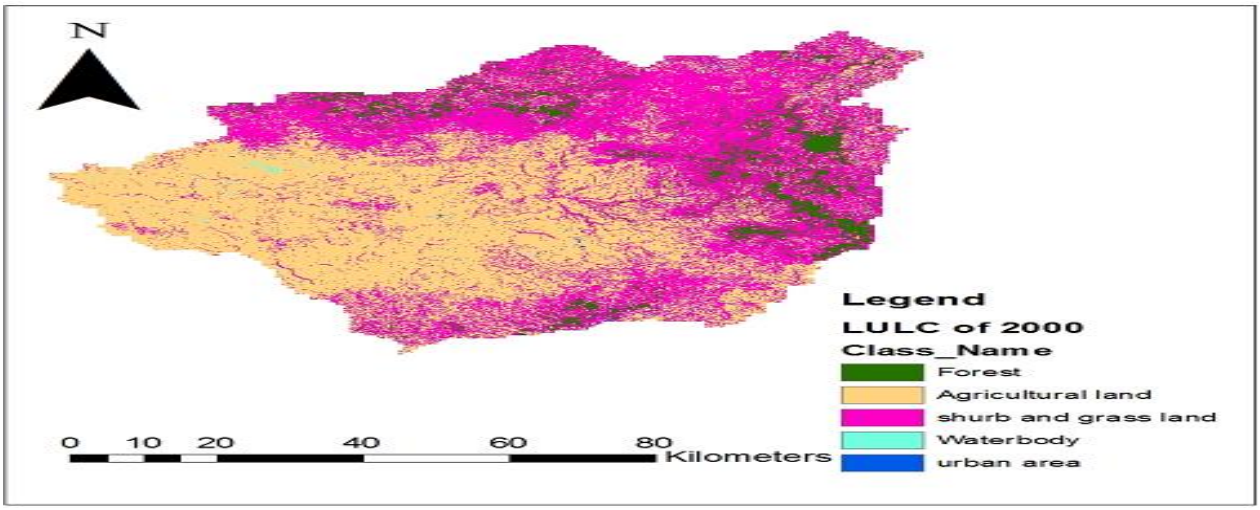

Figure 4-4 LULC classification during 2000 (GLCF wave site)

Land use / Land cover type	Land use according to SWAT database	SWAT code	Area	
			Km^2	%
Agricultural land	Agricultural land close to grown	AGRC	6590	82.5
Shrub and Grass land	Forest deciduous	FRSD	1031	12.9
Forest	Forest mixed	FRST	290	3.6
Built Up	Residential-Low Density	URLD	66	0.8
Water body	Water	WATR	9	0.1

Table 4-7 LULC Area during 2010

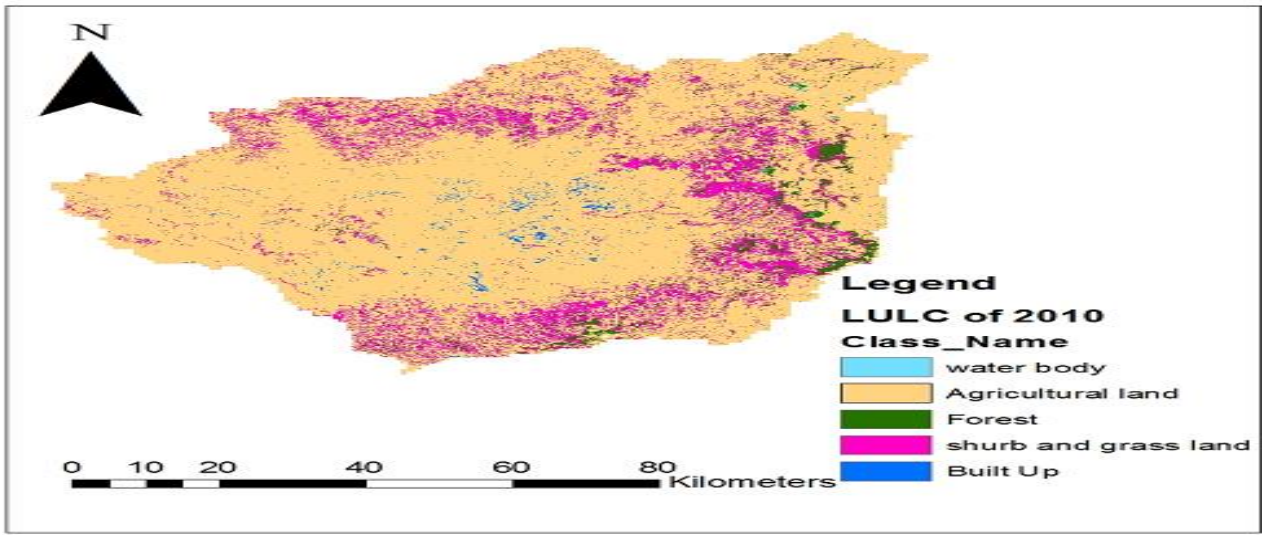

Figure 4-5 LULC classification during 2010(GLCF wave site)

4.3 Baseline Scenario developed for Anger station

4.3.1 Minimum temperature

The monthly mean minimum temperature downscaled in the baseline period shows a reasonably good agreement with the observed mean minimum temperature for all months as shown in figure 4.6. For other station presented in appendix E

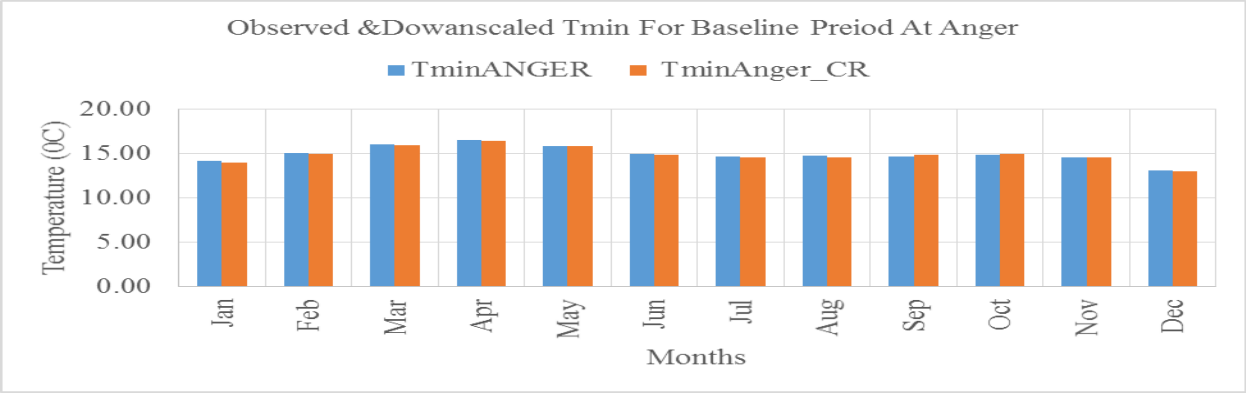

Figure 4-6 observed & Downscaled monthly mean Tmin for the baseline

The variability of monthly minimum temperature of observed values is well preserved in the downscaled value from April to November. From January to February and November to December the variance of observed value is slightly higher than the downscaled values but the general trend of both observed and downscaled values shows a similar pattern as shows Figure 4.7. For other station presented in appendix E

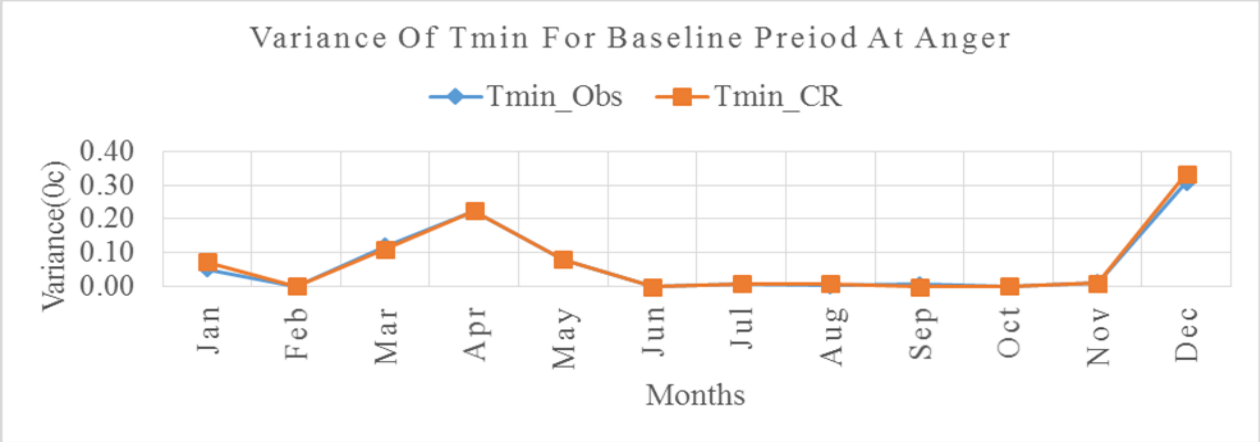

Figure 4-7 Variance of Observed & Downscaled Tmin for the Baseline period

4.3.2 Maximum Temperature

The downscaled monthly mean maximum temperature tells solid relations with the observed temperature for the baseline period as shown Figure 4.8. For other station presented in appendix F

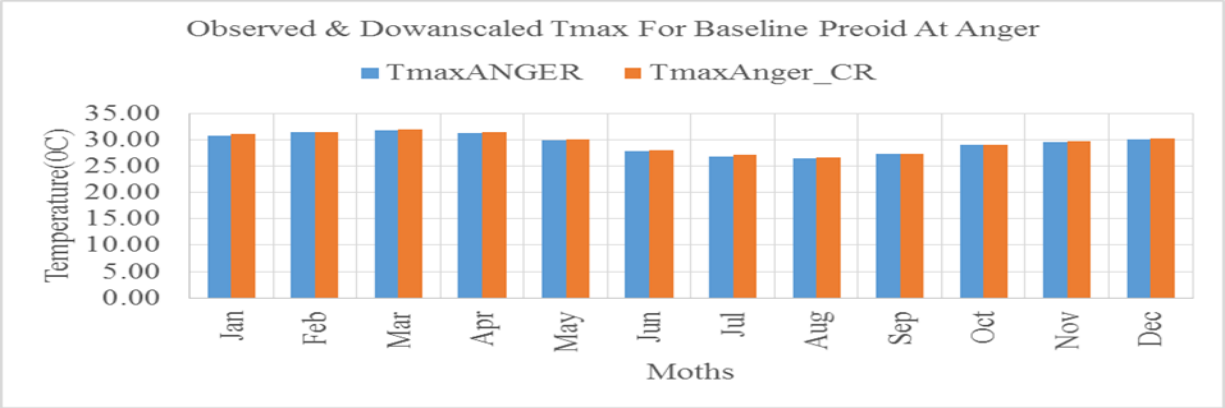

Figure 4-8 Observed & downscaled monthly mean Tmax for the baseline period

The variability of monthly maximum temperature of observed values is well preserved in the downscaled value from October to December. In February and July the variance of observed value is slightly higher than the downscaled values and in April and September the variance of observed value is slightly lower than the down scaled values but the general trend of both observed and downscaled values shows a similar pattern presented in figure 4.9. For other station presented in appendix F.

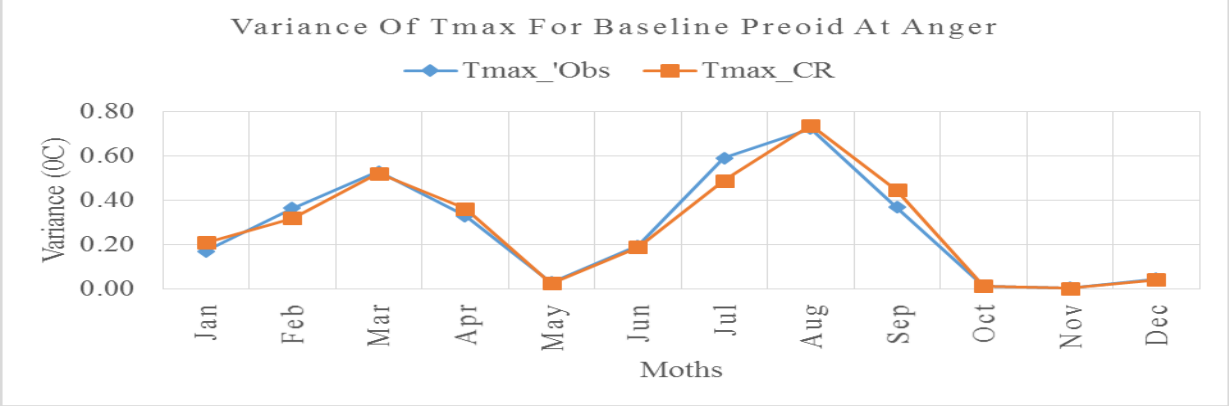

Figure 4-9 Variance of Observed & downscaled Tmax for baseline period

4.3.3 Precipitation

The GCM model performs soundly well in estimating the mean monthly precipitation in all months. The monthly precipitation downscaled for the baseline period is shown in Figure 4.10. For other station presented in appendix G.

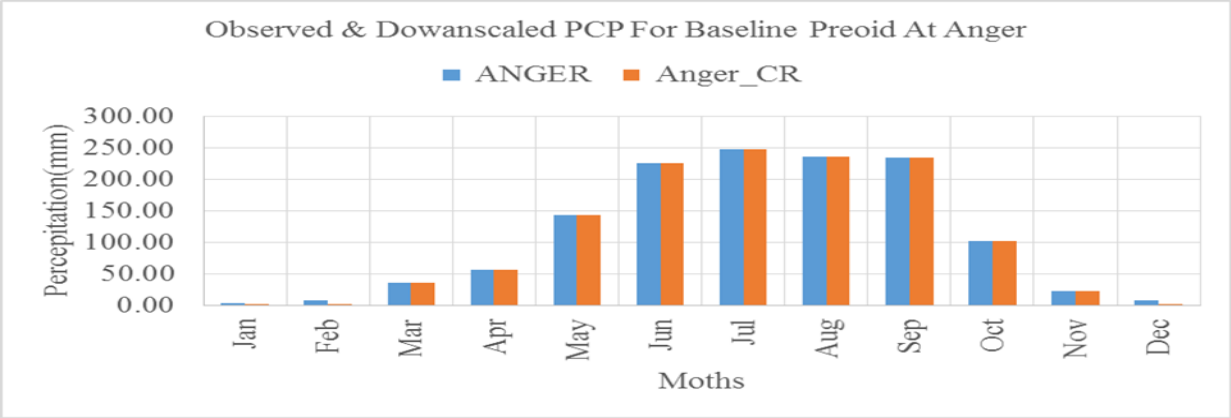

Figure 4-10 Mean monthly Observed & downscaled precipitation for the baseline period

The variability of observed and downscaled precipitation shows good agreement in all months. Generally talking the variance of observed and downscaled precipitation shows a similar pattern which was presented in figure 4.11. For other station presented in appendix G.

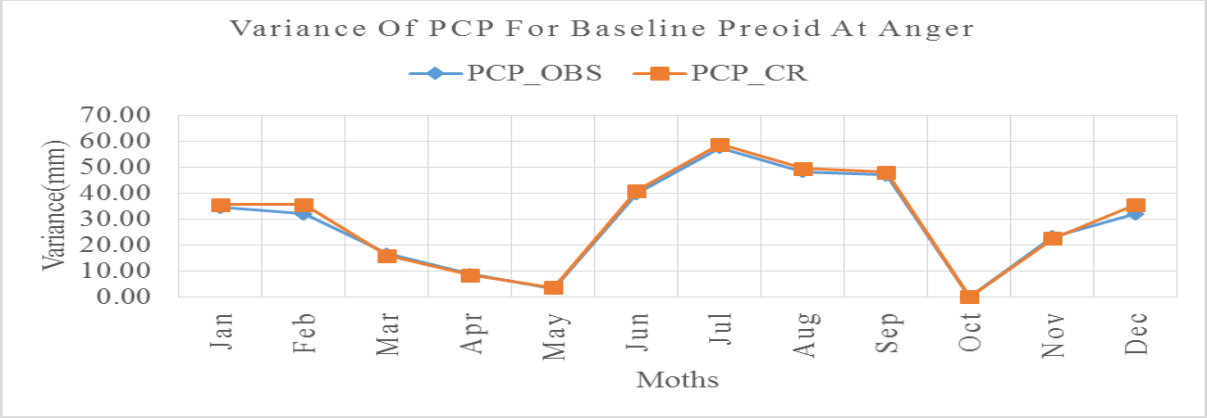

Figure 4-11 Variance of Observed & Downscaled Precipitation for the baseline period

4.4 Sub basin Climate change analysis

The annual precipitation and air temperature were evaluated for the base year and future seniors based on the metrological data from 1986 to 2100 From GCM which was bias corrected. Precipitation decreased during 2020s by 2.06%, during 2050s by 7.63% and during 2080s by 17.67%. And also, maximum and minimum temperature were increased during 2020s by 0.52 ^{0}C, 0.68 ^{0}C, during 2050s by 0.40 0C, 1.740C and during 2080s by 2.54 ^{0}C, 3.04 ^{0}C respectively in the sub basin. Increasing maximum temperature showed more variation at the monthly time step with arrange from -0.05oC to 1.32oC in 2020s, 0.58oC to 3.01oC in 2050s and 1.44oC to 4.50oC in 2080s. And also, increasing minimum temperature showed more variation at the monthly time

step with a range from 0.39oC to 1oC in 2020s, 1.17oC to 2.37oC in 2050s and 2.18oC to 3.80oC in 2080s.These result indicate that the climate is changed in sub basin during the study, and characterized by decreased precipitation and increased maximum and minimum temperature.

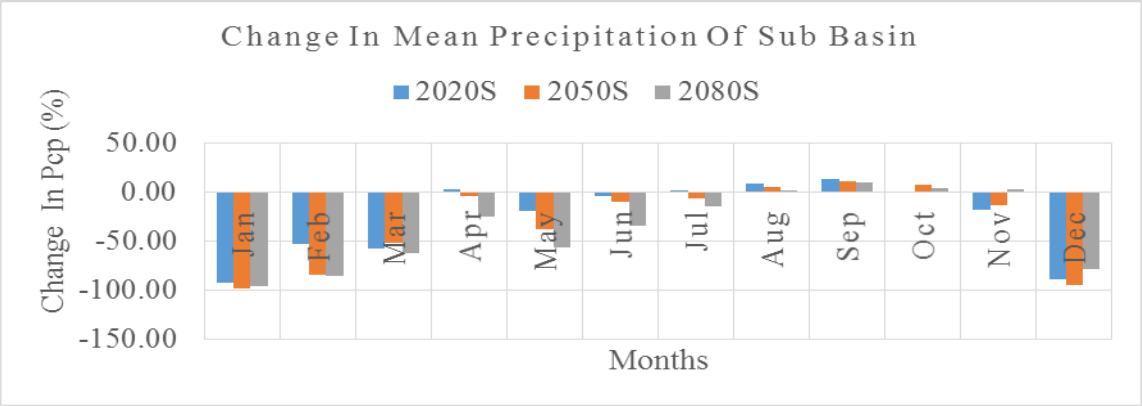

Figure 4-12 Change in mean monthly precipitation of sub basin

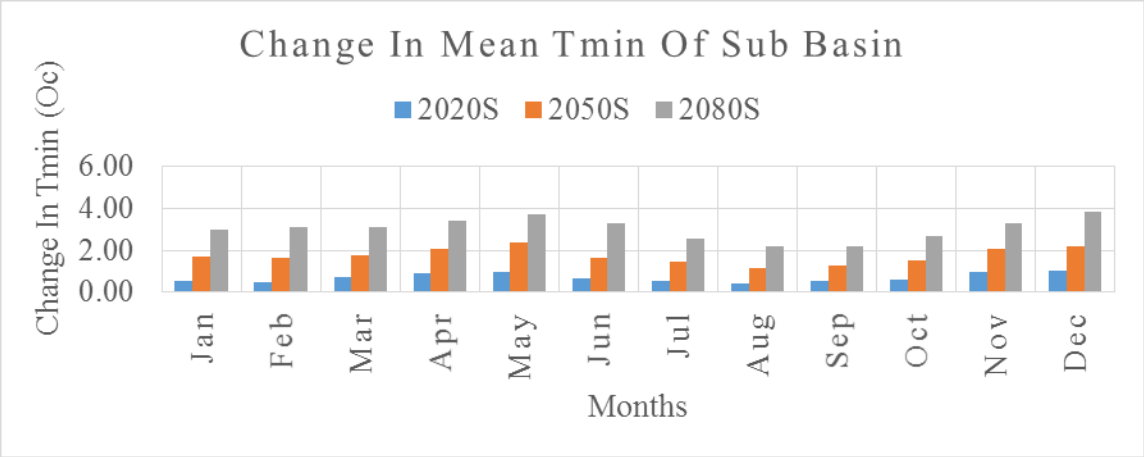

Figure 4-13 change in mean monthly Tmin of sub basin

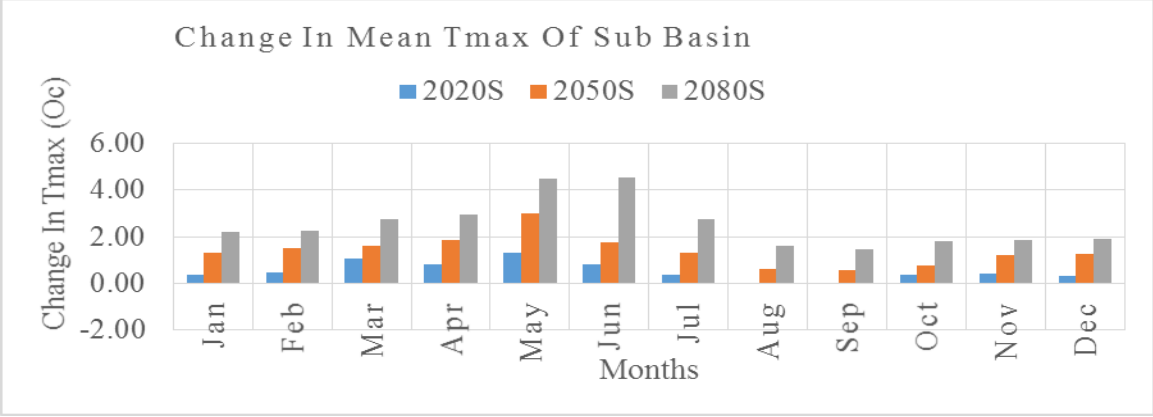

Figure 4-14 Change in mean monthly Tmax of sub basin

4.5 Annual average and monthly variability of Precipitation

For Anger station the downscaled Precipitation shows decreasing trend for all months in all future time horizons .The average annual precipitation in 2020s will be decreased by 2.59%. For the 2050s periods the average annual precipitation will be decreased by 12.76%. For the 2080s periods the average annual precipitation will be decreased by 21%. Decreasing precipitation showed more variation at the monthly time step with a range from -49.56% to 73.98% in 2020s, -99.23% to 1.62% in 2050s and -98.84% to 93.71% in 2080s.

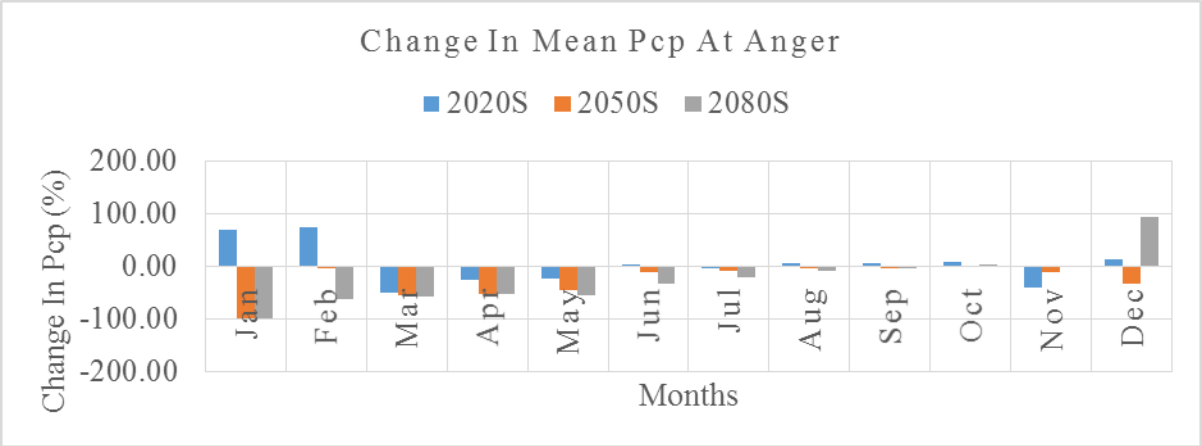

Figure 4-15 change in mean monthly Pcp at Anger

For G_Ayana station the downscaled Precipitation shows decreasing trend for all months in all future time horizons .The average annual precipitation in 2020s will be decreased by 1.97%. For the 2050s periods the average annual precipitation will be decreased by 7.62%. For the 2080s periods the average annual precipitation will be decreased by 18.43%. Decreasing precipitation showed more variation at the monthly time step with a range from -98.05% to 18.25% in 2020s, -99.65% to 20.79% in 2050s and -98.75% to 69.74% in 2080s.

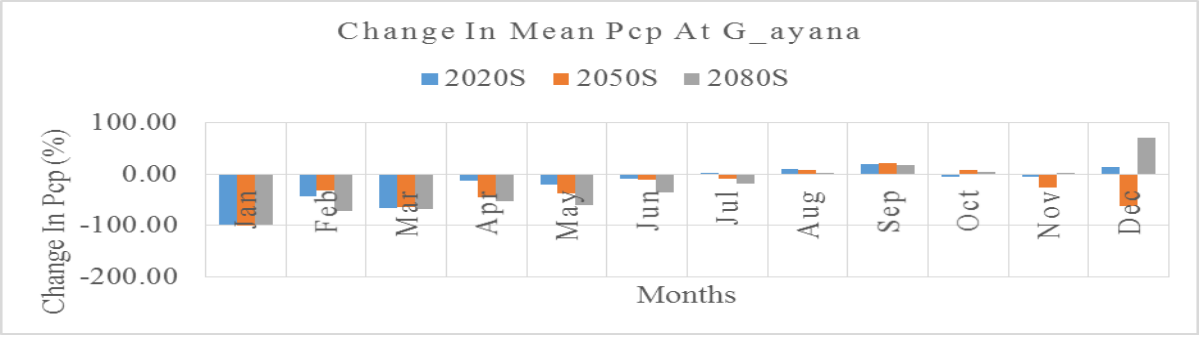

Figure 4-16 change in mean monthly Pcp at G_Ayana

For Nekemte station the downscaled Precipitation shows decreasing trend for all months in all future time horizons .The average annual precipitation in 2020s will be decreased by 2.66%. For the 2050s periods the average annual precipitation will be decreased by 12.35%. For the 2080s periods the average annual precipitation will be decreased by 19.81%. Decreasing precipitation showed more variation at the monthly time step with a range from -54.16% to 57.61% in 2020s, -99.48% to 48.18% in 2050s and -99.48% to 76.81% in 2080s.

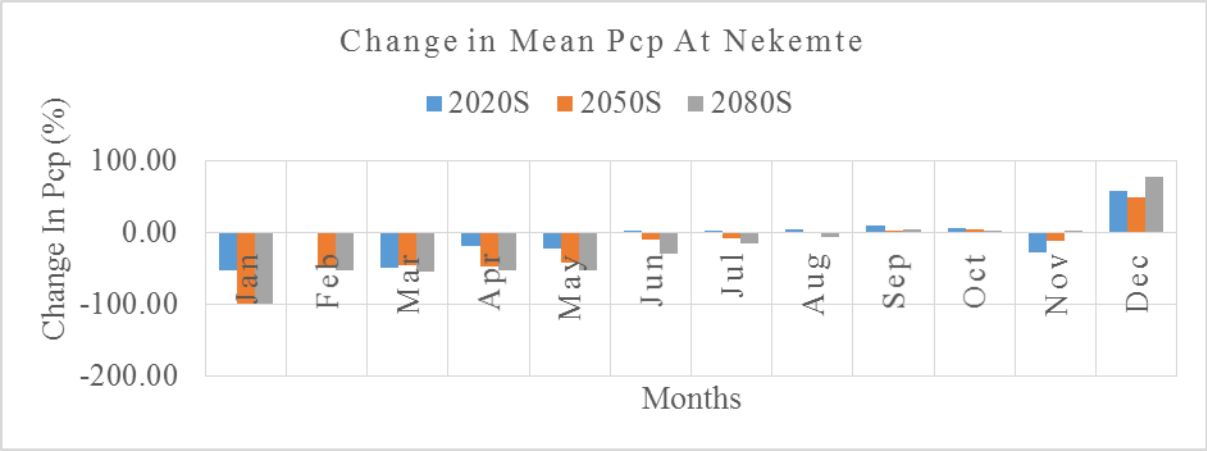

Figure 4-17 Change in mean monthly Pcp at Nekemte

For Shambu station the downscaled Precipitation shows decreasing trend for all months in all future time horizons .The average annual precipitation in 2020s will be decreased by 0.88%. For the 2050s periods the average annual precipitation will be decreased by 3.46%. For the 2080s periods the average annual precipitation will be decreased by 14.55%. Decreasing precipitation showed more variation at the monthly time step with a range from -79.08% to 63.35% in 2020s, -90.13% to 18.92% in 2050s and -82.70% to 72.83% in 2080s.

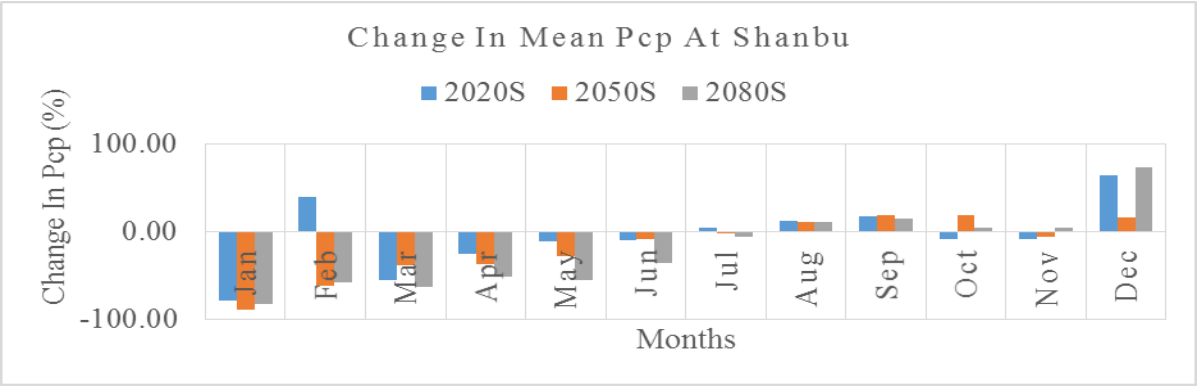

Figure 4-18 change in mean monthly Pcp at Shanbo

For Alibo station the downscaled Precipitation shows decreasing trend for all months in all future time horizons .The average annual precipitation in 2020s will be decreased by 2.25%. For the 2050s periods the average annual precipitation will be increased by 2.22%. For the 2080s periods the average annual precipitation will be decreased by 11.32%. Decreasing precipitation showed more variation at the monthly time step with a range from -69.33% to 19.57% in 2020s, -79.57% to 65.53% in 2050s and -69.73% to 98.02% in 2080s.

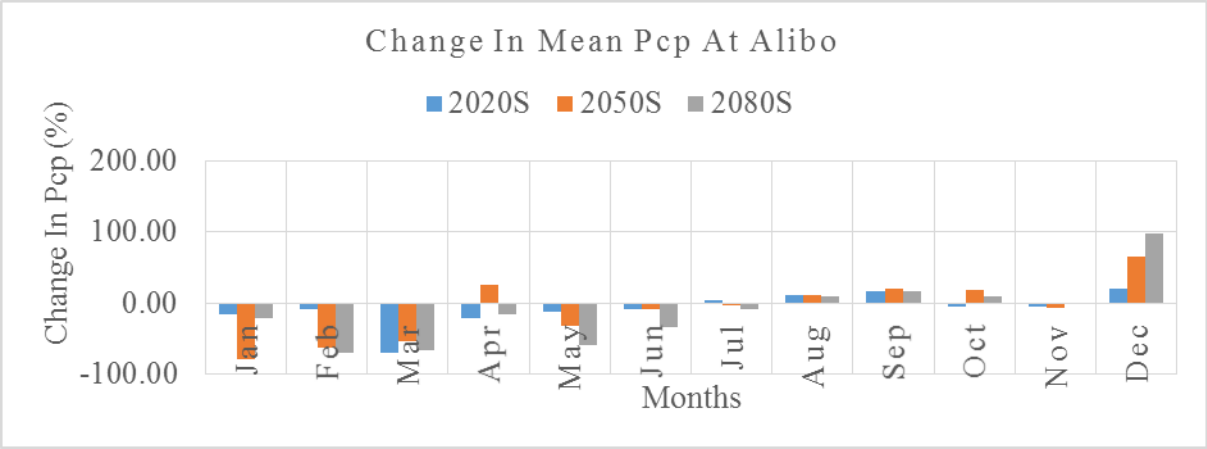

Figure 4-19 change in mean monthly Pcp at Alibo

4.6 Annual average and monthly variability of minimum temperature

For Anger station the downscaled minimum temperature shows an increasing trend for all months in all future time horizons .The average annual minimum temperature in 2020s will be increased by 0.54oC. For the 2050s periods the average annual minimum temperature will be increased by 0.98oC. For the 2080s periods the average annual minimum temperature will be increased by 1.21oC.Increasing minimum temperature showed more variation at the monthly time step with a range from 0.3oC to 1.1oC in 2020s, 1.1oC to 2.35oC in 2050s and 2.02oC to 3.80oC in 2080s.

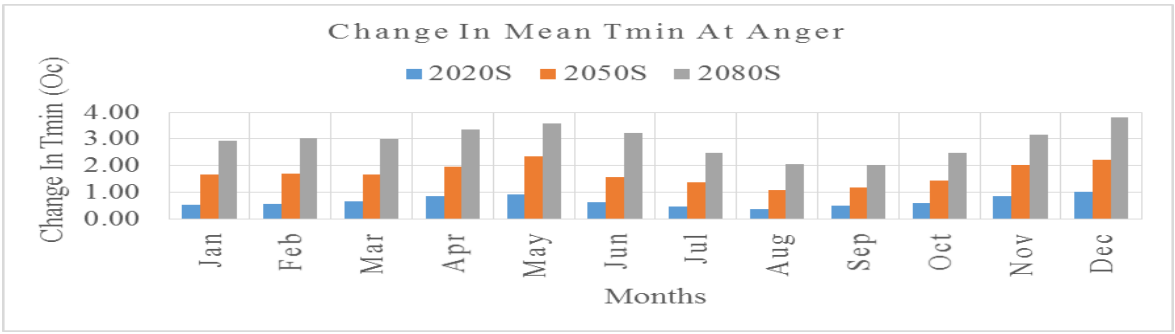

Figure 4-20 change in mean monthly Tmin at Anger

For G_Ayana station the downscaled minimum temperature shows an increasing trend for all months in all future time horizons .The average annual minimum temperature in 2020s will be increased by 0.78oC. For the 2050s periods the average annual minimum temperature will be increased by 2.0oC. For the 2080s periods the average annual minimum temperature will be increased by 3.49oC.Increasing minimum temperature showed more variation at the monthly time step with a range from 0.43oC to 1.16oC in 2020s, 1.33oC to 2.71oC in 2050s and 2.47oC to 4.44oC in 2080s.

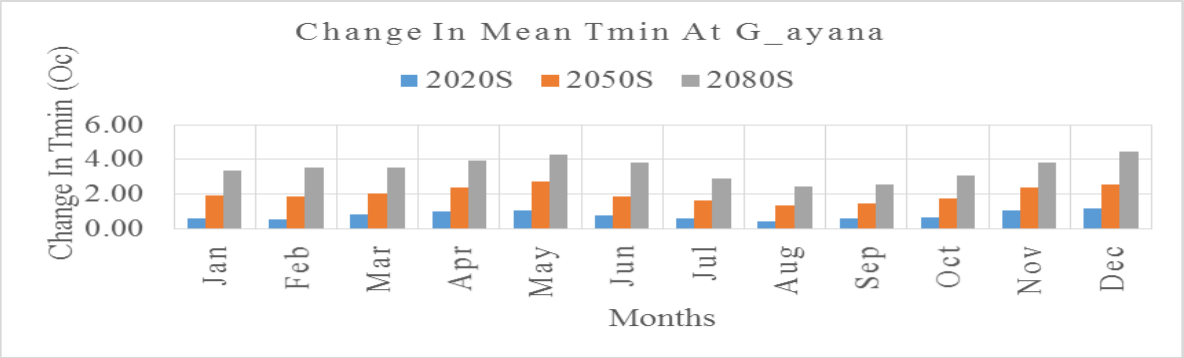

Figure 4-21 change in mean monthly Tmin at G_Ayana

For Nekemte station the downscaled minimum temperature shows an increasing trend for all months in all future time horizons .The average annual minimum temperature in 2020s will be increased by 0.51oC. For the 2050s periods the average annual minimum temperature will be increased by 1.31oC. For the 2080s periods the average annual minimum temperature will be increased by 2.30oC.Increasing minimum temperature showed more variation at the monthly time step with a range from 0.23oC to 0.77oC in 2020s, 0.85oC to 1.80oC in 2050s and 1.61oC to 2.96oC in 2080s.

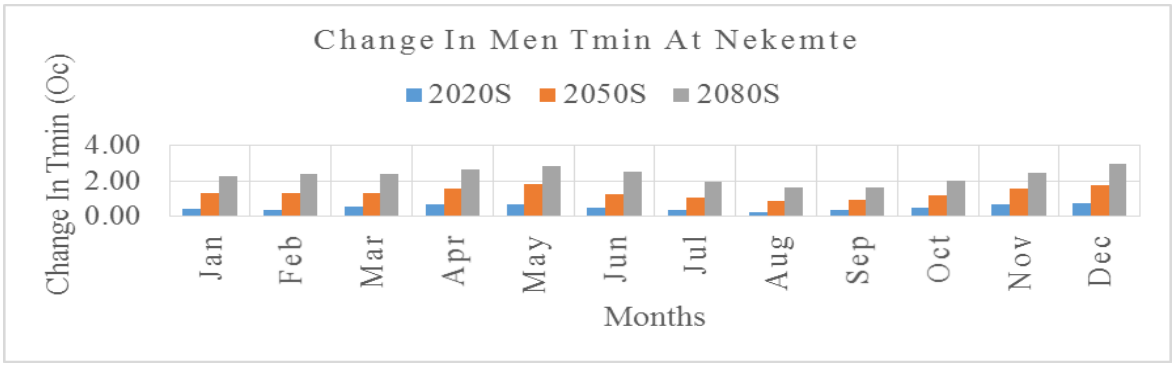

Figure 4-22 change in monthly Tmin at Nekemte

For Shambu station the downscaled minimum temperature shows an increasing trend for all months in all future time horizons .The average annual minimum temperature in 2020s will be increased by 0.56oC. For the 2050s periods the average annual minimum temperature will be increased by 1.43oC. For the 2080s periods the average annual minimum temperature will be increased by 2.52oC. Increasing minimum temperature showed more variation at the monthly time step with a range from 0.29oC to 0.83oC in 2020s, 1.02oC to 1.91oC in 2050s and 1.89oC to 3.06oC in 2080s.

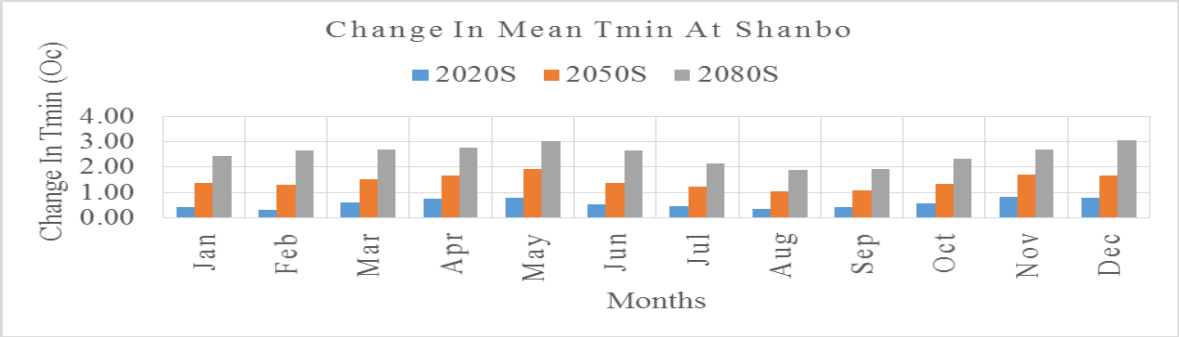

Figure 4-23 change in mean monthly Tmin at Shanbo

For Shambu station the downscaled minimum temperature shows an increasing trend for all months in all future time horizons .The average annual minimum temperature in 2020s will be increased by 0.93oC. For the 2050s periods the average annual minimum temperature will be increased by 2.37oC. For the 2080s periods the average annual minimum temperature will be increased by 4.18oC. Increasing minimum temperature showed more variation at the monthly time step with a range from 0.49oC to 1.39oC in 2020s, 1.66oC to 3.99oC in 2050s and 3.09oC to 5.66oC in 2080s.

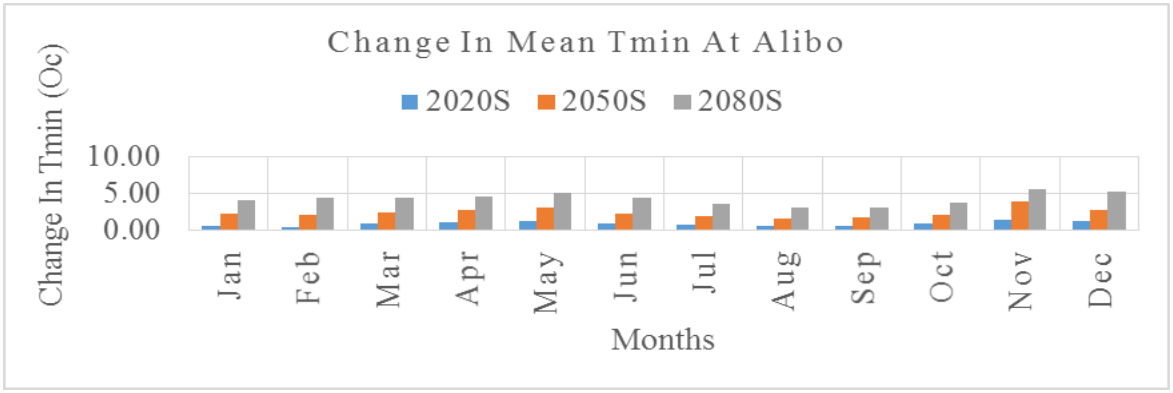

Figure 4-24 change in mean monthly Tmin at Alibo

4.7 Annual average and monthly variability of maximum temperature

For Anger station the downscaled maximum temperature shows an increasing trend for all months in all future time horizons .The average annual maximum temperature in 2020s will be increased by 0.54oC. For the 2050s periods the average annual maximum temperature will be increased by 0.98oC. For the 2080s periods the average annual maximum temperature will be increased by 1.21oC. Increasing maximum temperature showed more variation at the monthly time step with a range from -0.05oC to 1.41oC in 2020s, 0.69oC to 3.30oC in 2050s and 1.59oC to 5.03oC in 2080s.

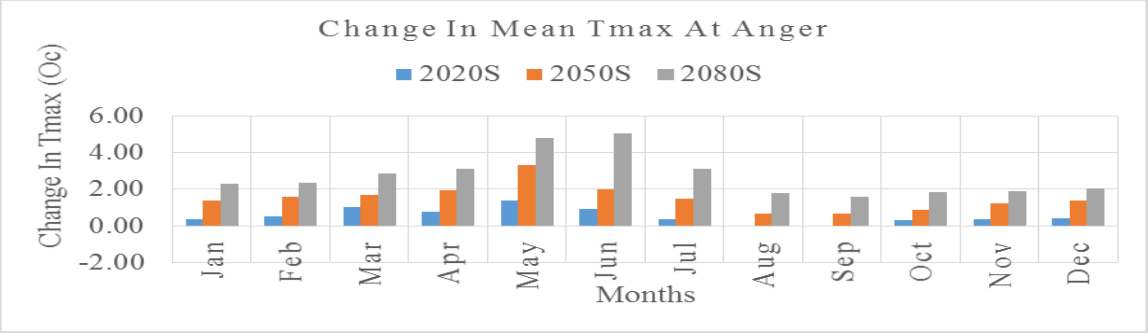

Figure 4-25 change in mean monthly Tmax at Anger

For G_Ayana station the downscaled maximum temperature shows an increasing trend for all months in all future time horizons .The average annual maximum temperature in 2020s will be increased by 0.49oC. For the 2050s periods the average annual maximum temperature will be increased by 1.29oC. For the 2080s periods the average annual maximum temperature will be increased by 2.34oC. Increasing maximum temperature showed more variation at the monthly time step with a range from -0.01oC to 1.20oC in 2020s, 0.51oC to 2.78oC in 2050s and 1.31oC to 4.20oC in 2080s.

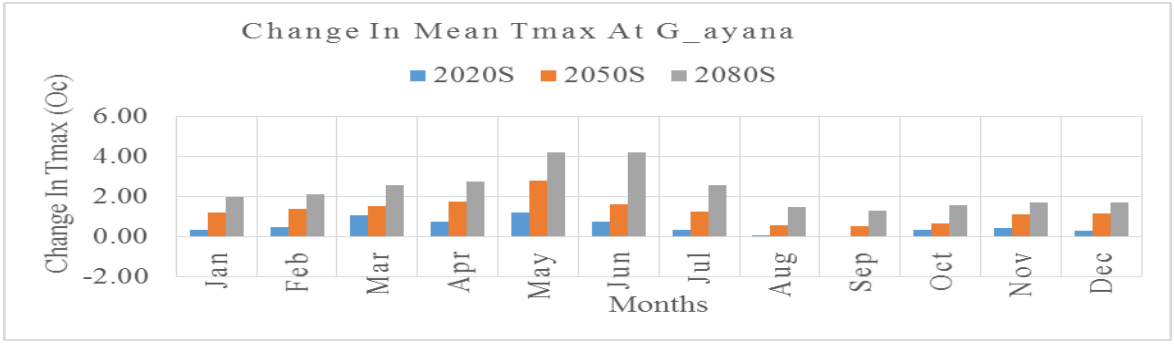

Figure 4-26 change in mean monthly Tmax at G_Ayana

For Nekemte station the downscaled maximum temperature shows an increasing trend for all months in all future time horizons .The average annual maximum temperature in 2020s will be increased by 0.59oC. For the 2050s periods the average annual maximum temperature will be increased by 1.63oC. For the 2080s periods the average annual maximum temperature will be increased by 2.95oC. Increasing maximum temperature showed more variation at the monthly time step with a range from -0.05oC to 1.53oC in 2020s, 0.71oC to 3.51oC in 2050s and 1.73oC to 5.39oC in 2080s.

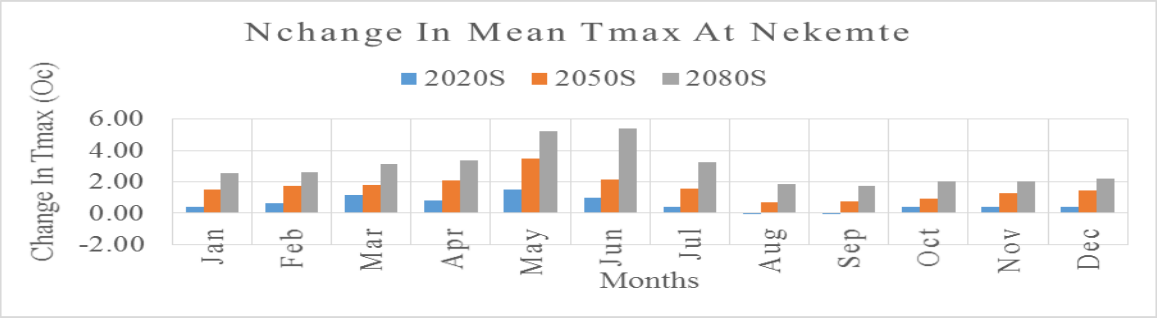

Figure 4-27change in mean monthly at Nekemte

For Shambu station the downscaled maximum temperature shows an increasing trend for all months in all future time horizons .The average annual maximum temperature in 2020s will be increased by 0.49oC. For the 2050s periods the average annual maximum temperature will be increased by 1.23oC. For the 2080s periods the average annual maximum temperature will be increased by 2.25oC. Increasing maximum temperature showed more variation at the monthly time step with a range from -0.11oC to 1.19oC in 2020s, 0.44oC to 2.58oC in 2050s and 1.22oC to 3.92oC in 2080s.

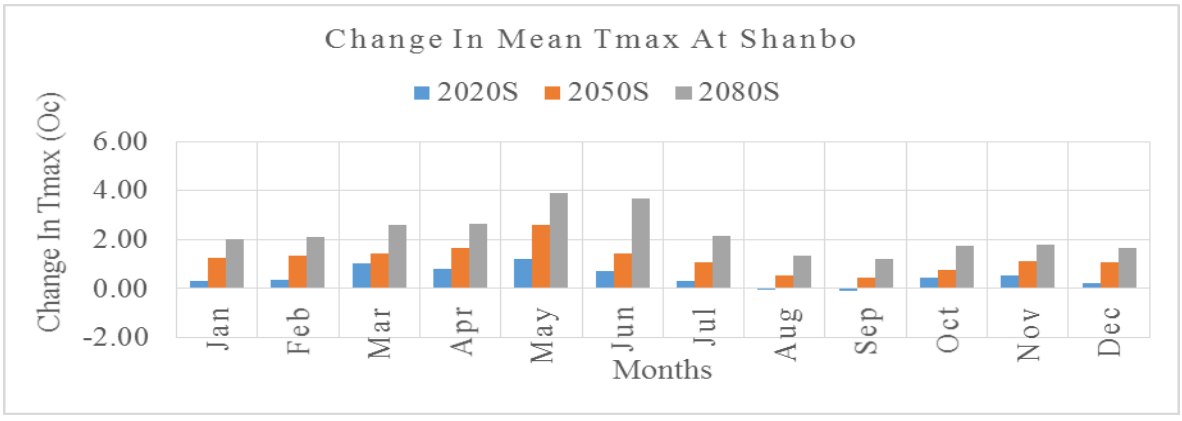

Figure 4-28change in mean monthly Tmax at Shanbo

For Alibo station the downscaled maximum temperature shows an increasing trend for all months in all future time horizons .The average annual maximum temperature in 2020s will be increased by 0.57oC. For the 2050s periods the average annual maximum temperature will be increased by 1.43oC. For the 2080s periods the average annual maximum temperature will be increased by 2.62oC. Increasing maximum temperature showed more variation at the monthly time step with a range from -0.11oC to 1.41oC in 2020s, 0.53oC to 3.07oC in 2050s and 1.41oC to 4.61oC in 2080s.

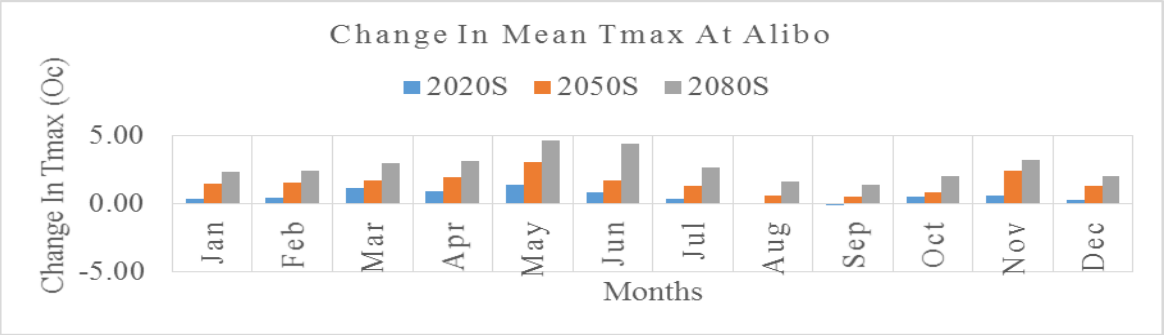

Figure 4-29change in mean monthly Tmax at Alibo

4.8 Dryness indexes (EO/P) Analysis

The difference in precipitation dryness index (E0/P) stated as a ratio of annual potential evapotranspiration calculated from the Penman-Monteith method to annual precipitation was evaluated for the base year and each seniors based on the metrological data between 1986 and 2100 (Jing Yin1, 2016). The dryness index showed that an increase during 2020s by 0.30%, during 2050s increased by 1.88% and during 2080s increased by 8.84%. According to (Jing Yin1, 2016) A little dryness index (<1.9) indicates the climate is wet. For detail information presented below (Figure 4-30).

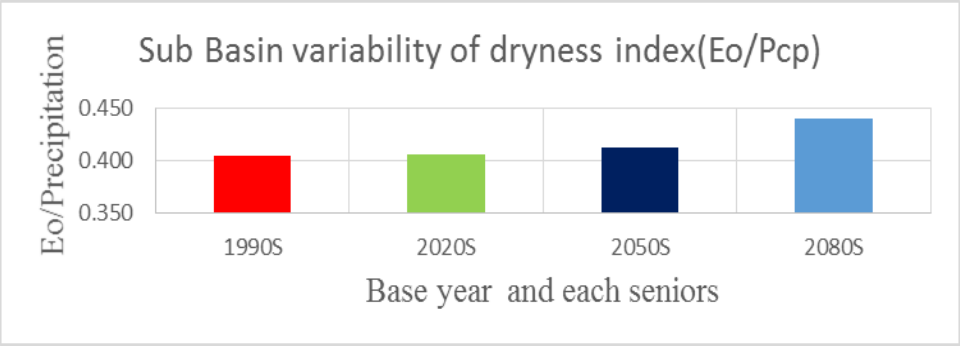

Figure 4-30 sub basin variability of dryness index

The monthly variability of dryness index showed that, the month November, December, January, February and March is high dryness index value and the month May, June, July, August and September is low dryness index value. For more detail illustrated in (Figure: 4-31) below.

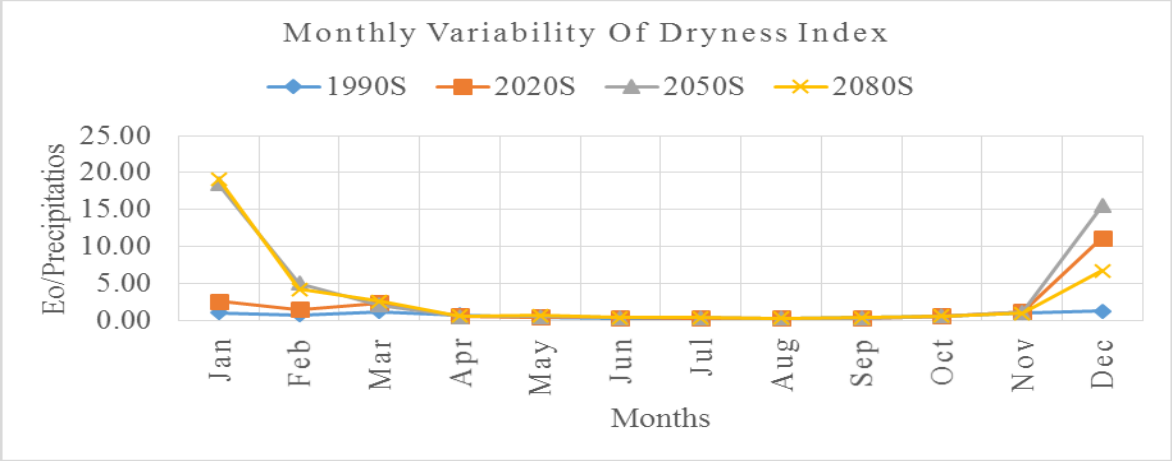

Figure 4-31monthly variability of dryness index

4.9 Stream Flow Modeling

4.9.1 Sensitivity Analysis

Sensitivity analysis of simulated stream flow for the sub basin was performed using the monthly observed flow data for identifying the most sensitive parameter and for further calibration of the simulated stream flow. Twenty-six flow parameters were checked for sensitivity and seven of them were found to be highly sensitive. For, detail information presented in (Table. 4-10) below.

Parameter Name	Sensitivity rank	t-Stat	P-Value	Min-value	Max-value	Fitted-value
4:V__CH_N2.rte	7	-0.49	0.62	0	0.3	0.1125
5:V__CH_K2.rte	6	0.66	0.51	5	130	126.875
6:V__ALPHA_BNK.rte	5	0.87	0.39	0	1	0.925
3:V__ESCO.hru	4	1.14	0.26	0.8	1	0.925
7:R__HRU_SLP.hru	3	1.57	0.12	0	0.2	0.195
1:R__CN2.mgt	2	2.36	0.02	35	98	78.88
2:V__GW_DELAY.gw	1	-3.78	0.00	30	450	145.5

Table 4-8: Sensitive parameters and their rank with t-stat and p-value for stream flow.

From those parameters Groundwater delay (GW_DELAY), SCS runoff curve number (CN2), Average slope steepness (HRU_SLP), Soil evaporation compensation factor (ESCO), Base flow alpha factor for bank storage (ALPHA_BNK), Channel effective hydraulic conductivity (CH_K2)

and Manning's n value for main channel (CH_N2) are sensitive parameters and ranked from 1 up to 7 respectively. The remaining parameters were not considered during model calibration, as the model simulation result was not sensitive to the sub basin.

4.9.2 Flow Calibration

The simulation of the model with the default value of parameters in Anger sub basin showed relatively weak matching between observed and the simulated stream flow. After sensitivity analysis has been done, the calibration of stream flow was done manually and Auto calibration. The model was run for the period of 10 years from 1990-1999. The result of calibration for the average monthly stream flow showed a good agreement between observed and simulated stream flow (Figure 4-32) with Nash –Sutcliffe simulation efficiency of 0.76 and coefficient of determination (R^2) of 0.90. For detail information attached in Appendix H

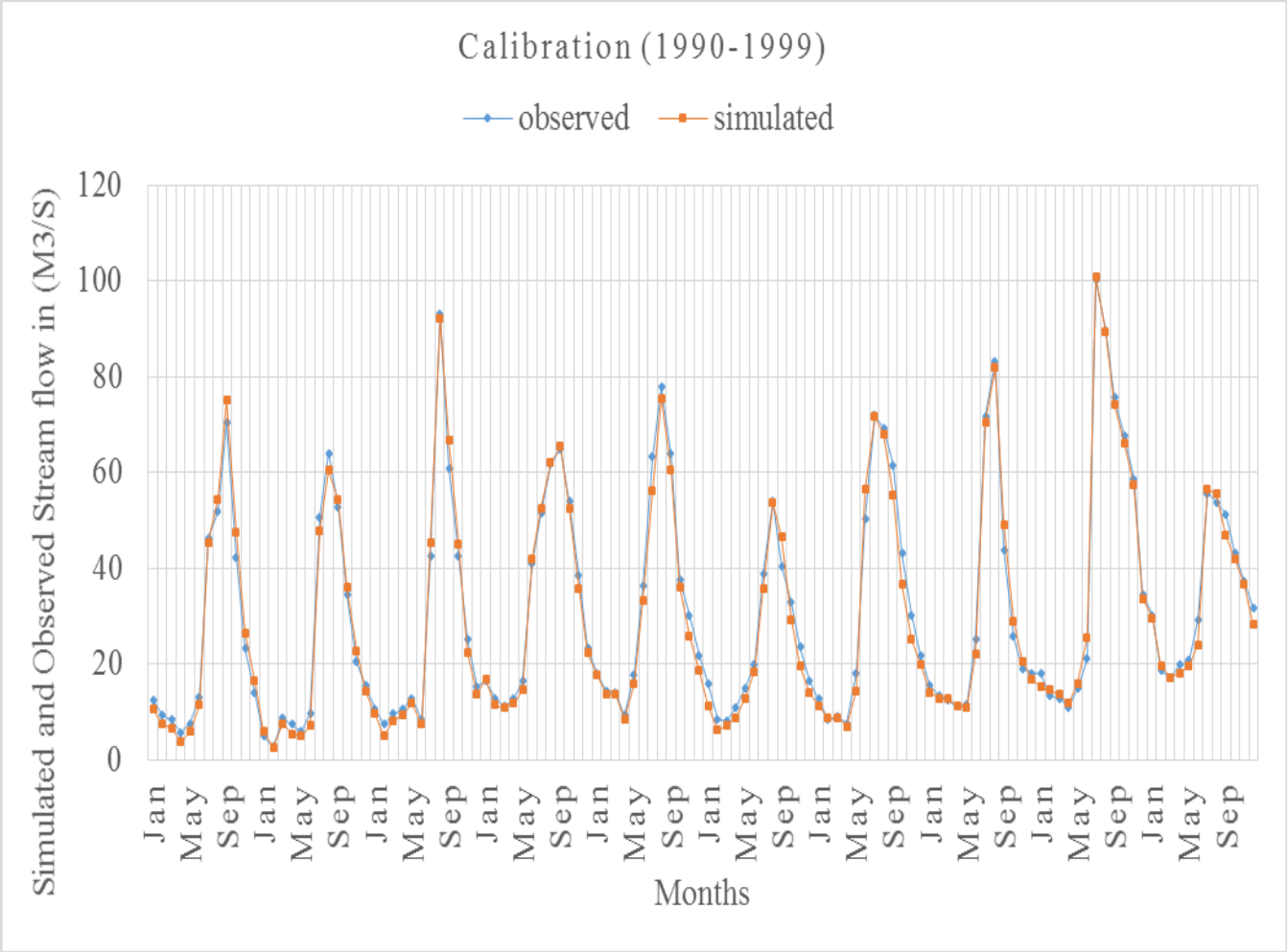

Figure 4-32: calibration of stream flow from (1990-1999).

4.9.3 Uncertainty

It is necessary to consider uncertainties in predicting of hydrology of the watershed. There are different sources of uncertainties, which lead not completely matching between observed and simulated graphs. Sources of uncertainty are:-

- Input data uncertainty, errors in meteorological data and hydrological data
- Output uncertainty, errors which is done by the model
- Model structural uncertainty and parametric uncertainty.

Hence, during this study the observed data collected were also having missing and outlier. Land use classifications were not fully accurate and it may have effects on HRU class determination. The other uncertainty is simulation or prediction uncertainty by the model. Therefore, with these uncertainties the model gave appreciable results.

4.9.4 Model Validation

After calibration was done manually and auto calibration getting acceptable values of NSE and R^2, validation of simulated flows for 6 years period from 2000–2005 were performed and validation were checked using monthly-observed flows. The model validation also showed a good agreement between simulated and measured monthly flow (Figure 4-33) with the NSE value of 0.63 and R^2value of 0.84.For detail information attached in Appendix H.

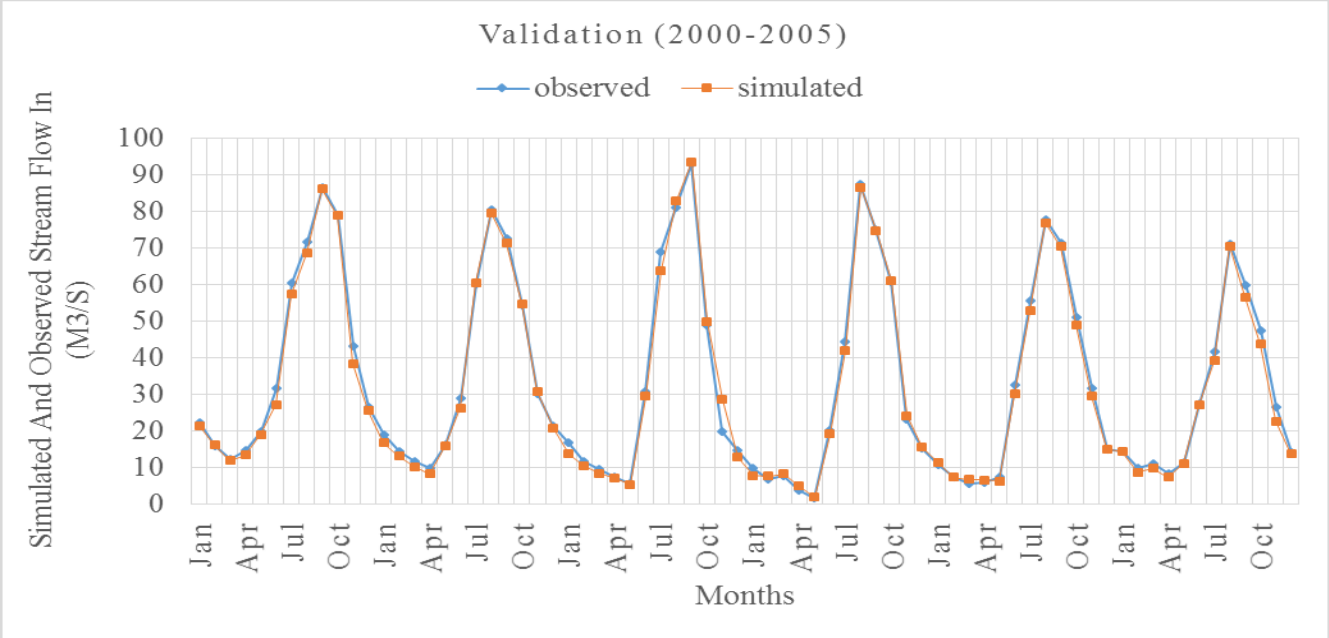

Figure 4-33: validation of stream flow from (2000-2005).

The calibrated and validated stream flow result shows a good agreement between observed and simulated stream flow. Therefore, the results of stream flows (Table 4-11) indicate that SWAT model is a good predicator for stream flow of Anger sub basin.

	Season	Observed flow (m^3/s)	Simulated flow (m^3/s)	R^2	Ens
Calibration (1990-1999)	DJF (Belg)	15.94	14.74	0.90	0.76
	MAM (Bega)	11.92	11.10		
	JJA (kiremt)	51.48	50.87		
	SON (Tsedey)	43.93	42.90		
	Annually	30.82	29.90		
	Season	Observed flow (m^3/s)	Simulated flow (m^3/s)	R^2	Ens
During Validation (2000-2005)	DJF (Belg)	14.86	14.08	0.84	0.63
	MAM (Bega)	9.52	9.09		
	JJA (kiremt)	54.00	52.22		
	SON (Tsedey)	54.15	53.55		
	Annually	33.13	32.24		

Table 4-9: Average monthly stream flow for calibration and validation.

Different studies that were conducted in the lower Blue Nile basin also showed similar result. For example, Minichli J., 2016) as cited in (Minchili J.,2016) reported that SWAT model showed a good match between measured and simulated flow of Didessa Sub basin both in calibration and validation periods with (ENS=0.76 and R^2=0.8) and (ENS =0.7 and R^2= 0.79), respectively. Through modeling upper Blue Nile basin of the Lake Tana basin, Shimelis indicated that the average monthly flow simulated with SWAT model were reasonably accurate with ENS =0.81and R^2=0.85 for calibration and ENS = 0.79 and R^2 = 0.80 for validation periods. This indicates that SWAT can give sufficiently reasonable result in the upper Blue Nile basin and hence the model can be used in this similar sub basin. The following figure shows that the scatter plots of observed and simulated value for both calibration and validation (Figure 4-34 and 4-35). This shows good linear correlation between observed and simulated values.

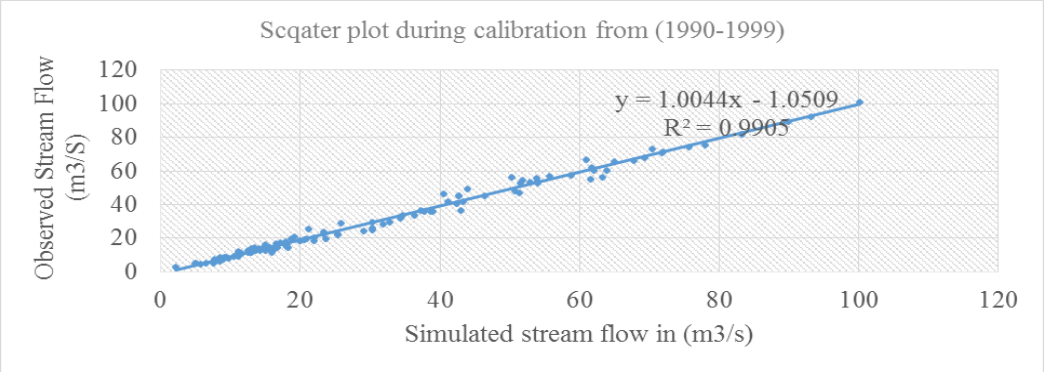

Figure 4-34 Fitted line between observed and simulated stream flow for calibration.

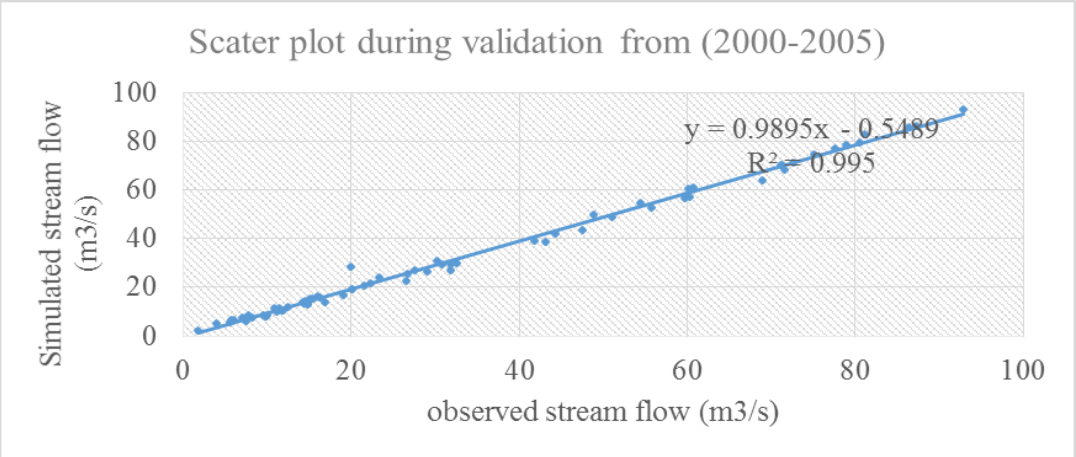

Figure 4-35: Fitted Line Between observed and simulated stream flow for validation

4.10 LULC and climate changes Impact analysis

4.10.1 Land use land cover change impact analysis

The effect of pas LULC change on average annual surface run off of Anger sub basin shown that surface run off volume increased due to LULC from 1986 to 2000,2000 to 2010 and 1986 to 2010 are $12.54Mm^3$ 12.54Mm^3,25.59Mm^3 and 38.13Mm^3 respectively. Increasing Surface run off showed more variation at the seasonal time step with a range of 0.3Mm^3 to 32.16Mm^3 in 1986 to 2000, 0.16Mm^3 to 60.36Mm^3 in 2000 to 2010 and -0.13Mm^3 to 92.52Mm^3 in 1986 to 2010 .

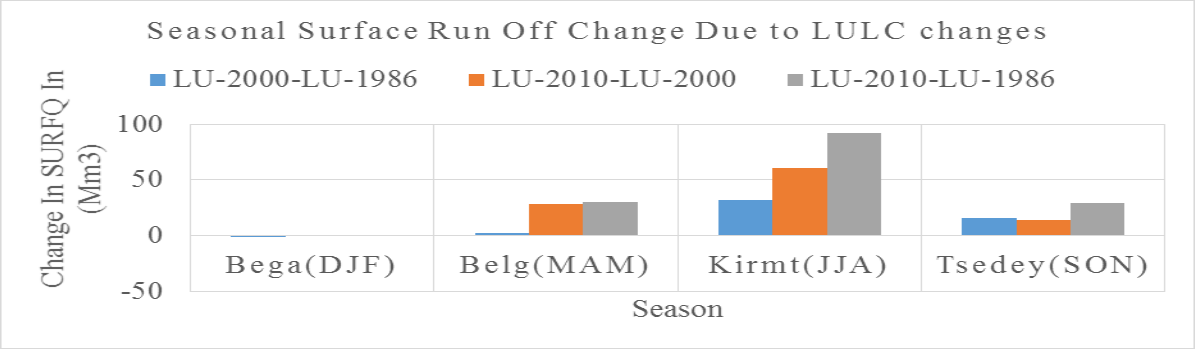

Figure 4-36 seasonal surface runoff change due to LULC change

The effect of LULC change on average annual Water yield of Anger sub basin shown that Water yield volume decreased due to LULC change from 1986 to 2000 ,2000 to 2010 and 1986 to 2010 are 22.16Mm^3, 20.76Mm^3 and 1.40Mm^3 respectively. Increasing and decreasing Water yield showed more variations at the seasonal time step with a range of -63.26Mm^3 to 27.35Mm^3 in 1986 to 2000,0.13Mm^3 to 33.41Mm^3 in 2000 to 2010 and -63.13Mm^3 to 60.76Mm^3 in 1986 to 2010.

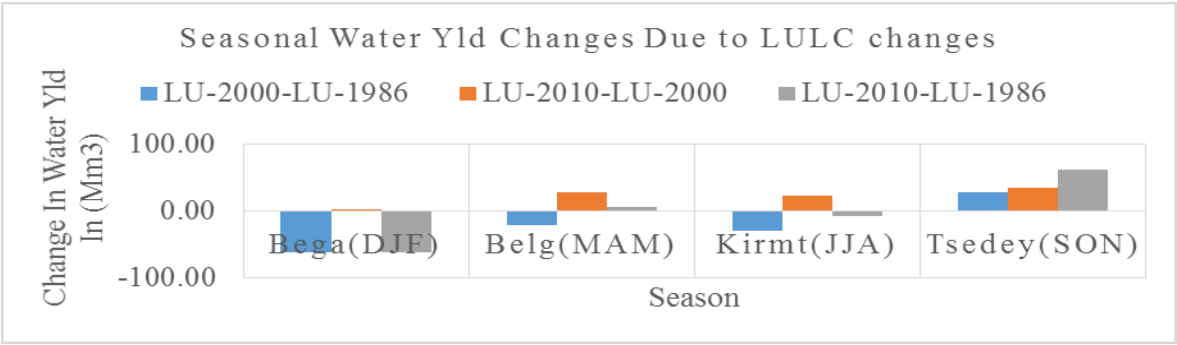

Figure 4-37seasonal water Yld change due to LULC change

4.10.2 Climate change impact analysis

The effect of climate change on average annual surface run off of Anger sub basin shown that surface run off volume will decrease from baseline period (1990s) due to climate change of 2020s by 16.76Mm^3, for 2050s by 44.96Mm^3 and for 2080s by 54.29Mm^3. The decreasing surface run off volume showed more variations at the seasonal time step with a range of -47.27Mm^3 to 11.31Mm^3 in 2020s, -65.38Mm^3 to -0.53Mm^3 in 2050s and -70.84Mm^3 to -0.40Mm^3 in 2080s.

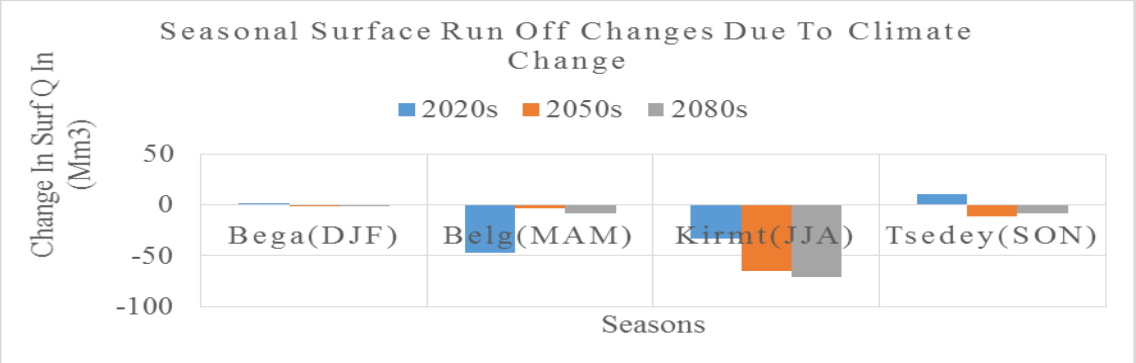

Figure 4-38seasonal surface runoff change due to climate change

The effect of climate change on average annual water yield of Anger sub-basin shown that water yield volume will decrease due to climate change of the 2020s, 2050s, and 2080s from the baseline period (1990s) by 14.50Mm3, 39.32Mm3, and 78.85Mm3 respectively. The decreasing and increasing water yield showed more variations at the seasonal time step with a range of-52.54Mm3 to 33.41Mm3,-89.22Mm3 to 9.05Mm3,and-88.63Mm3 to -0.40Mm3 during the 2020s,2050s, and 2080s respectively.

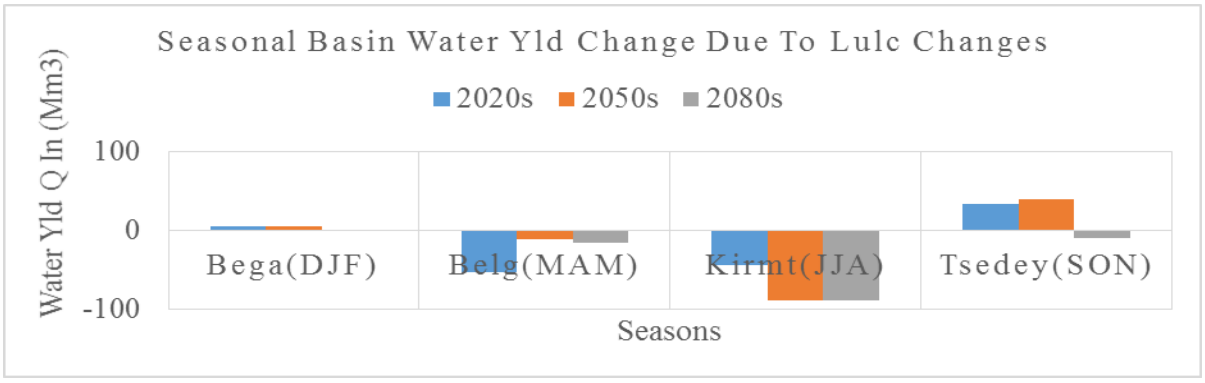

Figure 4-39 seasonal water Yld change due to climate change

4.10.3 The sub-basin reaches annual surface run off variability

Anger sub-basin had twenty-six sub reaches that had the spatial variability which relates surface runoff with sediment yields. The spatial and temporal variability of high surface runoff areas was identified and mapped using ArcGIS. As a result sub-basin Reach(R-10, R-11, R-12, R-16, and R-20) was required more attention than other reaches of the sub-basin. It was identified as more potential surface runoff areas due to past LULC, and future climate changes. These sub-watersheds requires attention for best management practices in the sub-basin. Due to sediment yield was the

function of surface runoff that means high surface runoff yields high sediment loads. For detail information presented in Figure 4-40.

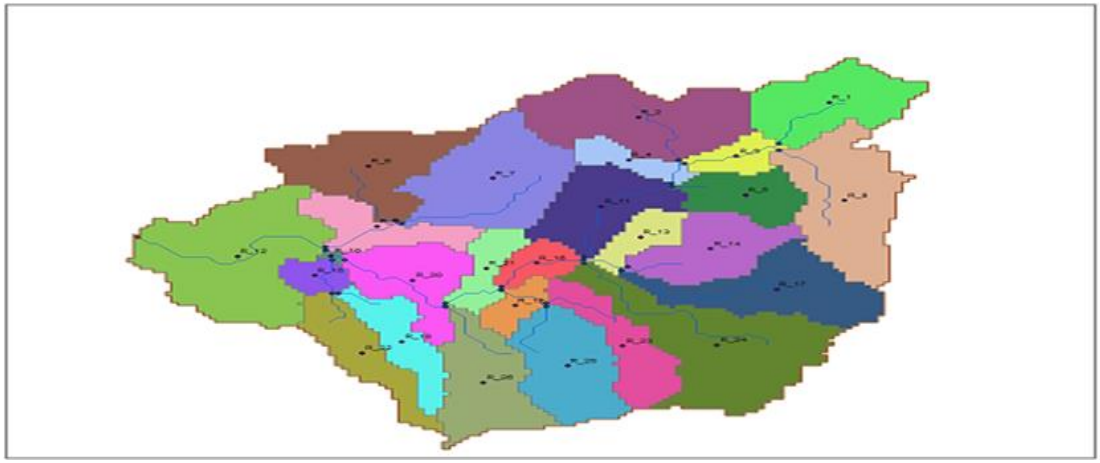

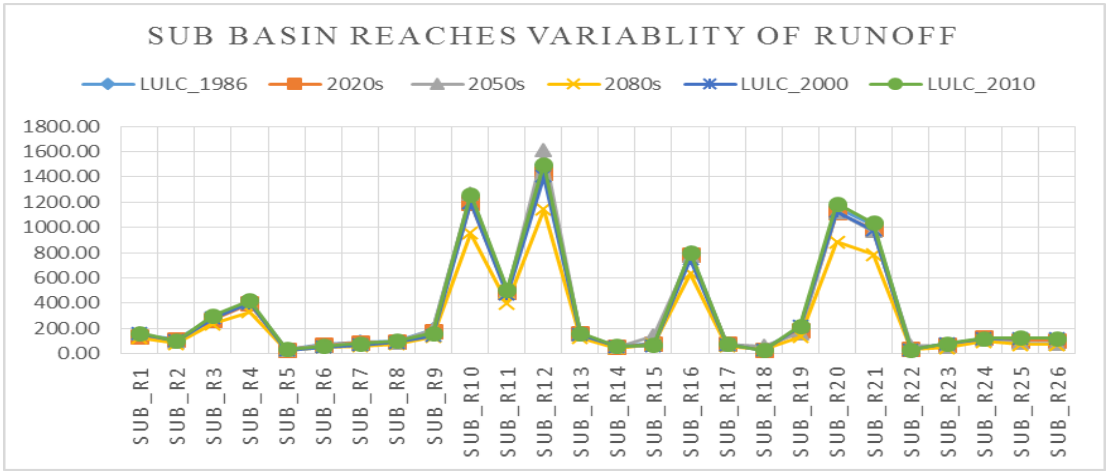

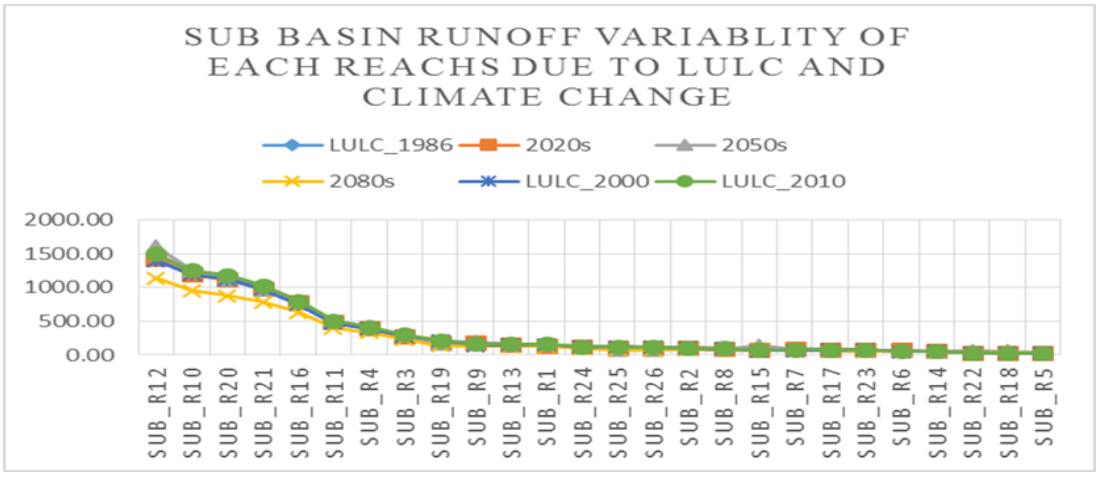

Figure 4-40: different reaches of Anger sub basin

5 CONCLUSION AND RECOMMENDATION

5.1 CONCLUSION

In Anger sub-basin, the SWAT model was used to simulate the effect of past LULC and future climate change on runoff volume change and Arc GIS was used to process preliminary data, extract, layer stake, mosaic satellite images, and image classification. Good performance of the SWAT model was confirmed, with a Nash-Sutcliffe model efficiency coefficient and determination coefficients of 0.76 and 0.90, respectively, for monthly stream-flow for the calibration period, and 0.63 and 0.84, respectively, for the validation periods.

Due to the effect of urbanization, deforestation and agricultural expansion the past LULC change increased runoff volume of the sub-basin by 12.54Mm^3, 25.29 Mm^3 during 1986-2000 and 2000-2010 respectively. And also the effect of future climate change will decrease runoff volume of the sub-basin differently during different scenarios from the baseline period (1990s). The run off volume will decrease by 16.76 Mm^3, 44.96 Mm^3, and 54.29 Mm^3 during 2020s, 2050s and 2080s respectively. From the research finding, it was observed that the maximum and minimum temperature of the sub basin increased while the precipitation decreased during the study period due to urbanization, deforestation and agricultural expansion in the study area.

As research findings shown that, much of the original forest in the sub-basin has already converted to agricultural lands, for instance agricultural land increased by 39.3% and built up area increased by 0.5% and also, shrub-land, forest area, and water body decreased by 32.9%, 6.6%, and 0.3% respectively. These change would aggravate already serious problem related to water scarcity in dry period and hill-slope erosion during wet period. The reason is mainly due to the population growth. This might be due to the population pressure caused high demand for additional land resulting shortage of cultivated land which is a major problem for farmers in the study area.

The accuracy of LULC Classification was achieved by: - overall accuracy, user's accuracy, and producer's accuracy and kappa coefficient. The kappa coefficient show good agreement between classified image and ground truth with 81%, 79.5% and 83.2% during 1986, 2000 and 2010 respectively. Anger sub-basin has twenty-six sub reach that had the spatial variability which relate surface runoff with sediment yield. The spatial and temporal variability of high surface runoff area were identified and mapped using ArcGIS. As a result sub-basin reach (R-10, R-11, R-12, R-16,

and R-20) were required more attention than other reach of the sub-basin due to past LULC and future climate change.

5.2 RECOMMENDATION

Generally, based on the results of the study, the following recommendations were made:

- Due to significant LULC and climate change, it needs effective participatory integrated watershed management.
- Change in LULC in Anger sub-basin are mainly caused by population growth. Due to this reforestation of shrub-land, steep slope land and some parts of agricultural land was mandatory. Mainly sub-basin reach (R-10, R-12, R-16, and R-20) was required more attention than other reach of the sub-basin which was located at upper middle and lower part of the watershed with other soil conservation measures.
- The sub-basin was sensitive to both past LULC and future climate change, so the government should give orientation for every stockholder to protect the sub-basin by protecting their own farmland as well as the surrounding area from deforestation. Otherwise, the deforestation leads to flooding during the wet season and water scarcity during the dry season in the sub--basin.
- Further researches like sedimentation effects on Anger sub-basin with reservoirs including the development of BMPs with detail land use survey shall have to be done. And also watershed should have to be modelled with climate data downscaled from different scenarios.

References

Aster D. Y. and Seleshi B. A. (2009). Characterization and Atlas of the Blue Nile Basin and its Sub basins. *International Water Management Institute January*.

Abayneh, A. (2011). Evaluation of Climate Change Impact on Extreme Evaluation of Climate Change Impact on Extreme Hydrological Event Addis Ababa University. Addis Ababa.

Abebe, S. (2005). Land-Use and Land-Cover change in headstream of Abbay watershed, Blue Nile Basin, Ethiopia. Addis Ababa University.

Abebe, S. (2005). Land-Use and Land-Cover change in headstream of Abbay watershed, Blue Nile Basin, Ethiopia. *Addis Ababa University*.

Arnold, J. G. (1993). A comprehensive surface- ground water flow model. *Journal of Hydrology,142:*, 47-69.

Arnold, J. G. (1993). A comprehensive surface- groundwater flow model. Journal of Hydrology. 142: 47-69.

Arnold, J. G. (1998). Large area hydrologic modeling and assessment Part I: Model Development. *Journal of the American Water Resources Association*, 30 (1): 73-89.

Asmamew, A. G. ((2013). Assessing the impact of land use and land cover change on hydrology of watershed. 1-3.

Atasoy, M. B. (2006). Monitoring land use changes and determinating the suitability of land for different uses with digital Photogrammetry. Remote Sensing and Photogrammetry, Cairo, Egypt.

Awulachew, S. B. ((2008). Impact of watershed interventions on runoff and sedimentation in Gumera watershed. Arba Minch University, . *Ethiopia Research Service and Texas A* .

Bawahidi, K. S. (2005). Integrated land use change analysis for soil erosion study in ulu kinta catchment. Universiti Sains Malaysia.

Bergström, S. (1995). The HBV model. In: Sing, V.P. (Ed), Computer models of watershed hydrology. *Water Resources Publications, Colorado*, 443-476.

Bewket, W. (2003). Towards integrated watershed management in highland Ethiopia: the Chemoga watershed case study . *PhD thesis, Wageningen University and Research Centre*, ISBN 90-5808-870-7. .

Bewket, W. a. (2005). Dynamics in land cover and its effect on stream flow in the Chemoga watershed, Blue Nile basin, Ethiopia. *Hydrological Processes, Hydrol. Process*, 19, 445-458.

Bezuayehu, T. O. (2008). Environmental impact of hydropower dam in Fincha'a watershed, EthiopiaLand use changes, erosion problems, and soil andwater conservation adoption.

Buishand, T. (1982). Some methods for testing the homogeneity of rainfall records. *Journal of Hydrology*, (58): 11 – 27.

Cibin, R. S. ((2010). (Sensitivity and identifiability of stream flow generation parameters of the SWAT model. *Department of Agricultural and Biological Engineering, Purdue University, West Lafayette*, IN 47907, USA. .

Cunderlik, J. (2003). Hydrological model selection for CFCAS project . *Assessment of water resource risk and vulnerability to change in climate condition, University of Western Ontario*.

Cunderlik, J. (2003). Hydrological model selection for CFCAS project, Assessment of water resource risk and vulnerability to change in climate condition, University of Western Ontario.

Denboba, M. A. ((2005). Forest conversion - soil degradation - farmers' perception nexus: Implications for sustainable land use in the southwest of Ethiopia . *Ecology and Development Series No. 26, 2005.* .

Elfert. S., and Bormann.H. (2010). Simulated impact of past and possible future land use changes on the hydrological response of Northern German lowland 'Hunte' catchment. *Journal of Hydrology*, 383, 245-255.

Emerta, A. (2013). climate change, growth, and poverty in Ethiopia. *The Roberts. Strauss center,working paper No.3.*

Endalkachew, G. (2012). Climate Change Impact on Surface Water Sources of Addis Abab case study Legedadi-Dire-Gefersa Catchments and Reservoirsa. *Addis Ababa institute of Technology,Addis Ababa.*

Essenfelder, A. H. (2016). SWAT Weather Database:. *A Quick Guide. Version: v.0.16.06. doi:.*, 10.13140/RG.2.1.4329.1927.

FAO and MoWIE . (2013). Developing a Water Audit for Awash River Basin. *GCP/INT/072/ITA Addis Ababa, Ethiopia*.

Gashaw G. and Mamaru A. (2015). Assessing the Land Use/Cover Dynamics and its Impact on the Low Flow of Gumara Watershed, Upper Blue Nile Basin, Ethiopia.

Gashaw, T. T. ((2017)). Evaluation and prediction of land use/ land cover changes in the Andassa watershed, Blue Nile Basin, Ethiopia.

Gassman, P. W. ((2007). The Soil and Water Assessment Tool: Historical Development, Applications, and Future Research Direction.American Society of Agricultural and Biological Engineers ISSN. 0001-2351.

Gebrehiwet, K. B. (2004). Land use and land cover changes in the central highlands of Ethiopia: The case of Yerer Mountain and its surroundings. *M.Sc Thesis, Addis Ababa University, Environmental Science*.

Getahun YS, V. L. (2015). Assessing the Impacts of Land Use-Cover Change on Hydrology of Melka Kuntrie Subbasin in Ethiopia, Using a Conceptual Hydrological Model. *Hydrol Current Res 6: 210. doi:10.4172/2157- 7587.*

Green. W.H. and Ampt G.A. (1911). Studies on soil physics, 1. The flow of air and water through soils. *Journal of Agricultural Sciences*, 4: 11-24.

H.Hardision, J. K. (1960). *GENERAL SURFACE RUNOFF TECHNIQUES.* USA: USA Government Printing office washngton.

Hadgu, K. M. (2008). Temporal and spatial changes in land use patterns and biodiversity in relation to farm productivity at multiple scales in Tigray,Ethiopia. *PhD Thesis Wageningen University, Wageningen, the Netherlands*.

Haile TA, E. K. (2011). Changes in land cover, rainfall and stream flow in Upper Gilgel Abbay catchment, Blue Nile basin – Ethiopia.

Houghton, J. T. ((1995). Climatic Change 1994: Radiative Forcing of Climatic Change and an Evaluation of IPCC IS92 Emission Scenarios. Intergovernmental panel on climate change. *Cambridge University press,Cambridge, UK*.

Hurni, H. ((1993). Degradation and conservation of the soil resource in the Ethiopian highlands. *A paper presented at the first international workshop on African mountains and highlands, Ethiopia*, 19-27.

IGBP-IHDP. (1999). Land-use and land-cover change, implementation strategy.IGBP Report 46/IHDP Report 10. Prepared by Scientific Steering Committee and International Project Office of LUCC. Stockholm and Bonn.

IPCC. (2007). Technical paper VI Climate change and Water.

IPCC. (2013). The Physical Science Basis: Contribution of working group I to the fifth assessment report of Intergovernmental Panel on climate change. *Cambridge University Press; Cambridge, UK and New York, NY*.

Jing Yin1, F. H. (2016). Effect of land use/land cover and climate changes on surface runoff in a semi-humid and semi-arid transition zone in Northwest China. 212.

Lambin, E. F. (2003). Dynamics of land use and land cover change in tropical regions. Annu. Rev. Environ. Resour. 2003. 28: 205- 41.

Legesse, D. V.-C. (2003). Hydrological response of a catchment to climate and land use changes in Tropical Africa: case study South Central Ethiopia. *Journal of Hydrology*, 275: 67-85.

Leng, G. T. (2016). Assessments of joint hydrological extreme risks in a warming climate in China. *International Journal of Climatology, 36,* 1632–1642.

Lenhart, T. E.-G. ((2002). Comparison of two different approaches of sensitivity analysis. *Physics and Chemistry of the Earth 27: ,* 645-654.

Li, Z. L. (2009). Impacts of land use change and climate variability on hydrology in an agricultural catchment on the loess plateau of China. *J. Hydrol.,* 377,35-42.

Ma X, X. J. (2009). Responses of hydrological processes to land-cover and climate changes in Kejie watershed,. *south-west China. Hydrological Processes 23*, 1179-1191.

Mann, H. B. (1945) : Kendall, M. G. ((1975). Nonparametric tests against trend,Rank Correlation Methods. *Charles Griffin, London , Econometrical*, 13,245-259.

Minichil.J. (2012). Evaluation of land use land cover change on Stream flow. *a case study of dedissa sub basin, abay basin, south western Ethiopia,Ariba Minch University*.

Minichil.J. (2016). Evaluation of land use land cover change on Stream flow. *a case study of dedissa sub basin, abay basin, south western Ethiopia,Ariba Minch University*.

Moriasi, D. N. ((2007). Model evaluation guidelines for systematic quantification of accuracy in watershed simulations . 885-900.

Ndomba, P.2002, and Tripathi. (2003). SWAT model application in a data scarce tropical complex catchment in Tanzania. *Physics and chemistry of the Earth*.

Neitsch S, A. J. (2005). Soil and Water Assessment Tool Theoretical Documentation-Version 2005. *Grassland, Soil & Water Research Laboratory, Agricultural Research Service, and Blackland Agricultural Research Station, Temple, Tex*.

Neitsch, S. A. (2005). Soil and Water Assessment Tool, Theoretical documentation: Version 2005. *Temple, TX.USDA Agricultural Research Service and Texas A & M Black land Research Centre*.

NMSA . (2001). National Meteorological Service Agency. *Initial National Communication of Ethiopia to the United Nations Framework Convention on Climate Change (UNFCCC) Addis Ababa, Ethiopia*.

Pechlivanidis I.G., J. B. (2011). Catchment scale hydrological modelling. *A review of model types, calibration approaches and uncertainty analysis methods in the context of recent developments in technology and applications, Global NEST Journal*, 13, 193–214.

Priestley, C. H. (1972). On the Assessment of Surface Heat Flux and Evaporation Using Large-Scale Parameters. *Division of Atmospheric Physics, Commonwealth Scientific and Industrial Research Organization, Aspendale, Victoria, Australia*.

Richards, H. M. (1998). *Hydrologic Analysis and Design.* Department of Civil Engineering University of Maryland, Prentice Hall Upper Saddle River, New Jersey 074582ndEdition.

Sage, C. (1994). Population and Income. In Meyer, W.B. and Turner, B. L. Change in land use and land cover. *A Global perspective Cambridge university press: Cambridge*, (pp. 263-285).

Santhi. C., J. A. (2001). Validation of the SWAT model on a large river basin with point and non point sources the American water resources association. 1169-1188.

Seleshi G. Yalew, *. M.-I., & A., a.-i. (2016). Land-Use Change Modelling in the Upper Blue Nile Basin.

Setegn, S. S. ((2008). Spatial delination of soil erosion vulnerability in the Lake Tana Basin, Ethiopia. *Hydrological Processes, Hydrol. Process. (2009)*.

Setegn, S. S. (2008). Spatial delination of soil erosion vulnerability in the Lake Tana Basin, Ethiopia. *Hydrological Processes, Hydrol. Process. (2009)*.

Solomon, H. . (2005). GIS-Based Surface Runoff Modeling and Analysis of Contributing Factors; a Case study of the Nam Chun watershed . *Thailand. M.Sc Thesis, ITC, the Netherlands*.

Tadesse T. (2016). Development of Water Allocation and Utilization System for Koka Reservoir under Climate Change and Irrigation Development Scenarios (Case Study Downstream of Koka Dam to Metahara). *Addis Ababa Ethiopia,*, page 28.

Tekle, A. (2010). Assessment of Climate change impact on Water availability of Bilate watershed, Ethiopian Rift valley basin. *M.Sc Thesis, Arba Minch University, Ethiopia*.

U. S. ACE. (2001). Hydrologic Modeling System HEC- HMS User's Manual. *Hydrologic Engineering Center, Davis, CA.*

USDA - SCS. (1972). *National Engineering Handbook, Section 4: Hydrology.* U.S. Government Printing Office,: Washington, DC.

Van Griensven, A. M. (2006). A global sensitivity analysis tool for the parameters of multi-variable catchment models. *Journal of Hydrology 324:*, 10-23.

Wang, R. K. (2014). Individual and combined effects of land use/cover and climate change on Wolf Bay watershed streamflow in southern Alabama,. *Hydrol. Process 28*, 5530–5546.

Yang, J. R. (2008). Comparing uncertainty analysis techniques for a SWAT application to the Chaohe Basin in China. *J. Hydrol., 358,* 1–23.

Zeleke, G. a. (2001). Implications of Land use and land cover dynamics for mountain resource degradation in the northwestern Ethiopia. *highlands Mountain Research and Development*, 21: 184-191.

Appendix: A

A. mean monthly rainfall, maximum and minimum Temperature of sub basin

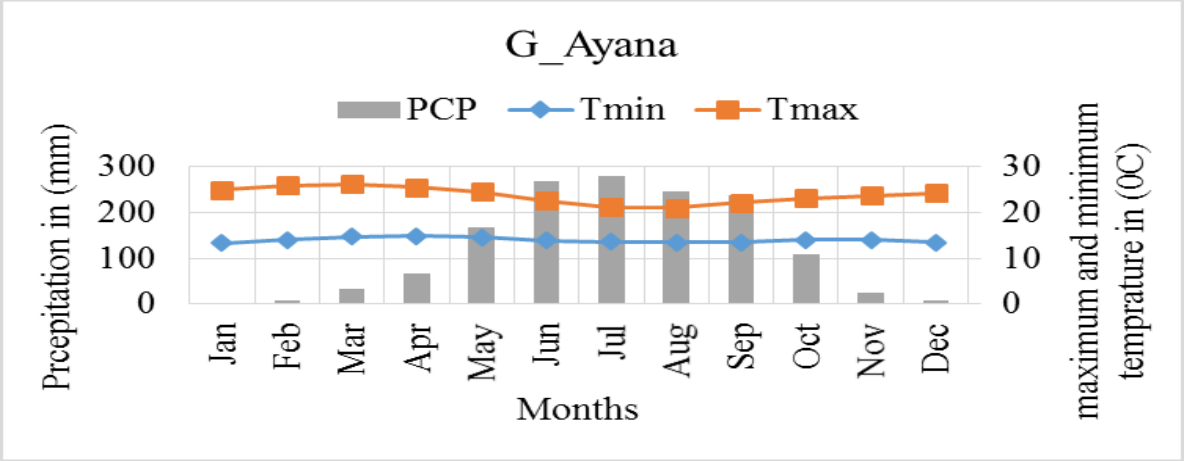

B. Mean monthly rainfall, maximum and minimum Temperature of sub basin

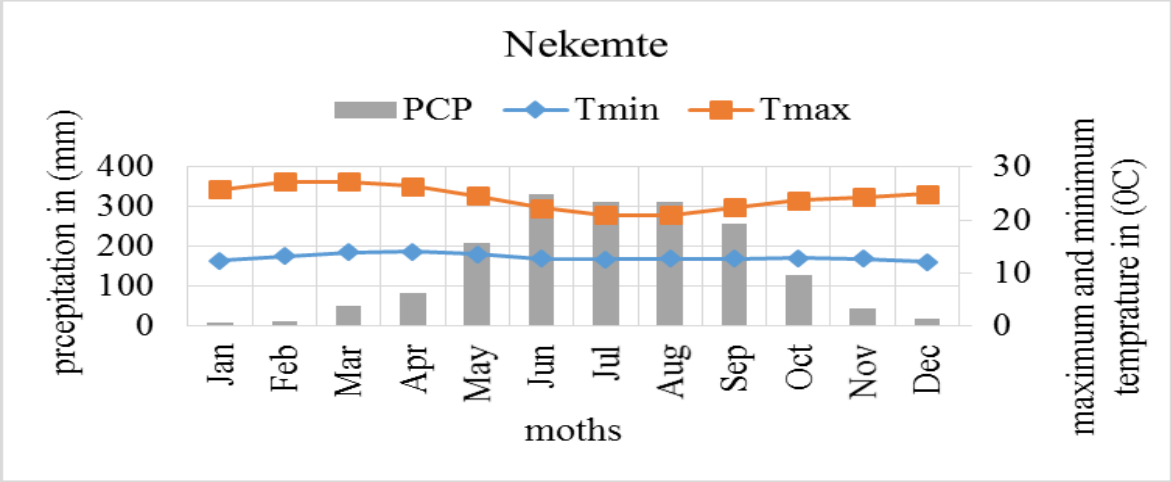

C. Mean monthly rainfall, maximum and minimum Temperature of sub basin

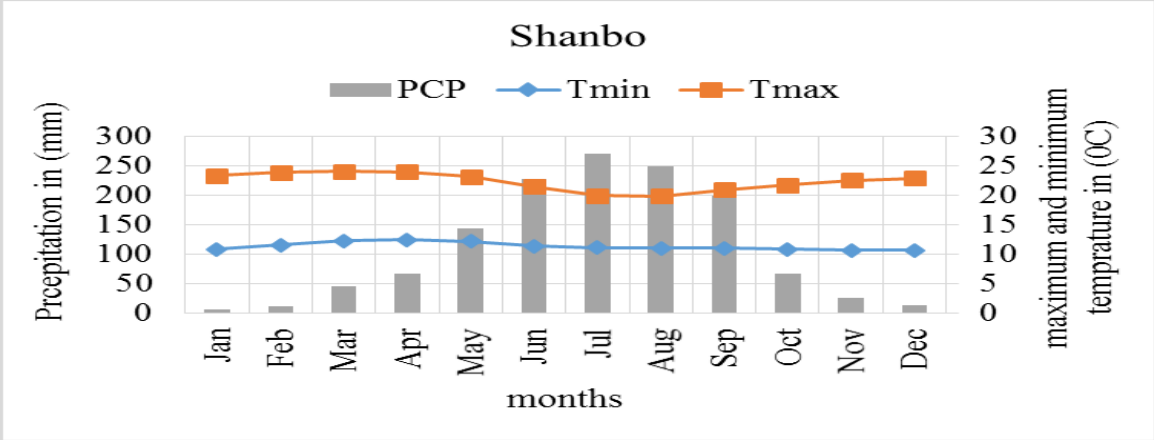

D. mean monthly rainfall, maximum and minimum Temperature of sub basin

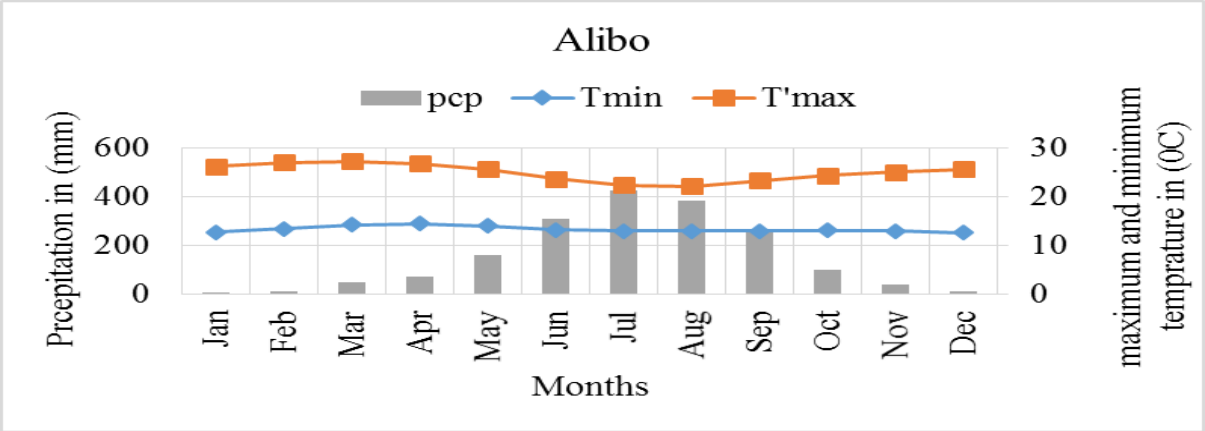

Appendix _B value of constant a and b for each station

G_Ayana Station

months	Jan	Feb	Mar	Apr	May	Jun	Jul	Aug	Sep	Oct	Nov	Dec
a	1.01	1.32	1.53	1.34	1.16	1.55	1.57	1.22	1.51	1.87	1.16	0.59
b	1.23	0.57	0.69	0.90	0.91	0.82	0.78	0.85	0.80	0.75	0.78	0.81

Nekemte Station

months	Jan	Feb	Mar	Apr	May	Jun	Jul	Aug	Sep	Oct	Nov	Dec
a	2.35	1.24	2.87	1.46	1.55	2.17	1.79	2.04	1.85	1.48	3.27	1.25
b	1.52	0.45	0.60	0.89	0.89	0.78	0.77	0.75	0.77	0.88	0.57	0.97

Shanbo Station

months	Jan	Feb	Mar	Apr	May	Jun	Jul	Aug	Sep	Oct	Nov	Dec
a	1.02	7.05	1.84	1.46	1.19	1.22	1.22	1.15	1.78	1.18	2.23	2.03
b	0.20	0.80	0.65	0.77	0.92	0.90	0.85	0.87	0.73	0.83	0.60	0.55

Alibo Station

months	Jan	Feb	Mar	Apr	May	Jun	Jul	Aug	Sep	Oct	Nov	Dec
a	3.68	9.51	1.82	0.79	0.66	1.85	2.57	2.08	1.94	1.33	3.58	1.16
b	0.43	0.40	0.73	1.55	1.16	0.83	0.73	0.80	0.76	0.90	0.56	0.52

Appdeix_C Trend analysis of Tmax and Tmin for each station

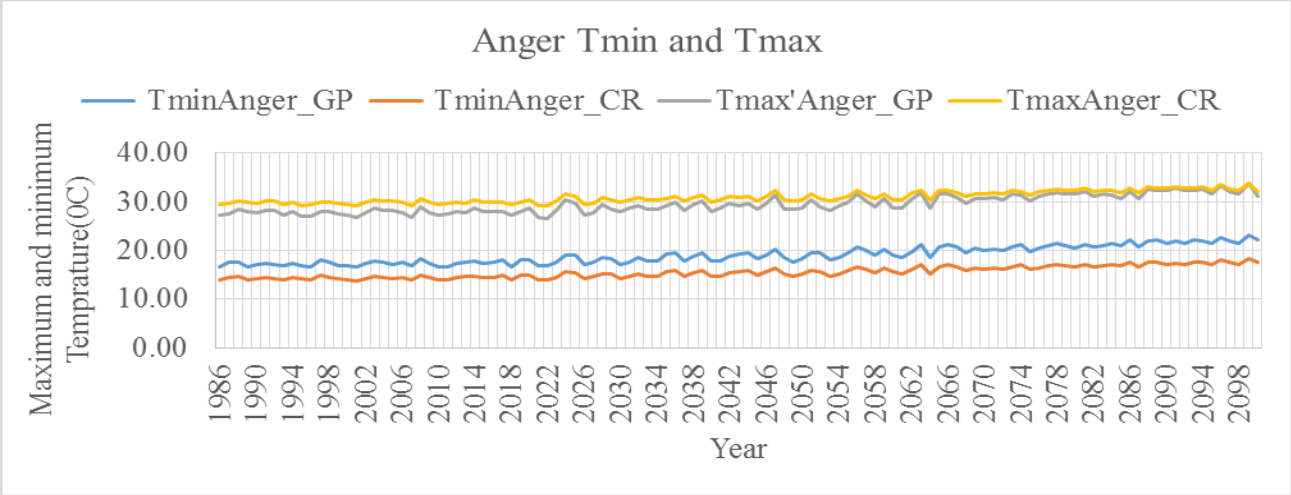

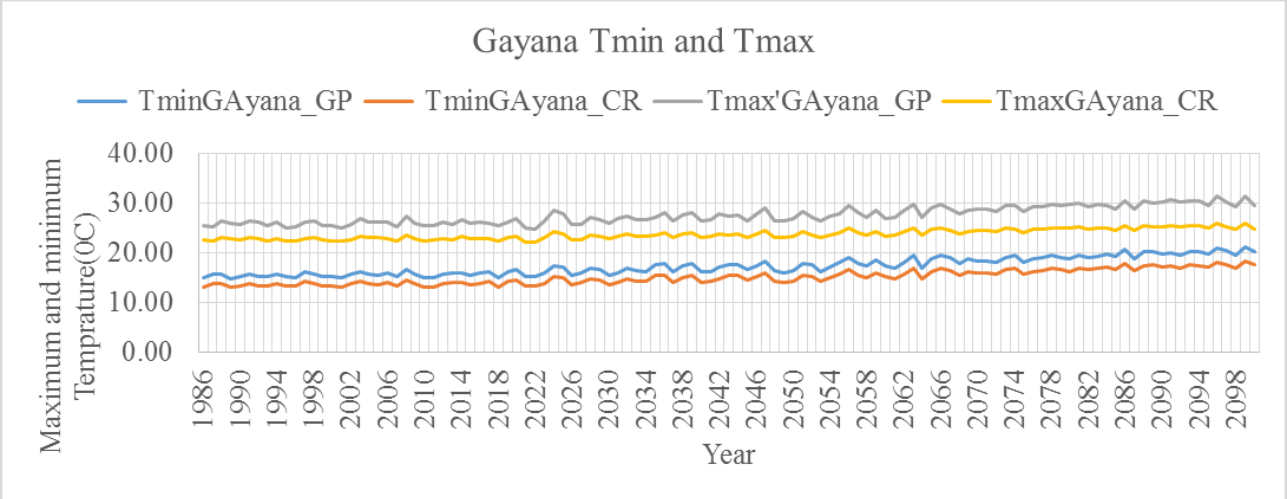

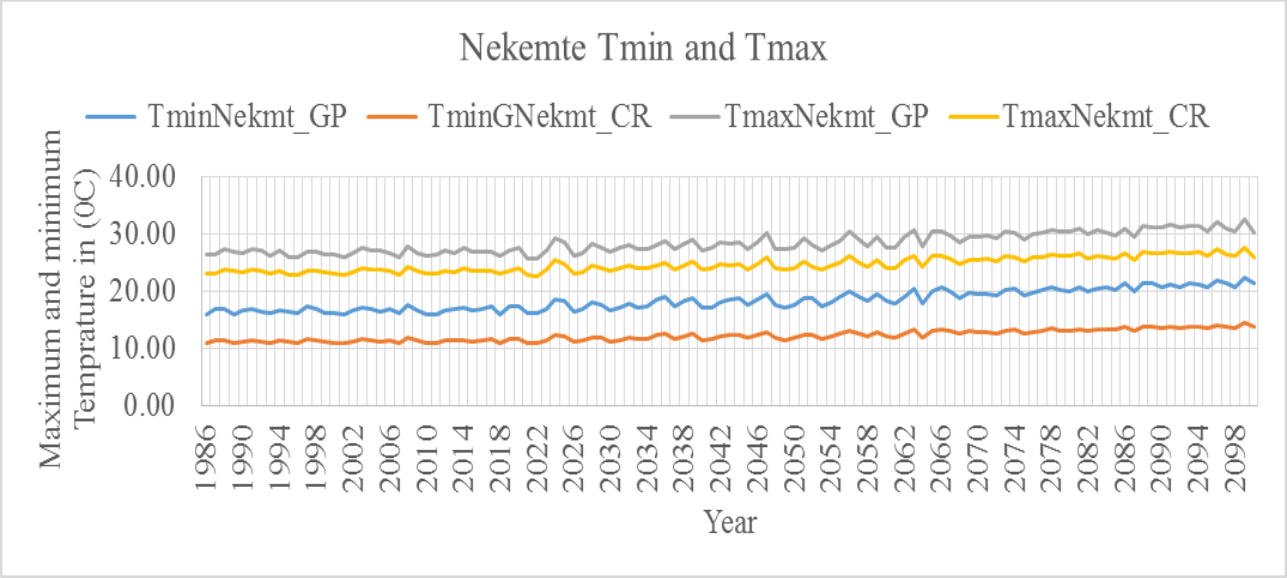

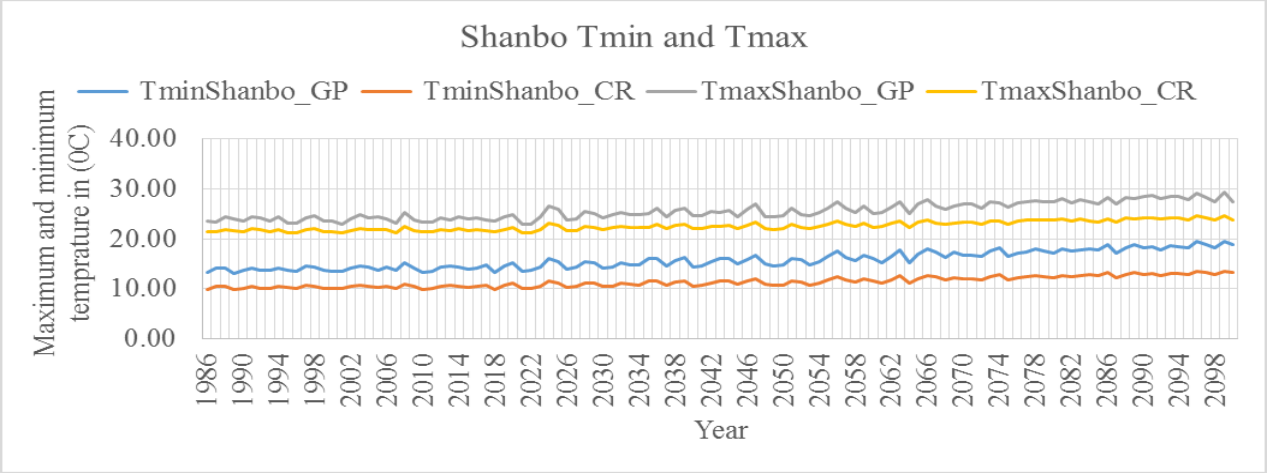

Appendix-D Trend analysis of Precipitation for each station

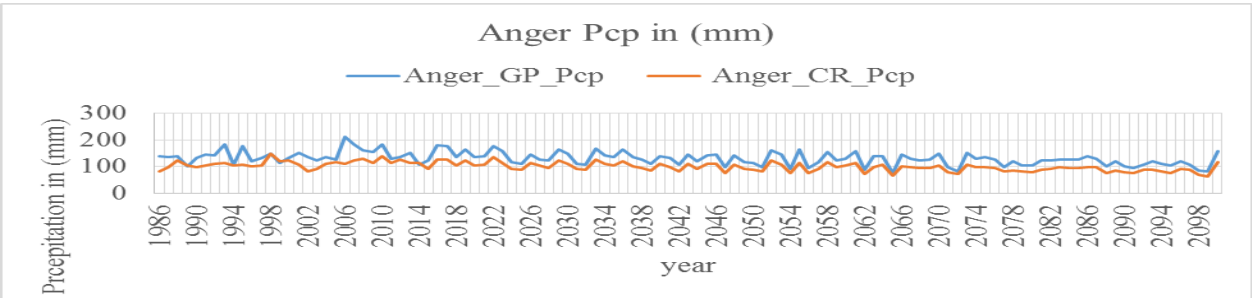

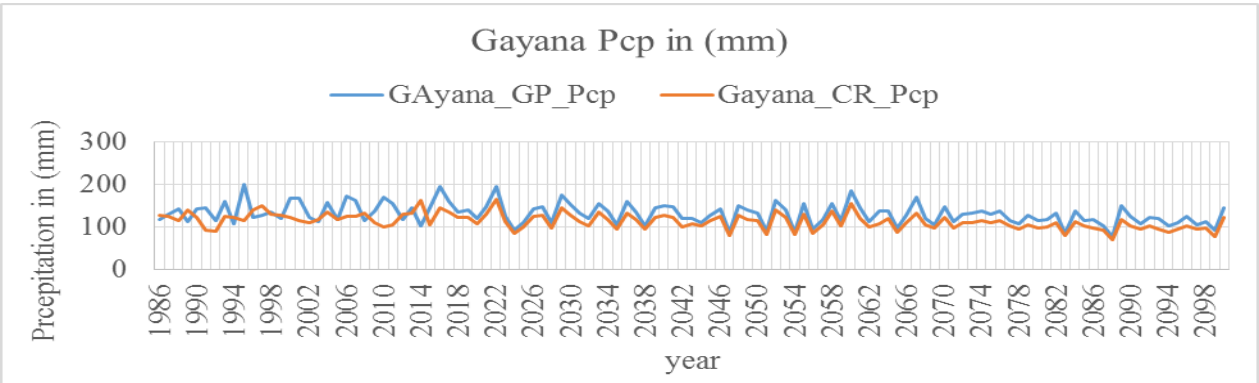

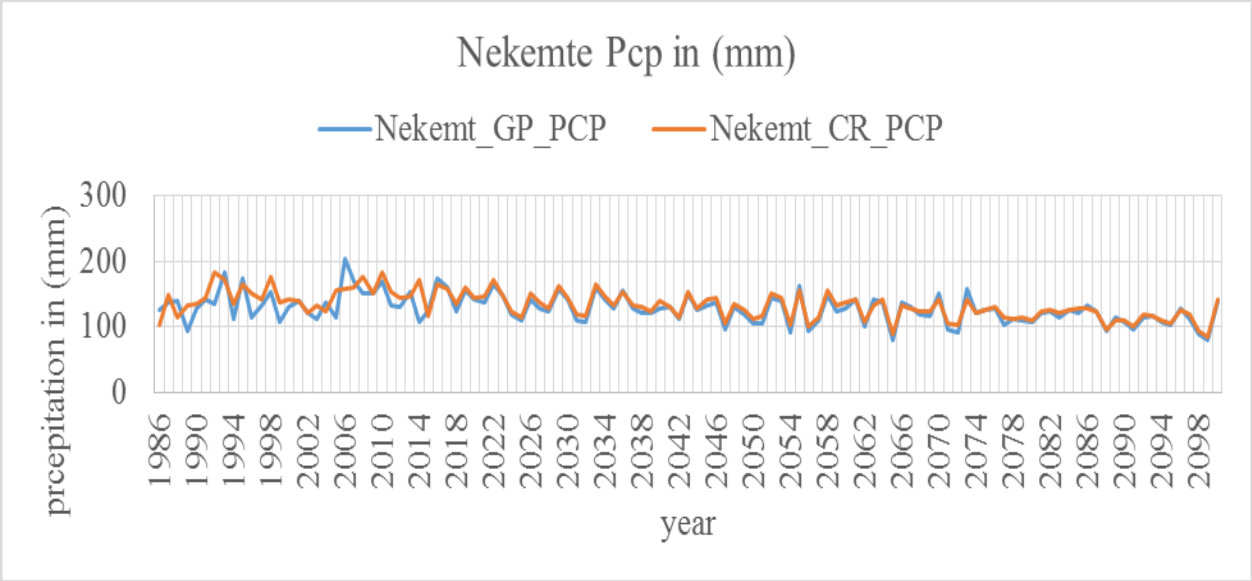
Nekemte Pcp in (mm)
Nekemt_GP_PCP
Nekemt_CR_PCP
precipitation in (mm)
300
200
100
0
1986 1990 1994 1998 2002 2006 2010 2014 2018 2022 2026 2030 2034 2038 2042 2046 2050 2054 2058 2062 2066 2070 2074 2078 2082 2086 2090 2094 2098
year

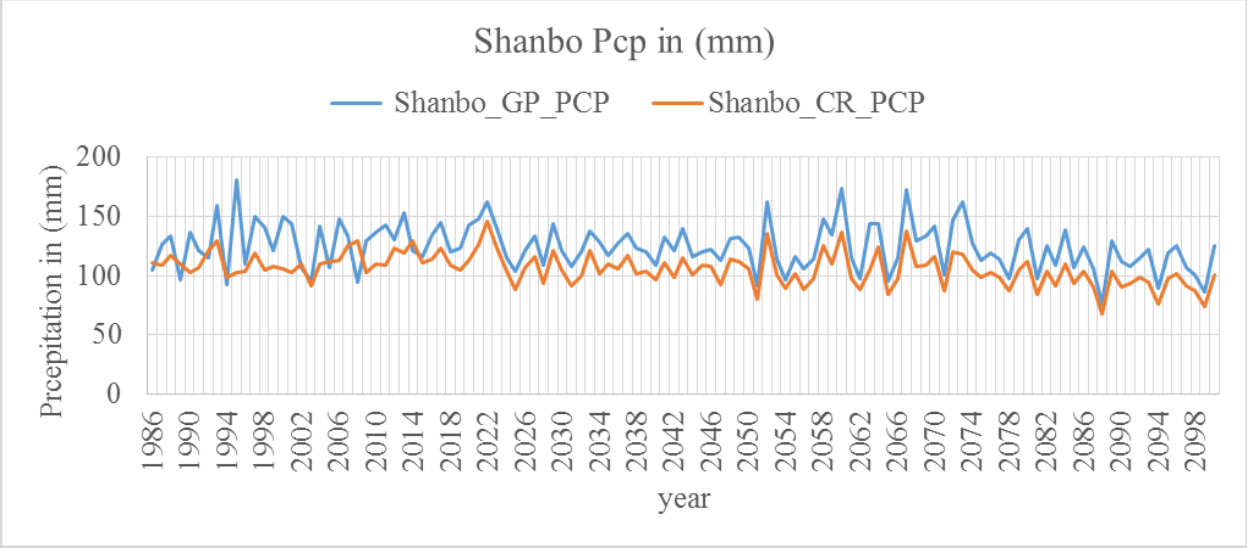
Shanbo Pcp in (mm)
Shanbo_GP_PCP
Shanbo_CR_PCP
Precipitation in (mm)
200
150
100
50
0
1986 1990 1994 1998 2002 2006 2010 2014 2018 2022 2026 2030 2034 2038 2042 2046 2050 2054 2058 2062 2066 2070 2074 2078 2082 2086 2090 2094 2098
year

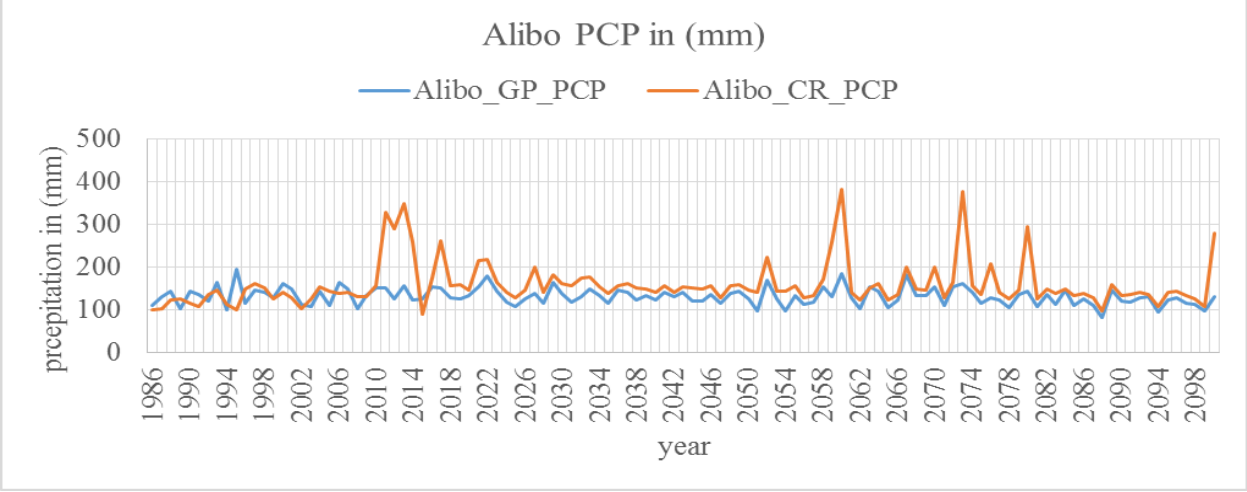
Alibo PCP in (mm)
Alibo_GP_PCP
Alibo_CR_PCP
precipitation in (mm)
500
400
300
200
100
0
1986 1990 1994 1998 2002 2006 2010 2014 2018 2022 2026 2030 2034 2038 2042 2046 2050 2054 2058 2062 2066 2070 2074 2078 2082 2086 2090 2094 2098
year

Appendix_ E Base line Tmin Scenario developed for all station

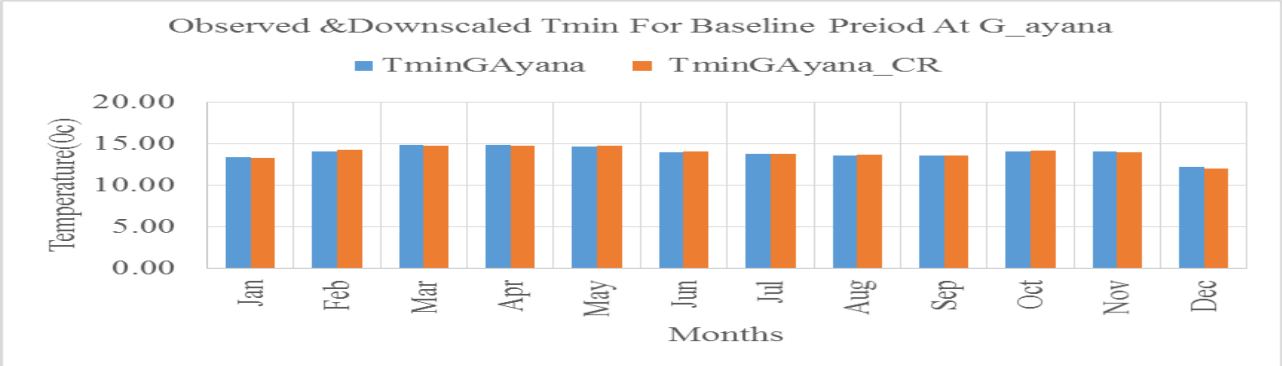

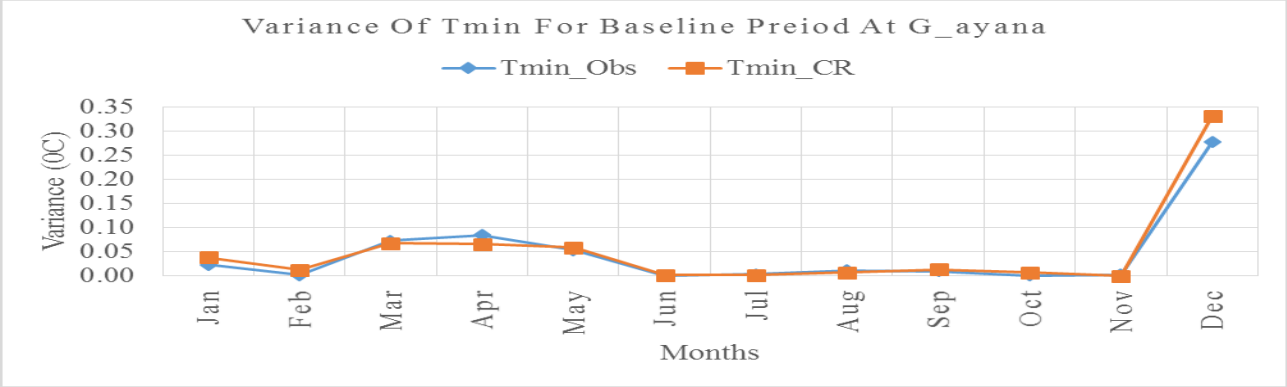

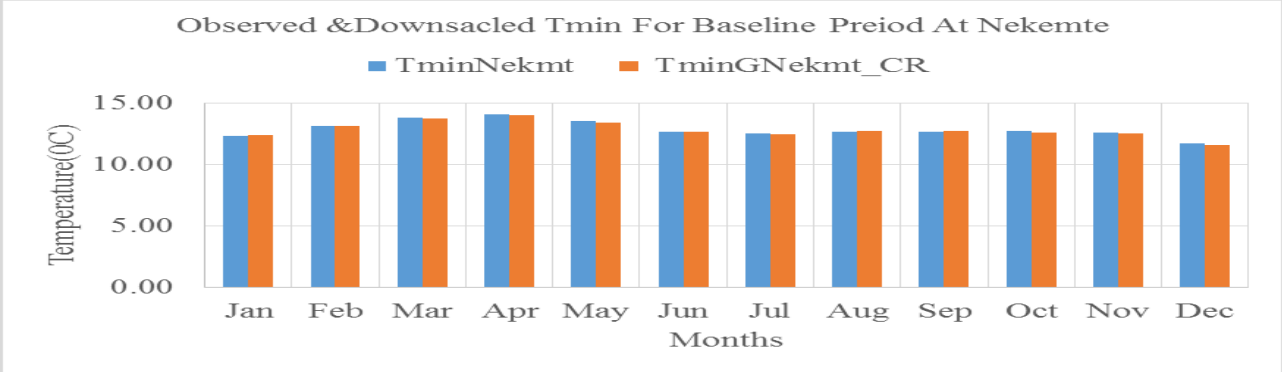

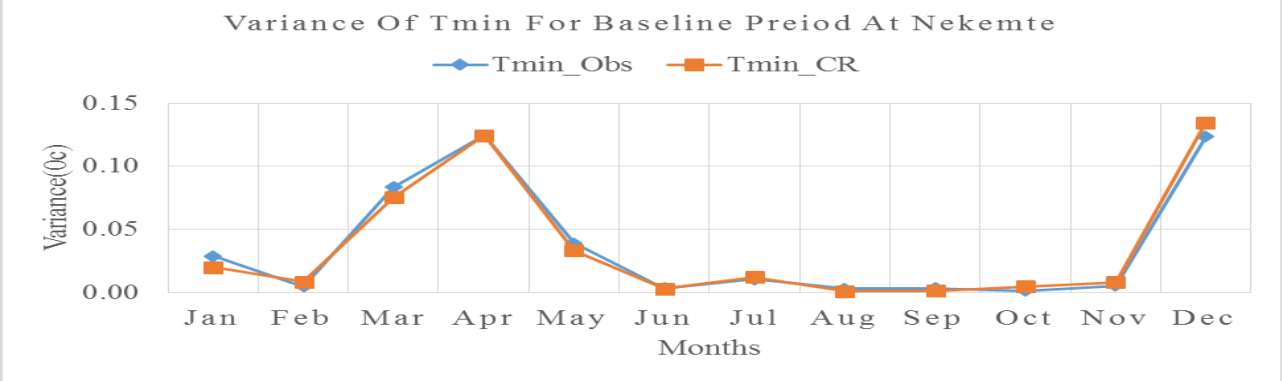

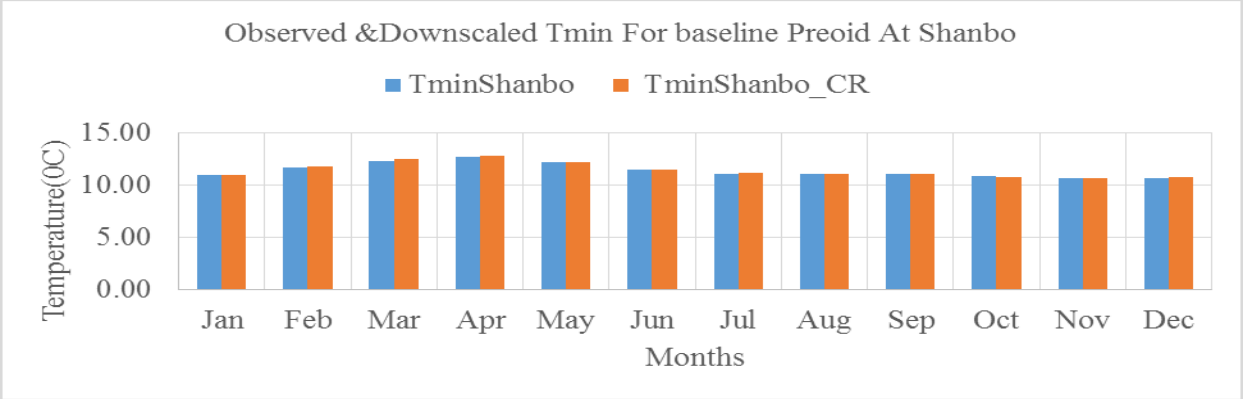
Observed &Downscaled Tmin For baseline Preoid At Shanbo
TminShanbo
TminShanbo_CR
Temperature(0C)
15.00
10.00
5.00
0.00
Jan
Feb
Mar
Apr
May
Jun
Jul
Aug
Sep
Oct
Nov
Dec
Months

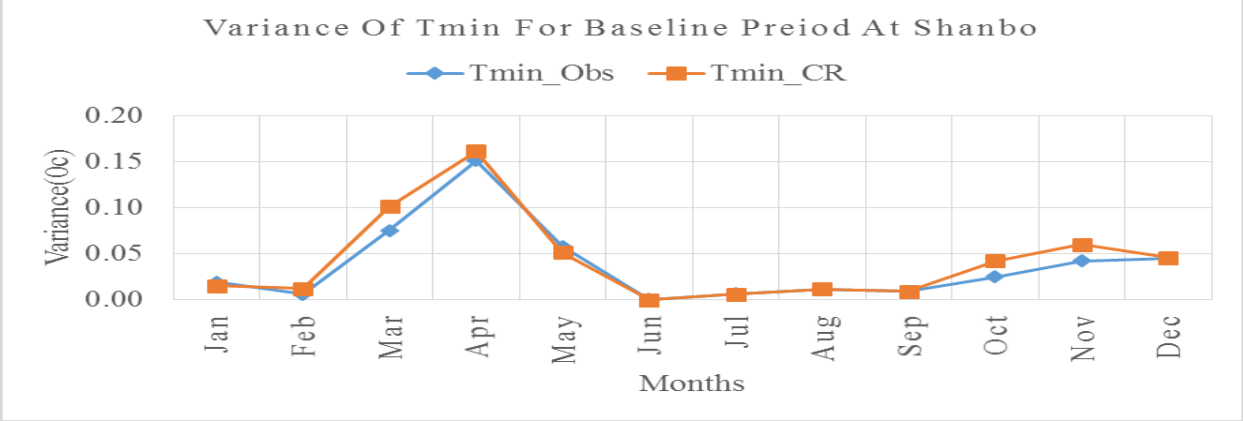
Variance Of Tmin For Baseline Preoid At Shanbo
Tmin_Obs
Tmin_CR
Variance(0c)
0.20
0.15
0.10
0.05
0.00
Jan
Feb
Mar
Apr
May
Jun
Jul
Aug
Sep
Oct
Nov
Dec
Months

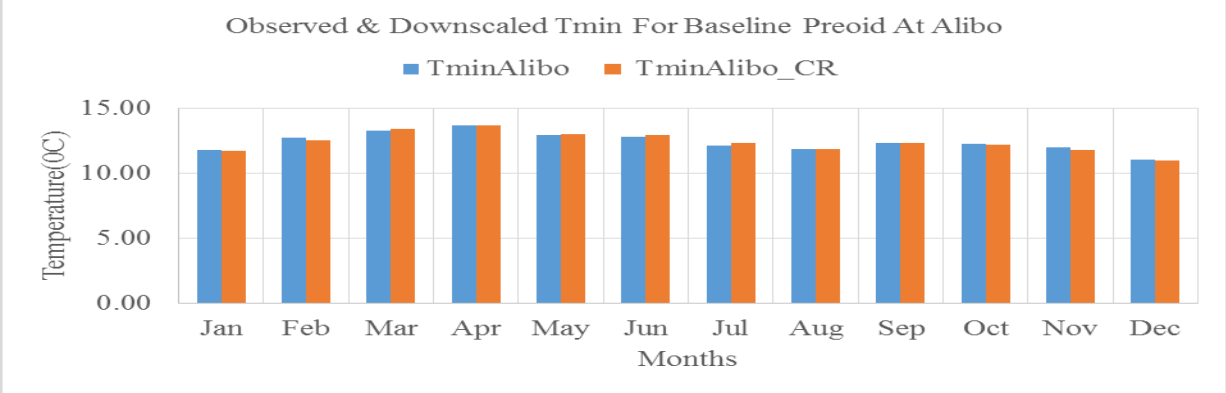
Observed & Downscaled Tmin For Baseline Preoid At Alibo
TminAlibo
TminAlibo_CR
Temperature(0C)
15.00
10.00
5.00
0.00
Jan
Feb
Mar
Apr
May
Jun
Jul
Aug
Sep
Oct
Nov
Dec
Months

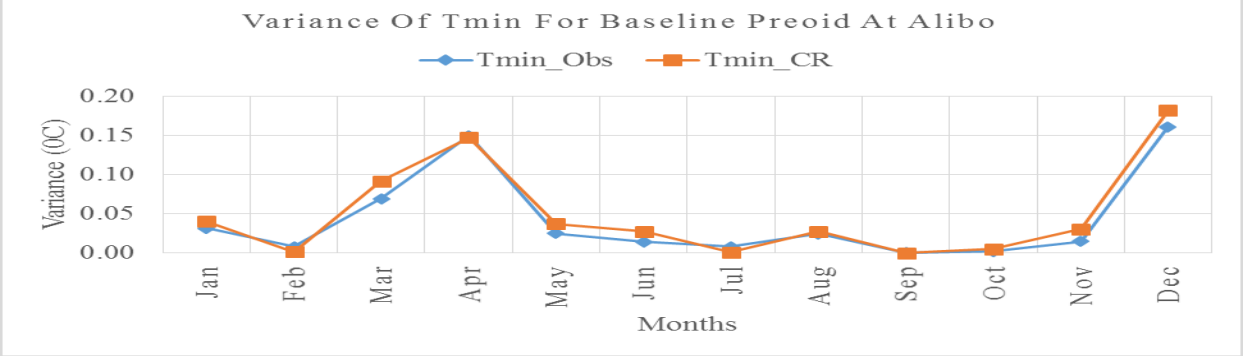
Variance Of Tmin For Baseline Preoid At Alibo
Tmin_Obs
Tmin_CR
Variance (0C)
0.20
0.15
0.10
0.05
0.00
Jan
Feb
Mar
Apr
May
Jun
Jul
Aug
Sep
Oct
Nov
Dec
Months

Appendix _ F Base line Tmax Scenario developed for all station

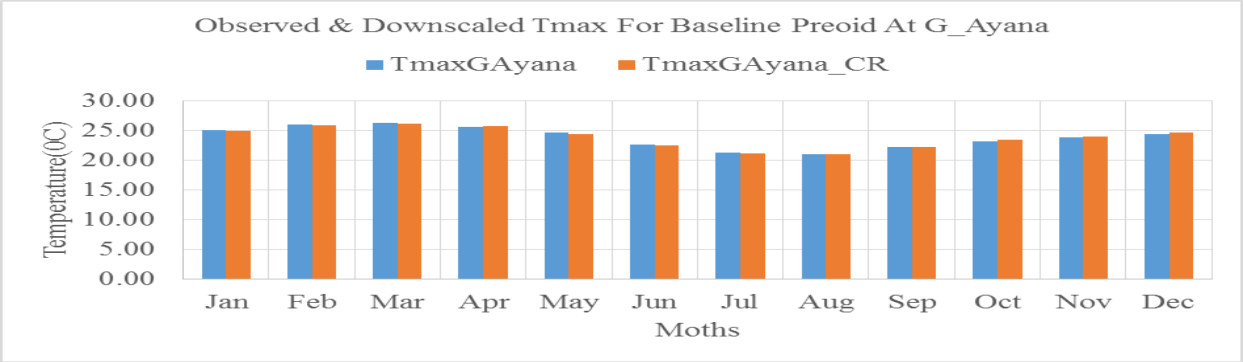

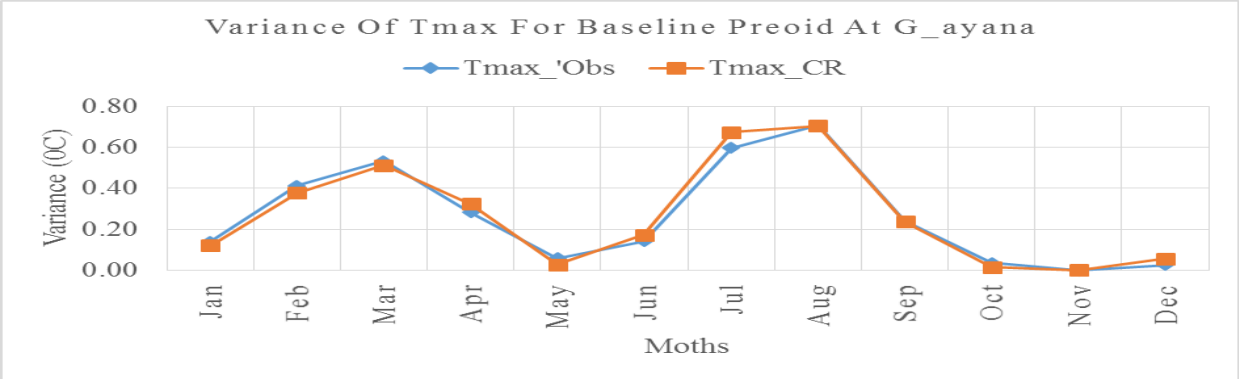

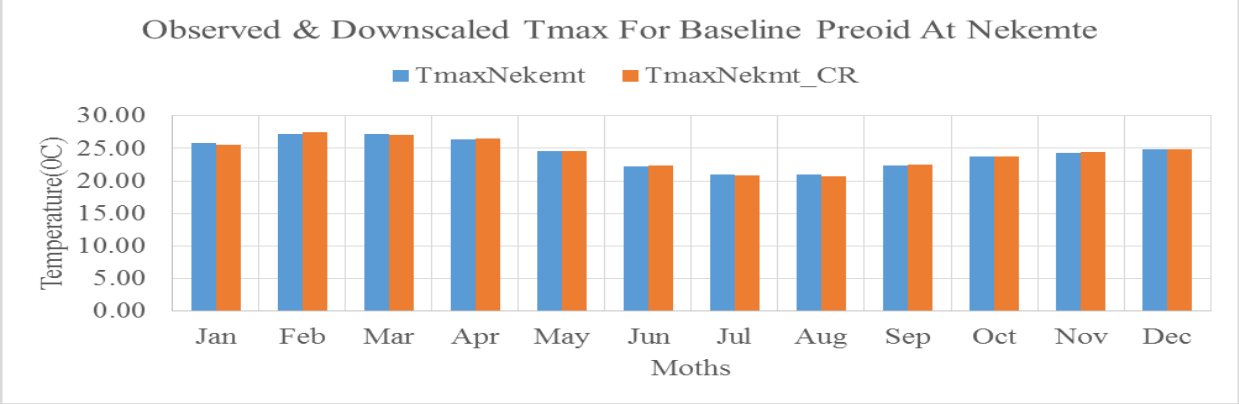

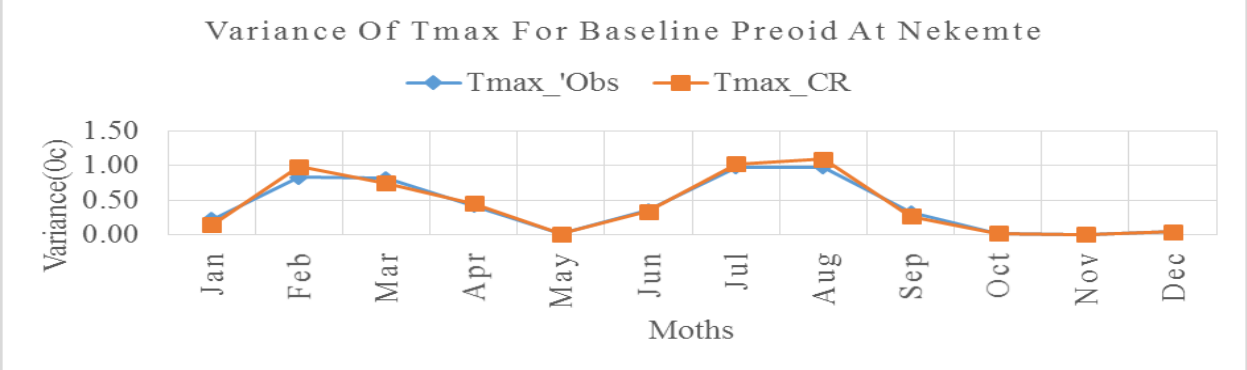

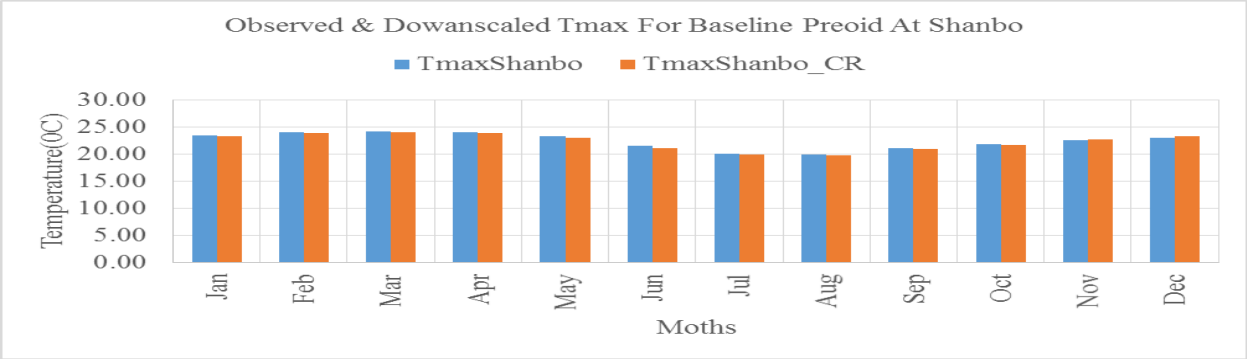

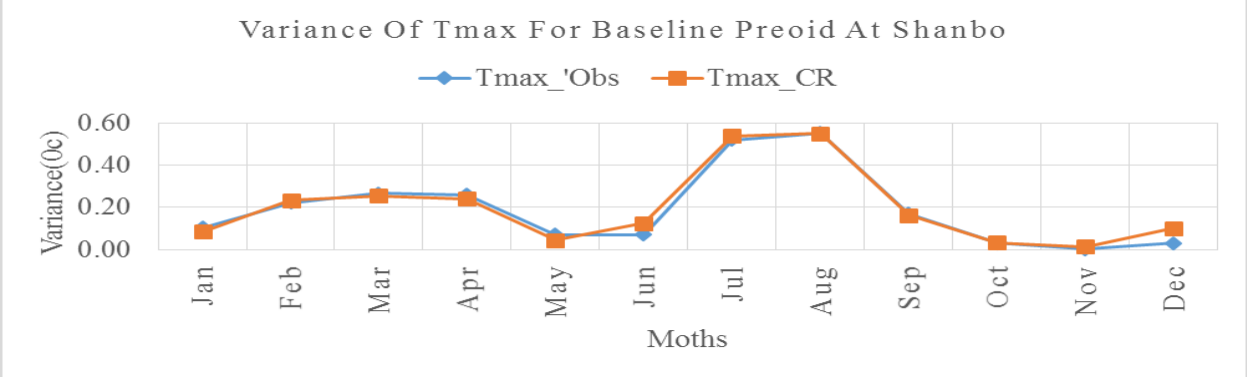

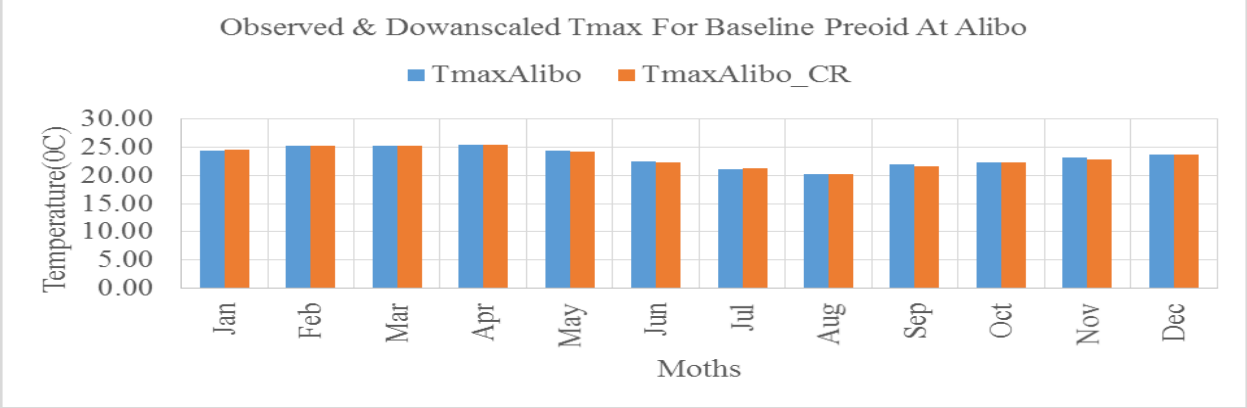

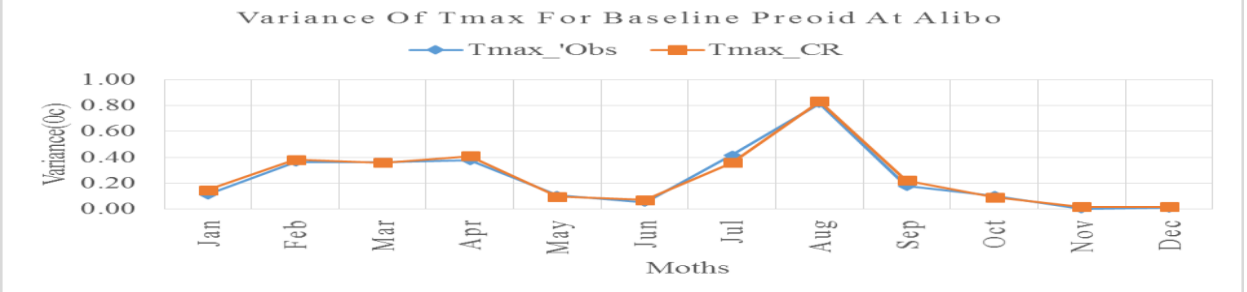

Appendix G Base line PCP Scenario developed for all station

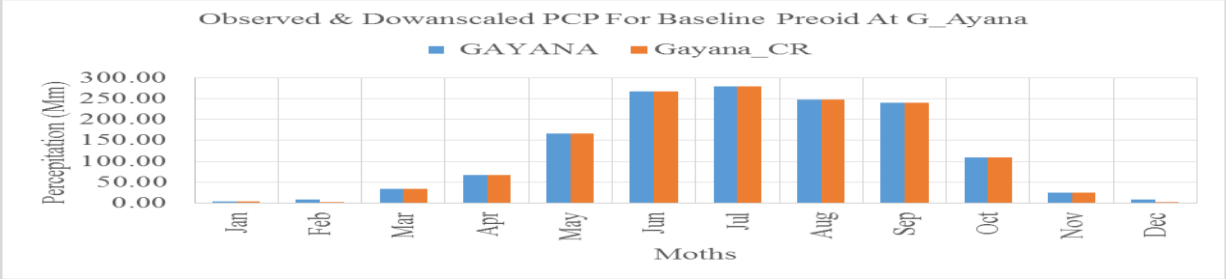
Observed & Dowanscaled PCP For Baseline Preoid At G_Ayana
GAYANA
Gayana_CR
Percepitation (Mm)
300.00
250.00
200.00
150.00
100.00
50.00
0.00
Jan
Feb
Mar
Apr
May
Jun
Jul
Aug
Sep
Oct
Nov
Dec
Moths

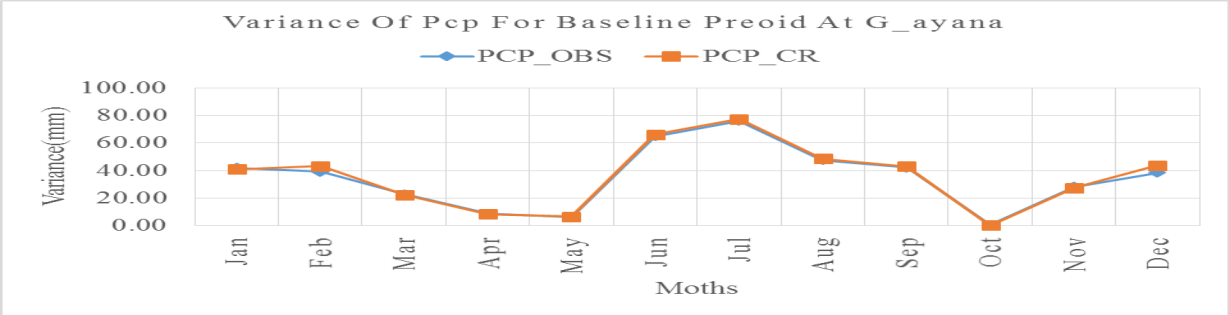
Variance Of Pcp For Baseline Preoid At G_ayana
PCP_OBS
PCP_CR
Variance(mm)
100.00
80.00
60.00
40.00
20.00
0.00
Jan
Feb
Mar
Apr
May
Jun
Jul
Aug
Sep
Oct
Nov
Dec
Moths

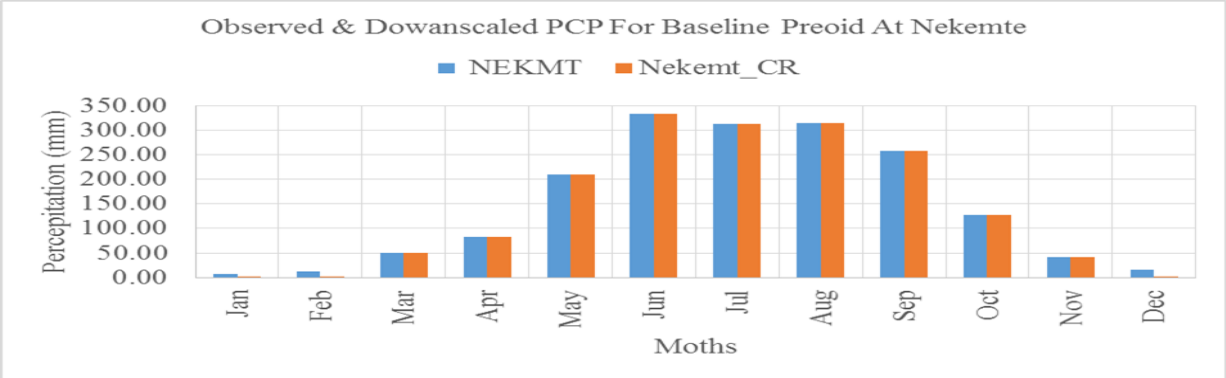
Observed & Dowanscaled PCP For Baseline Preoid At Nekemte
NEKMT
Nekemt_CR
Percepitation (mm)
350.00
300.00
250.00
200.00
150.00
100.00
50.00
0.00
Jan
Feb
Mar
Apr
May
Jun
Jul
Aug
Sep
Oct
Nov
Dec
Moths

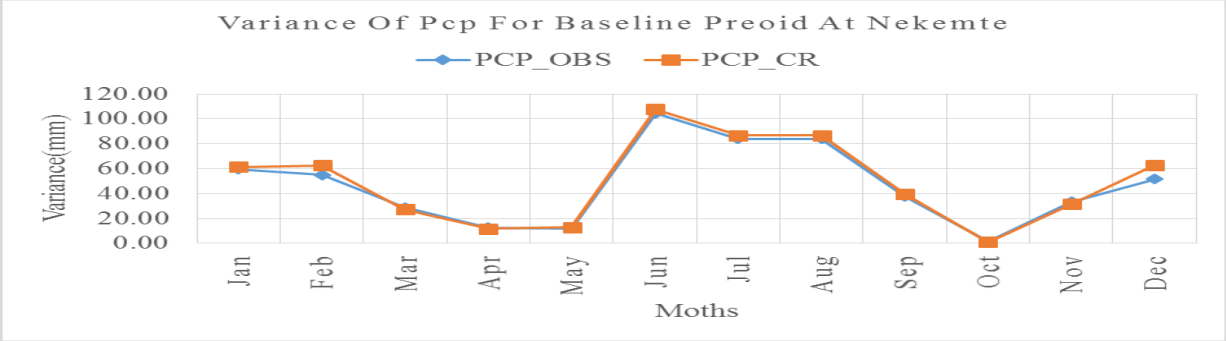
Variance Of Pcp For Baseline Preoid At Nekemte
PCP_OBS
PCP_CR
Variance(mm)
120.00
100.00
80.00
60.00
40.00
20.00
0.00
Jan
Feb
Mar
Apr
May
Jun
Jul
Aug
Sep
Oct
Nov
Dec
Moths

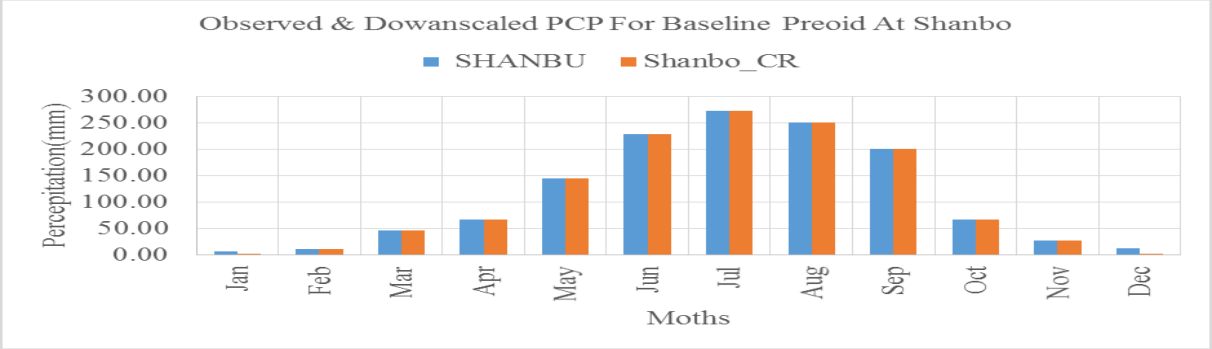
Observed & Dowanscaled PCP For Baseline Preoid At Shanbo
SHANBU
Shanbo_CR
Percepitation(mm)
300.00
250.00
200.00
150.00
100.00
50.00
0.00
Jan
Feb
Mar
Apr
May
Jun
Jul
Aug
Sep
Oct
Nov
Dec
Moths

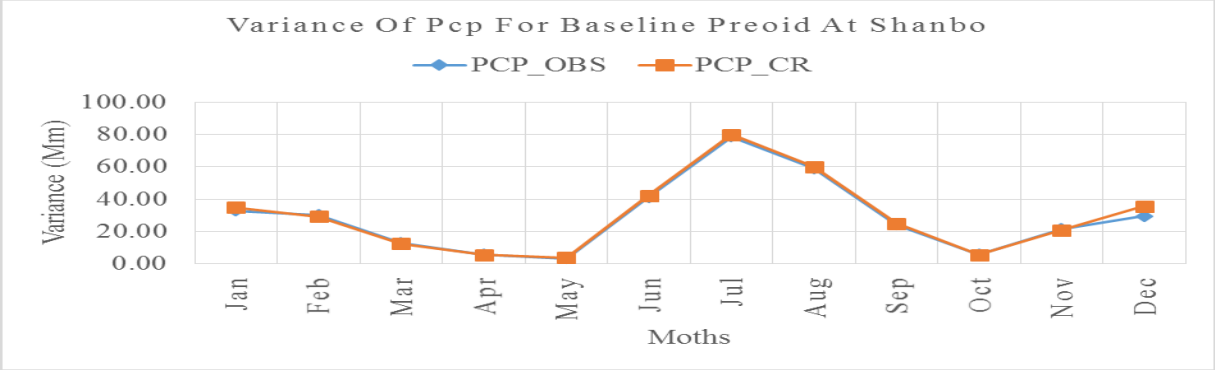
Variance Of Pcp For Baseline Preoid At Shanbo
PCP_OBS
PCP_CR
Variance (Mm)
100.00
80.00
60.00
40.00
20.00
0.00
Jan
Feb
Mar
Apr
May
Jun
Jul
Aug
Sep
Oct
Nov
Dec
Moths

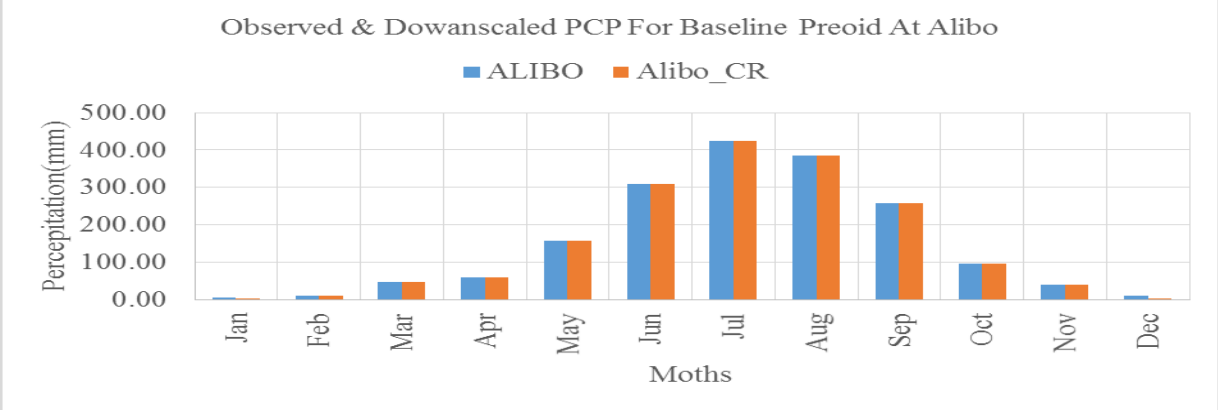
Observed & Dowanscaled PCP For Baseline Preoid At Alibo
ALIBO
Alibo_CR
Percepitation(mm)
500.00
400.00
300.00
200.00
100.00
0.00
Jan
Feb
Mar
Apr
May
Jun
Jul
Aug
Sep
Oct
Nov
Dec
Moths

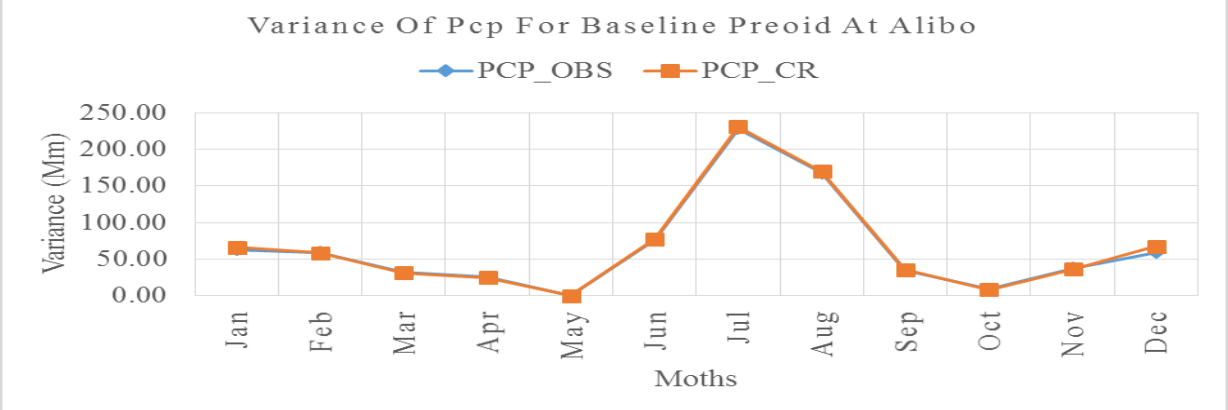
Variance Of Pcp For Baseline Preoid At Alibo
PCP_OBS
PCP_CR
Variance (Mm)
250.00
200.00
150.00
100.00
50.00
0.00
Jan
Feb
Mar
Apr
May
Jun
Jul
Aug
Sep
Oct
Nov
Dec
Moths

Appendix –H observed stream flow for calibration and validation (1990-2005)

Year \ Months	Jan	Feb	Mar	Apr	May	Jun	Jul	Aug	Sep	Oct	Nov	Dec
1990	12.55	9.33	8.44	5.77	7.61	13.13	46.46	51.89	70.42	42.40	23.36	14.21
1991	5.06	2.17	7.69	6.46	4.90	8.90	50.68	61.99	52.90	34.40	20.55	15.56
1992	10.79	7.52	9.69	10.59	12.99	8.46	42.66	93.15	60.90	42.68	25.34	15.34
1993	16.52	12.87	11.17	12.71	16.66	41.20	51.56	61.76	64.93	53.96	38.68	23.30
1994	18.00	14.50	14.05	9.39	17.88	36.35	63.30	77.91	63.96	37.78	30.34	21.91
1995	15.99	8.54	8.11	11.08	14.98	19.89	38.97	54.02	40.46	32.86	23.70	16.45
1996	12.83	8.50	9.11	7.69	18.25	50.35	71.96	69.40	61.54	43.08	30.31	21.92
1997	15.63	13.56	12.46	11.21	11.53	25.30	71.74	83.28	43.96	25.84	19.17	18.13
1998	18.03	13.43	12.99	11.12	15.00	21.20	100.20	89.84	75.65	67.85	58.83	34.69
1999	30.26	18.69	17.25	19.98	20.88	29.13	55.74	53.83	51.30	43.30	37.30	31.90

a. observed stream flow in (m3/s) for calibration from (1990-1999)

Year \ Months	Jan	Feb	Mar	Apr	May	Jun	Jul	Aug	Sep	Oct	Nov	Dec
2000	22.24	16.02	12.47	14.79	20.04	31.76	60.28	71.52	86.42	78.91	43.16	26.69
2001	19.05	14.34	11.87	9.78	16.28	29.04	60.13	80.46	72.68	54.36	30.27	21.54
2002	16.83	11.79	9.53	7.54	5.63	30.80	68.94	81.08	92.91	48.88	19.99	14.76
2003	9.83	7.01	7.83	3.90	1.69	20.14	44.31	87.30	75.08	60.66	23.32	15.33
2004	10.89	7.49	5.70	5.96	7.47	32.58	55.74	77.57	71.31	51.08	31.83	15.04
2005	14.49	9.90	11.20	8.28	11.36	27.55	41.74	71.13	59.75	47.53	26.61	14.26

b. Observed stream flow in (m3/s) for validation from (2000-2005).